

Studies on the Inhibitory and Additive Effects of Withaferin A in Experimental Visceral Leishmaniasis



Thesis Submitted to the University of Hyderabad
for the Award of

Doctor of Philosophy

By

Bharadwaja Vadloori

(13LAPH01)

Supervisor:

Dr. Radheshyam Maurya

DEPARTMENT OF ANIMAL BIOLOGY
SCHOOL OF LIFE SCIENCES
UNIVERSITY OF HYDERABAD
Hyderabad, 500046, India

June 2018



हैदराबाद विश्वविद्यालय

University of Hyderabad

(A Central University Established in 1974 by the Act of Parliament)

Hyderabad – 500046, India.

“DECLARATION”

I, Bharadwaja Vadloori, hereby declare that this thesis entitled **“Studies on the Inhibitory and Additive Effects of Withaferin A in Experimental Visceral Leishmaniasis”** submitted by me is based on the results of research work done under the guidance and supervision of Dr. Radheshyam Maurya at Department of Animal Biology, School of Life Sciences, University of Hyderabad. The research work presented in this thesis is original and plagiarism free. I also declare that no part or in full of this thesis has been submitted previously to this University or any other University or Institution for the award of any degree or diploma.

Bharadwaja Vadloori

(Research Scholar)



हैदराबाद विश्वविद्यालय

UNIVERSITY OF HYDERABAD

(A Central University Established in 1974 by the Act of Parliament)
Hyderabad – 500046, India.

“CERTIFICATE”

This is to certify that the thesis entitled **“Studies on the Inhibitory and Additive Effects of Withaferin A in Experimental Visceral Leishmaniasis”** submitted by **Mr. Bharadwaja Vadloori** bearing registration number **13LAPH01** in partial fulfilment of requirements for the award of Doctor of Philosophy in **School of Life Sciences** is a bonafide work carried out by him under my supervision and guidance. This thesis is free from plagiarism and has not been submitted previously in part or in full to this or any other University or Institution for the award of any degree or diploma.

A. Published in the following publications:

1. BMC Research Notes. 2018 11:246
2. Scientific Reports. 2017 Nov 7; 7:14664.

B. Presented in the following conferences:

1. AS-UOH joint workshop on “Frontiers in Life Sciences” in Sep 2016 at School of Life Sciences, University of Hyderabad. (International)
2. ‘International Conference on Innovations in Pharma and Bio-Pharma Industry Challenges and Opportunities for Academy and Industry’ in Dec 2017 at School of Life Sciences, University of Hyderabad. (International)

The Student has passed the following courses towards fulfilment of coursework requirement for Ph.D.

Course Code	Name	Credits	Pass/Fail
1. AS 801	Seminar	1	Pass
2. AS 802	Research Ethics & Management	2	Pass
3. AS 803	Biostatistics	2	Pass
4. AS 804	Analytical Techniques	3	Pass
5. AS 805	Lab Work	4	Pass

Supervisor

Head of Department

Dean of School

Acknowledgements

I owe a great debt to many people who have contributed to my thesis. Firstly I thank my supervisor, Dr. Radheshyam Maurya for giving me an opportunity to pursue Ph.D., studies under his guidance. I thank my doctoral committee members Dr. Srinivasulu Kurukuti, Dr. Irfan Ahmed Ghazi, for their time and valuable suggestions.

I thank the present Dean, School of Life Sciences Prof. K.V.A Ramaiah, and the former Deans; the present Head, Department of Animal Biology, Prof. Anita Jagota, and the former heads for providing good scientific infrastructure for the School and the Department to carry out research work.

I thank all Ph.D. scholars, Post-Doctoral Fellows, Faculty and Non-Teaching Staff of the School of Life Sciences.

I thank Mr. Devender, the metabolomics facility technician, for helping me in performing LCMS/MS. My thanks are also due to Dr. Jerald Mahesh, CCMB and Mr. Yadagiri for their help in histological studies.

I thank the previous and the present research scholars in the lab. I thank the staff of animal house facility.

I thank DST, DBT, UGC, ICMR, DST-PURSE, and UPE II for funding the lab. I acknowledge the infrastructure support provided by DBT-CREBB, DST-FIST to the Dept. of Animal Biology and School of Life Sciences.

I thank the University of Hyderabad for supporting me with BBL fellowship.

I am grateful to Dr. Balraj Kashi, for benevolently sending *Withania somnifera* leaves.

I have no words of gratitude for the unconditional love and support of my parents and my sister. I am grateful to have them in my life. I am deeply indebted to them for their patience and encouragement. I offer my obeisance to the God for blessing me with good health, patience, and strength to fulfil my endeavors successfully.

Bharadwaja Vadloori

Abstract

Leishmaniasis is a neglected tropical disease with limited drugs available for treatment. Toxicity and emergence of resistance to this disease calls for an urgent need to explore alternative treatment. *Leishmania* has Dihydrofolate reductase-thymidylate synthase (DHFR-TS) and Pteridine reductase (PTR1) enzymes in the folic acid pathway. DHFR-TS is an essential enzyme whose inhibition leads to disruption of the nucleotide metabolism. Withaferin A (WA) is major withanolide from *Withania somnifera*, known for different properties, but its mechanism of action on *Leishmania* is not known. Our docking studies reveal that Lys 173 forms H-bond with WA. The molecular dynamics simulations confirm that H-bonds were stable and the binding energies of WA with *Ld* DHFR-TS were calculated using MM-PBSA. Our *in silico* study reveals that WA has higher binding affinity to *Ld* DHFR-TS than the Human enzymes. The *Ld* DHFR-TS gene was cloned during the study; the recombinant protein was expressed, purified and refolded from the inclusion bodies. The DHFR activity was determined spectrophotometrically by monitoring a decrease in absorbance at 340 nm which accompanies the conversion of substrates NADPH and dihydrofolate to the products NADP⁺ and tetrahydrofolate. The enzyme inhibition was performed with WA (1.2 μM) and Methotrexate (2 μM). The results suggest that WA is an uncompetitive inhibitor of *Ld* DHFR-TS. The combination of existing drugs with the natural products is one of the most rational alternative approaches to prevent resistance, improve efficiency, reduce the duration and lower the treatment failure. The study evaluated *in vivo* safety and efficacy of Miltefosine (Milt) and WA combination. Milt is the first and only available oral drug for Leishmaniasis. A combination trial was performed on the female BALB/c mice and IgG2a and IgG1 levels by an indirect ELISA, spleen parasite load by microscopy, Haematoxylin-Eosin staining of liver tissue, glucose, cholesterol and triglyceride concentrations in the serum, spleen and whole body weight were estimated. The results of the combination trial suggest that, an oral administration of Milt (2.5 mg/kg BW) with an *i.p* delivery of WA (2 mg/kg BW) can be considered safe, effective and show an additive effect. WA + Milt combination may reduce the drug resistance problem in the endemic areas. However, the combination study requires further research after which it can be developed for the control of VL in the endemic regions.

Contents

Contents	Page Number
Chapter I: Introduction	1-23
Chapter II: Review of literature	24-43
Chapter III: Materials and Methods	44-69
Chapter IV: Results and Discussion	70-100
Chapter V: Summary	101-103
Chapter VI: References	104-121

Abbreviations

%	Percentage
°C	Degree centigrade/Degree Celsius
2D	Two dimensional
3D	Three dimensional
Å	Angstrom units
AmB	Amphotericin B
APC	Antigen Presenting Cells
ATB	Automated Topology Builder
ATCC	American Type Culture Collection
atm	Atmospheres
B.W	Body Weight
BBB	Blood Brain Barrier
BCG	Bacillus Calmette Guérin
BPL	Below Poverty Line
CaCl ₂	Calcium Chloride
CaCO ₂	Calcium Carbonate
CD	Cluster of Differentiation
CL	Cutaneous Leishmaniasis
CMI	Cell-Mediated Immunity
CNS	Central Nervous System
CO ₂	Carbon Dioxide
DALYs	Disability Adjusted Life Years
DC	Dendritic Cell
DCL	Diffuse Cutaneous Leishmaniasis
DD8	<i>Leishmania donovani</i> strain MHOM/IND/80/DD8
DHFA	Dihydrofolic acid
DHFR	Dihydrofolate reductase
dNTP	Deoxynucleotide triphosphate
DTT	Dithiothreitol
EDTA	Ethylene Diamine Tetra Acetic acid
ELISA	Enzyme-Linked Immunosorbent Assay
ER	Endoplasmic Reticulum
FASTA	Fast Alignment
FBS	Fetal Bovine Serum
GIPL	Glycosyl Inositol Phospho Lipids
GMQE	Global Model Quality Estimation
gp63	Glycoprotein 63
H ₂ SO ₄	Sulphuric acid
H ₂ O ₂	Hydrogen Peroxide
HBA	Hydrogen bond acceptors
HBD	Hydrogen bond donors
H-E	Haematoxylin-Eosin
HIV	<i>Human Immunodeficiency Virus</i>
HPLC	High Performance Liquid Chromatography
HRP	Horse Radish Peroxidase
i.c.	Intra Cardiac
i.d.	Intra Dermal
i.l.	Intra-Lesional

<i>i.m</i>	Intra Muscular
<i>i.p</i>	Intra Peritoneal
<i>i.v.</i>	Intra Venal
IAEC	Institutional Animal Ethics Committee
IC ₅₀	Half-inhibitory Concentration
ICT	Immunochromatographic Test
IFN- γ	Interferon- γ
Ig	Immunoglobulin
IL	Interleukin
iNOS	Inducible Nitric Oxide Synthase
IPTG	Isopropyl β -D-1-Thiogalactopyranoside
k	Kelvin
kDa	Kilo Dalton(s)
Kg	Kilo gram
LAT	Latex Agglutination Test
LB Media	Luria-Bertani Media
LC-MS/MS	Liquid Chromatography- Mass Spectrophotometry
LDU	Leishman-Donovan Units
LINCS	LINear Constraint Solver
Log P	Octanol-Water partition coefficient
LPG	Lipophosphoglycan
M199	Medium-199
MAB	Monoclonal Antibody
MCP	Monocyte Chemotactic Protein
MDS	Molecular Dynamics Simulations
mg	Milli gram
MgCl ₂	Magnesium Chloride
MHC	Major Histocompatibility Complex
ml	Milli litre
MM-PBSA	Molecular Mechanics-Poisson-Boltzmann Surface Area
mRNA	Messenger Ribonucleic Acid
MTX	Methotrexate
MW	Molecular Weight
NaCl	Sodium Chloride
NaHCO ₃	Sodium Bicarbonate
NCBI	National Center for Biotechnology Information
NF- κ B	Nuclear Factor kappa-light-chain-enhancer of activated B cells
ng	Nano gram
NH ₄ Cl	Ammonium Chloride
NK cells	Natural Killer cells
nm	Nano meter
NO	Nitric Oxide
NOS	Nitric Oxide Synthase
NPT ensemble	isothermal (constant temperature T)-isobaric (constant pressure P)
ns	Nano seconds
NVT ensemble	Number of particles (N), absolute temperature (T) and volume (V)
OD	Optical Density
PBMCs	Peripheral Blood Mononuclear Cells
PBS-T	Phosphate Buffer Saline-Tween
PCR	Polymerase Chain Reaction

PDB	Protein Data Bank
BLAST	Basic Local Alignment Search Tool
pg	Pico gram
PKDL	Post <i>Kala-Azkar</i> Dermal Leishmaniasis
PMSF	Phenyl Methyl Sulphonyl Fluoride
ps	Pico seconds
PSA	Polar Surface Area
PSG	Promastigote Secretion Gel
PSP	Promastigote Surface Protease
PTR	Pteridine reductase
PV	Parasitophorous Vacuole
QMEAN	Qualitative Model Energy Analysis
QSPR	Quantitative Structure-Property Relationship
RFLP	Rapid Fragment Length Polymorphism
RMSD	Root mean square deviation
RMSF	Root mean square fluctuations
RNI	Reactive Nitrogen Intermediate
ROI	Reactive Oxygen Intermediate
ROS	Reactive Oxygen Species
RPMI	Roswell Park Memorial Institute
RT	Room Temperature/Retention Time
SAVES	Structure Analysis and Verification Server
SbV	Pentavalent Antimonial
SDS-PAGE	Sodium Dodecyl Sulphate-Poly Acrylamide Gel Electrophoresis
SLA	Soluble <i>Leishmania</i> Antigen
SPC/E water models	Extended simple point charge model
TAE	Tris Acetate-EDTA
TB	Tuberculosis
TBS	Tris Buffered Saline
TBS-T	Tris-Buffer Saline-Tween
TEMED	N,N,N',N'-Tetramethylethylenediamine
TGF- β	Transforming Growth Factor beta
Th	T-helper
TMB	3,3', 5,5;-tetramethylbenzidine
TNF- α	Tumor Necrosis Factor- α
Tris-HCl	Tris-Hydrochloric acid
VL	Visceral Leishmaniasis
V-rescale	Velocity rescale
WA	Withaferin-A
WB	Western Blotting
WHO	World Health Organization
λ	Wave length
μg	Micro gram
μl	Micro litre
μM	Micro molar
μm	Micro meter
μn	Micron
Φ	Macrophage
Ψm	Mitochondria membrane potential

Chapter: 1

Introduction

1.1 Leishmaniasis – an overview:

Leishmaniasis is one of the major and relatively unnoticed epidemic tropical diseases. World Health Organization (WHO) has recognized it as one among the six significant parasitic infections and it stands ninth among the global infectious diseases. It is a complicated disease which is diverse in terms of clinical manifestation and epidemiology. The humid and semi humid territories in the world with the majority of population poorer are affected by this disease, which is a serious public health impediment. Approximately 350 million individuals are presently in danger and every year two million fresh individuals are affected. About 50,000 deaths occur annually by visceral leishmaniasis (VL) and 23,57,000 disability-adjusted life years (DALY) are lost (WHO 2010). Nearly 100 countries are endemic to the disease and more than 90% of patients are from Bangladesh, Brazil, Ethiopia, India, Nepal, and Sudan. The visual external symptoms may include mild self-healing lesions on the skin as in cutaneous leishmaniasis (CL), damage to the mucocutaneous regions of the face as mucocutaneous leishmaniasis (MCL), depending on the species involved. VL is potentially fatal if left untreated (Freitas et al. 2012). The factors like malnutrition, stress, immune deficiency, poverty, famine, war, increase the severity of this disease (Alvar et al. 2012; Ready 2014).

The protozoan parasite *Leishmania* causes VL and is transmitted by the phlebotomine sand fly vector. The disease is sensitive to the climatic conditions such as temperature, rainfall, and humidity. Further, in the adult HIV patients, VL occurs as an opportunistic infection manifesting atypical clinical features, with increased chances of relapse and death (WHO 2010). The polymorphic outcome of VL depends on the parasite's virulence, the immunosuppressive capability of sand fly's saliva, the host's genetic makeup and the immune response. As it is currently unpreventable and uncontrollable, a modernistic approach to control is the need of the hour. A successful vaccination program can most likely control the disease. The fact that, the host becomes resistant to further infections after recovering from a primary infection and parasite's simple life cycle, provides encouragement to develop vaccines (Kaye and Aebischer 2011; Loría-Cervera and Andrade-Narváez 2014). The elimination of VL depends largely on research breakthroughs in the cost-effective case management and vector control. The major achievements in treatment, diagnosis, prevention have taken place in the last decade and the cost of medication has come down (Faleiro et al. 2014; WHO 2010).

1.2 Historical Background:

Archaeological and historical evidence shows that Leishmaniasis affected humans in the pre-historic times. On the inscriptions of the seventh-century king, Ashurbanipal, illustrations of clearly visible lesions similar to CL were reported. In the tenth century, a Persian physician, Avicenna, gave a detailed account of Balkh sore. Alexander Russell in 1756, after inspecting a patient in Turkey, elaborately described the clinical symptoms and called the disease as 'Aleppo boil'. In the Americas, pottery belonging to the periods before Inca Empire, show carvings of lesions on the skin and damaged faces which are the archaeological and historical evidence of CL in Ecuador and Peru from the first century. During the 15th - 16th century, the Inca empire and the Spanish colonial period's many texts have been written in which "Valley sickness, Andean sickness, and White leprosy" diseases are mentioned which probably is CL (<https://en.wikipedia.org/wiki/Leishmaniasis>).

Vianna, Lindenberg, Borovsky, Leishman, Wright, Cunningham, and Donovan have independently identified Leishmaniasis causing parasite in the later part of the 19th century. New microorganisms were identified by Leishman in 1901, in the spleen biopsy of an army personnel expired of "dum-dum fever" and reported them to be *Trypanosomes* in *The British Medical Journal* on May 30, 1903, with the title '*On the possibility of the occurrence of Trypanosomiasis in India*'. Charles Donovan after observing the same kind of organism in smears of a patient from Madras has written a memorandum to Leishman's article in the same journal on July 11, 1903. It was Sir Ronald Ross who identified that the 'new microorganisms' are not *Trypanosomes*, and called them 'Leishman Bodies'. He wrote an article with title the '*Further notes on Leishman's Bodies*' in *The British Medical Journal* on Nov 28, 1903. Later he coined the generic name '*Leishmania donovani*' and described '*Leishman-Donovan*' (LD) bodies as intracellular stages of a new parasite. Charles Bentley discovered *L. donovani* in patients with *Kala-Azar* after Charles Donovan suggested the relation between LD Bodies and *Kala-Azar*. During the Second World War many soldiers of allied troops died of this disease. (<https://en.wikipedia.org/wiki/Leishmaniasis>) (Bray and Modabber 2000).

Before the 1820s, the documentation about *Kala-Azar* was uncertain. William Twining initially described fever and enlargement of the spleen as symptoms caused by *Kala-Azar*. During 1824-1825 in '*Mahomedpore*', situated about 30 miles to the east of *Jessore* in Lower Bengal, the first outbreak of Leishmaniasis occurred that was mistaken for Malaria and the

cause of endemicity was due to unhealthy conditions of villages and unsanitary habits of villagers. A few years later in 1858, in Burdwan, another epidemic fever occurred which was resistant to quinine. Eight to ten years later, in the south-west of Assam, fever with the enlargement of spleen, anemia, and darkening of the skin occurred that was locally called as *Kala-Azar*. During 1898 Ronald Ross investigated *Kala-Azar* in Darjeeling, Purnea in Upper Bengal and in Assam, and felt that it is the same disease present in both places and concluded that the disease was Malaria coinfecting with other opportunistic pathogens. In 1904 Donovan found *L. donovani* in peripheral circulation and other internal organs. *L. donovani* for the first time was cultured *in vitro* at 27°C by Leonard Rogers in 1904. Saul Adler, a British-Israeli parasitologist in 1942 demonstrated and proved that sand fly is the vector which transmits *Kala-Azar* (Gibson 1983).

1.3 Morphology and Life Cycle of *Leishmania*:

The life cycle of *Leishmania* alters across the invertebrate sand fly vector and the vertebrate host, thus it is digenetic. It exists in two morphological forms namely, the amastigotes, (which dwell within the cells of the mammalian host/vertebrate host) and the promastigotes, (which dwell outside the cells in the phlebotomine sand fly gut/invertebrate host). The morphology of these two forms is shown in the fig. 1.1. The promastigotes pass through the diverse developmental stages like procyclic, nectomonad, haptomonad and metacyclic which have their own characteristic forms and functions. The development of the parasite in the mammalian host is relatively simple whereas in the sand fly it is intricate and less discovered (Gossage, Rogers, and Bates 2003; Wheeler, Gluenz, and Gull 2011).

Amastigotes:

They are intracellular, non-motile, non-flagellated 3-5 µm long ovoid forms in the mammalian host which are smaller in size compared to the promastigotes. The flagellum barely extrudes from the cell body. They dwell in the parasitophorous vacuoles of the macrophages. The outer membrane is composed of polysaccharides but lacks a coat on the surface. They have very low endoplasmic reticulum (ER) enveloped by a nuclear membrane and Golgi apparatus and also have distinctively organized lysosomal compartment (Herwaldt 1999) (fig. 1.1.C)

Promastigotes:

They are extracellular, flagellate forms in sand fly measuring about 15-20 μm by 1.5-3.5 μm in size with a long spindle-shaped motile body with 15-28 μm flagellum in the anterior region. The flagellum is thrice the cell length in some promastigotes. The plasma membrane is coated with the glycoproteins, lipophosphoglycan (LPG), highly cross-linked sub-pellicular microtubules and mannose receptors, which create an association between molecules on the surface of the parasite and the macrophage receptors. The flagellar pocket is an invagination at the anterior end of the plasma membrane, where the ER and Golgi apparatus are situated and negotiate in the exocytosis and endocytosis. It holds the base of the flagellum and helps in the anterior motility (Herwaldt 1999) (fig. 1.1.B.)

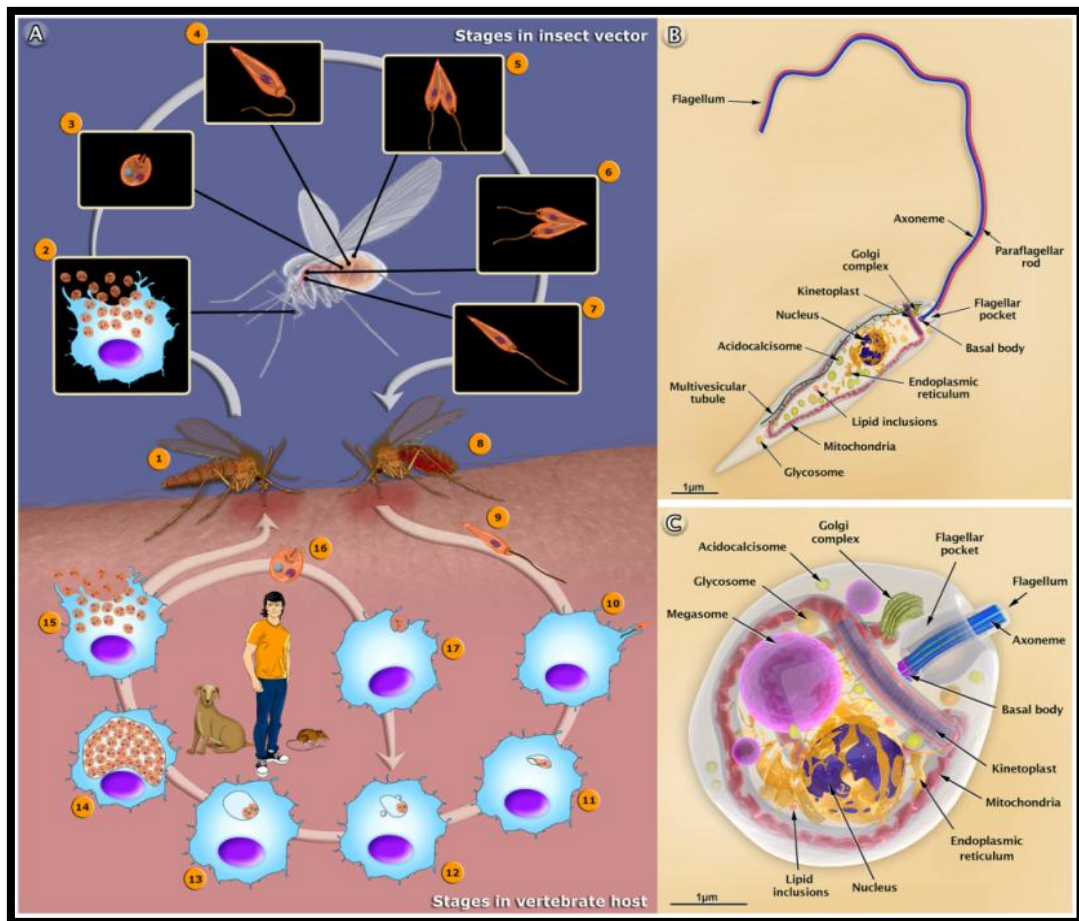


Fig 1.1: A) Life cycle of Leishmania B) Promastigote C) Amastigote

Source: <http://www.ncbi.nlm.nih.gov/pmc/articles/PMC3795027/pdf/ppat.1003594.pdf>

Life cycle:

An infected sand fly bites and injects the metacyclic promastigotes into the vertebrate host's skin (fig. 1.1 A). After the invasion, by phagocytosis, into the susceptible host cells consisting of the mononuclear phagocyte lineage (Monocytes, Macrophages, and Langerhans cells), the metacyclic promastigotes transform into amastigotes. The spleen, liver and the bone marrow accumulate the macrophages with parasites migrated from the skin. The phagosome and lysosome combine to form phagolysosome in the macrophages, within which promastigotes differentiate into amastigotes, influenced by the pH, temperature, and CO₂ (Freitas et al. 2012). In the phagocytic vacuole, the amastigotes develop and multiply by the binary fission. At some stage the cell ruptures and releases the free amastigote forms which start infecting the other cells. The sand fly saliva suppresses the host immune system by disrupting the antigen presentation, NO generation, and expression of co-stimulatory molecules and thus aggravates the disease (Loría-Cervera and Andrade-Narváez 2014). In the next bite of the sand fly, the infected cells are sucked into its gut. The sand flies obtain energy from sugar meals and this also helps the parasites to grow in their gut (Wheeler, Gluenz, and Gull 2011; WHO 2010).

In the sand fly, the parasite takes 8-20 days to complete its cycle. About four days after ingestion, the amastigotes reach lumen and move towards the stomodeal valve situated near the anterior midgut and secrete the promastigote secretion gel (PSG) which forms a plug and blocks the midgut and pharynx region. The amastigotes face adverse conditions, digestive enzymes and peritrophic matrix in the midgut. They bind to the midgut cells mediated by LPG, the major surface glycoconjugate, to avoid their excretion and for the protection from the enzymes. The amastigotes differentiate into several promastigote types denominated as per their form, as procyclic, haptomonad, nectomonad, promastigote, and metacyclic forms (Freitas et al. 2012). During the metacyclogenesis, a few changes like deflation of the body size, extension of the flagellum, increase in the motility occur in the amastigotes which replicate by the longitudinal binary fission and differentiate into the infective metacyclic promastigotes, which move towards the midgut's anterior portion and the sand fly's mouthparts to move on to next host and the cycle continues (fig.1.1 A) (Freitas et al. 2012).

1.4 Taxonomical Classification of *Leishmania*:

According to the monothetic Linnaean classification, the genus *Leishmania* is branched into

- (i) *Leishmania* - existent in the old and new world countries
- (ii) *Viannia* - narrowed only to the new world countries.

The genus *Leishmania* belongs to:

Phylum: Sarcomastigophora

Sub. Phylum: Mastigophora

Class: Zoomastigophora

Order: Kinetoplastida

Sub-order: Trypanosomatina

Family: Trypanosomatidae

To organize the *Leishmania* taxonomy, the iso-enzyme analysis is considered as the ‘gold standard’ till date, as it is a reliable indicator for bunches of geographical isolates in a species. The modern taxonomical procedures comprised of the rapid fragment length polymorphism (RFLP), the polymerase chain reaction (PCR) with a diversity of primers and monoclonal antibody (MAB) typing (WHO 2010). *Leishmania*’s detailed taxonomical classification is shown in fig.1.2.

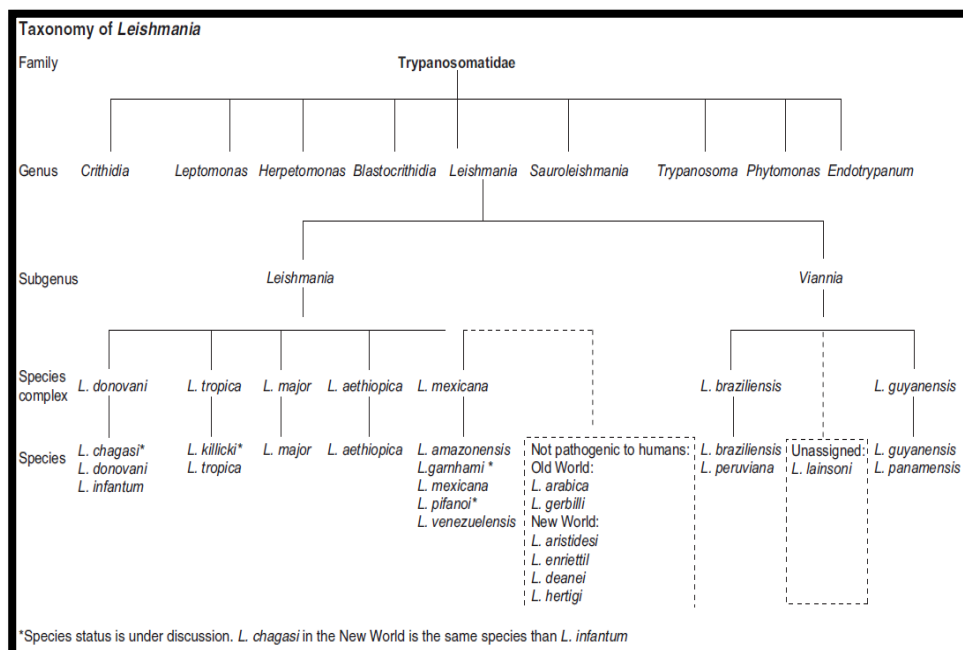


Fig 1.2: Taxonomy of *Leishmania* (WHO 2010)

1.5 Geographical Distribution:

The endemicity of Leishmaniasis is seen all over the world except the Arctic and Antarctic regions where neither the parasite nor the host can survive for long (fig.1.3 a). The confirmed VL cases have been declared in 66 countries, out of which 90% are from Bangladesh, Brazil, India, Nepal, and Sudan. Ninety percent of CL patients are from the African and South American continents. The HIV-*Leishmania* co-infection is reported in Spain, Italy, France and Portugal (Desjeux 1999) (fig.1.3 b). The changes in climate and environment decide the geographic reach of the vectors. The geographical distribution depends on the sand fly species, its ecology, and the parasite's internal developmental conditions. CL also occurred in the new world regions like Southern Europe, Mexico, Central and South America and in the old world regions like Africa, Asia, and the Middle East. Ninety percent of the infections are due to *L. major* and *L. aethiopica* in Syria, Algeria, Iran, Iraq, Afghanistan and Saudi Arabia (Ready et al. 2014; Reithinger et al. 2007; WHO 2010) (<https://en.wikipedia.org/wiki/Leishmaniasis>).

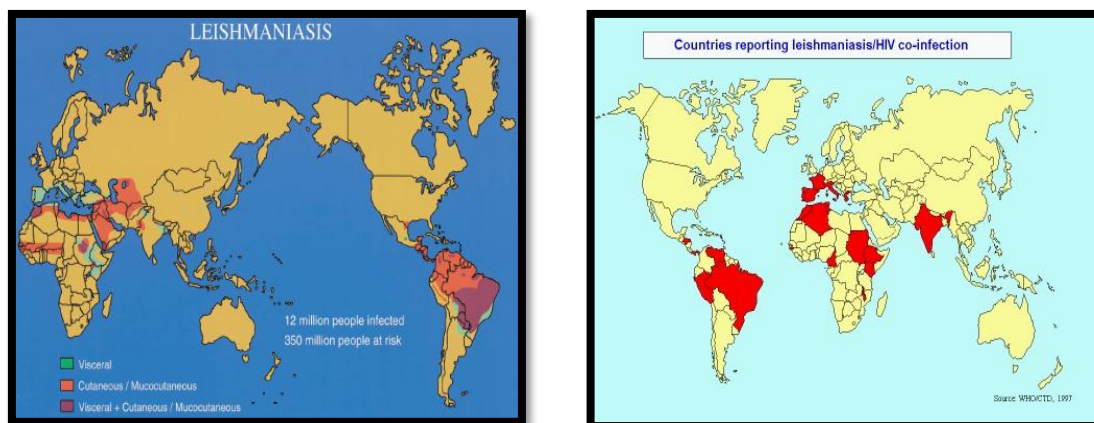


Fig1.3 (a) Prevalence of Leishmaniasis worldwide

(b) VL-HIV coinfecting areas

Source: (a) <http://www.emedmd.com/content/leishmaniasis>

(b) <http://web.stanford.edu/group/parasites/ParaSites2003/Leishmania/leish%20epi.html>

Leishmaniasis in India:

VL is endemic in Bihar, and thus is the 'Heartland of *Kala-Azar*' and the 'Hotspot of VL' (52 districts), West Bengal (eight districts), small pockets of Himachal Pradesh, Eastern U.P (two districts) and the North-Western part of India are the other endemic areas (fig. 1.4). In Bihar, 50% of the total VL burden of India is recorded, and 75% of the cases live below poverty line (BPL) earning less than one dollar per day. Between 1990 and 2008, 68,358 VL cases were reported in Muzaffarpur. In Bihar, only 1 in 8 cases are reported officially and about 20% of the death cases are undiagnosed. Nepal (12 districts),

Bangladesh (45 districts) and Bhutan are also affected by VL (Hasker et al. 2012; Varma and Naseem 2010; WHO 2010).

The Post *kala-azar* dermal leishmaniasis (PKDL) was illustrated in 1922 by Brahmachari. In the skin of cured VL patients, he confirmed erupted plaques as LD bodies in the slit skin smear and termed it as dermal leishmanoid. Swaminathan, Shortt, and Anderson demonstrated in the 1940s that *L. donovani* and *L. tropica* (presumably *L. major*) are transmitted by the sand flies of phlebotomine. In the 1950s during the malaria eradication programme in the Ganges-Brahmaputra basin, the epidemic anthroponotic VL almost disappeared but later reappeared in the 1970s and remains till date.

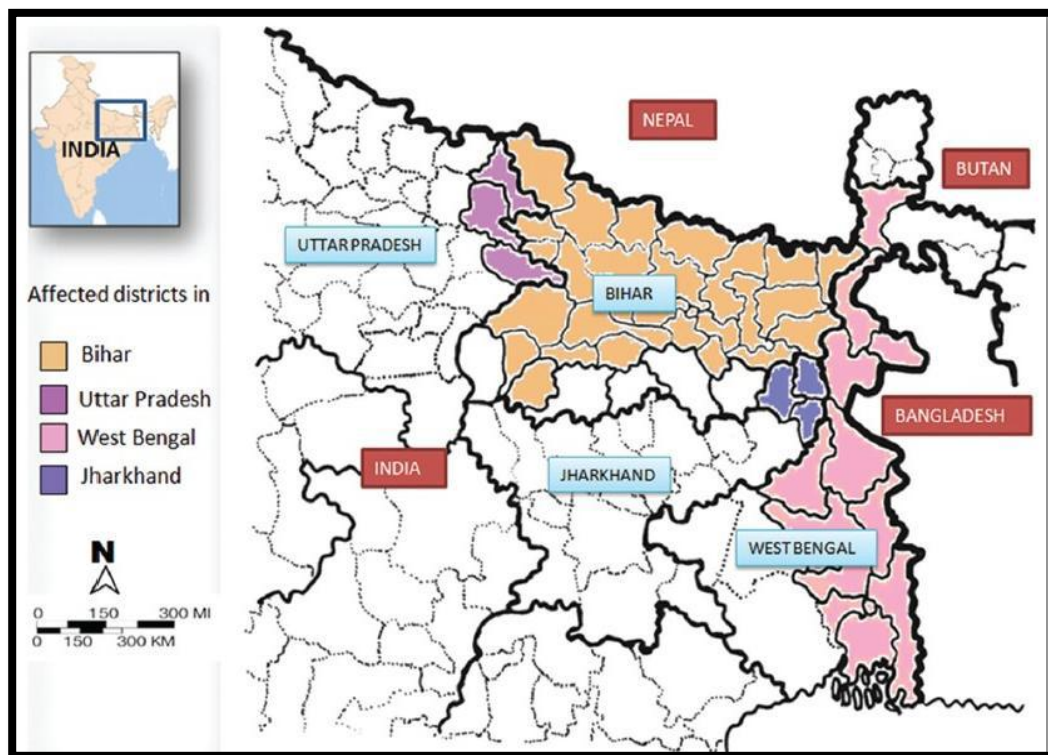


Fig 1.4: Prevalence of Leishmaniasis in Indian subcontinent

Source: http://www.tropicalparasitology.org/viewimage.asp?img=TropParasitol_2014_4_1_10_129143_u1.jpg

Epidemiology and ecology:

Leishmaniasis mostly occurs in the African, South American, and Asian continents. It has not been reported from the Australia and Antarctica. The regions with an altitude less than 600 m above the sea level, relative humidity greater than 70%, heavy rainfall, temperatures ranging between 38°C and 15°C with less than 7°C change during the day, abundant vegetation, alluvial soil with subsoil water, human habitations with thatched roofs, earthen floors and mud walls with livestock nearby are the most favourable conditions for the sand fly survival and the disease transmission. The sand flies are seen in the cattle sheds taking

the blood meal from the cattle and humans. Sleeping under the acacia trees or on the ground during the hot season, increase the risk of infection. The migration during the drought, famine, floods and the cross-border movements across the Indo-Nepal border spread the disease, and these factors contribute to about 40% of the cases in these regions (Quinnell and Courtenay 2009).

VL is also a poverty-related disease. The dwelling of a large number of people in small congested areas and poor sanitary conditions like open sewerage and improper waste disposal etc., attract the sand flies. The anthropogenic events like urbanization, the occupation of forest areas and their conversion to agricultural farms and settlements, incorporation of the sand-fly mediated transmission cycle into the human dwellings increase the chances of occurrence of the disease. The highest rate of infection is seen in the people dwelling at the perimeter of the natural convergence points like the forests, deserts etc., which are nearer to the wild flora and fauna. Further, malnutrition which generally is associated with the poverty contributes to VL. The disease occurs in the individuals who take diets that contain low amounts of proteins, vitamin A, iron, and zinc (Quinnell and Courtenay 2009).

VL is a climate-related disease. The host and the vector population size, dispersal and the ability to survive are determined by the distortions in humidity, rainfall, and temperature. A temperature change affects the parasite's life cycle within the sand fly and favors its transmission into the unaffected areas. The other rare routes of transmission for VL are the venereal transmission, blood transfusion, congenital transmission and through partaking of syringes by the intravenous route among drug addicts (Quinnell and Courtenay 2009).

The patients with the HIV-VL co-infection exhibit great load of the parasite, which sometimes includes the drug-resistant strains and can spread the infection. These patients act as the effective infection reservoirs and cannot be cured as they have the CD4⁺ counts less than 200 cells/ μ l and the antileishmanial drugs do not show any effect on them. In the areas of VL-HIV co-endemicity there could be a disaster at any time but in the Indian subcontinent, where the two focal points do not really lap over (as VL occurs in the rural and HIV in the urban), the extreme effects have not been reported till date (Desjeux 1999). A careful monitoring of the situation is very essential as it is swiftly changing. The peri-domestic sand flies have been controlled with the insecticide spraying for mosquito

control. The use of impregnated bed nets has affected the transmission in some areas. The organized killing of dogs can be substituted by an efficient vaccination programme. The dogs can be safeguarded from 96% of the sand fly bites by using the impregnated collars. Since 2005, the eradication programme is being implemented in Bangladesh, India, and Nepal with an aim to limit VL cases to less than 1 in 10,000 by the year 2015 (Ready et.al. 2014; WHO 2010).

Vectors for Leishmaniasis:



Fig 1.5: (a) *Lutzomyia longipalpis*

(b) *Phlebotomus argentipes*

Source: http://www.raywilsonbirdphotography.co.uk/Galleries/Invertebrates/vectors/sand_fly.html

The sand flies (Order: Diptera, Class: Insecta, Family: Psychodidae Phylum: Arthropoda) are the vectors which transmit the disease. The specific vectors are specific only to one particular species of *Leishmania*, whereas the permissive vectors can harbor many species. Only 93 out of 800 sand fly species are proven vectors. *Phlebotomus* sand flies in the old world countries and *Lutzomyia* sand flies in the new world countries infect the humans. The best studied species are *Lutzomyia longipalpis* (fig. 1.5 a) and *Phlebotomus argentipes* (fig. 1.5 b). The sand flies dwell in cool, humid niches, breed in the cattle sheds, and lays eggs on the water surface. The female sand flies transmit the disease as they have well developed sharp proboscis to perforate the skin. The male sand flies cannot transmit the disease as their mouth parts are suitable only to suck plant juices. The male flies call female flies for mating by their characteristic ‘songs’ from their vibrating wings and pheromones. The female sand flies lay about 200 eggs on the water surface but the larvae and pupae stages are not aquatic. The eggs usually hatch within 7-10 days in the laboratory conditions. Then the larva develops. After three weeks, the pupa develops from which the adult flies emerge after 10 days. It is difficult to control the female sand fly population by spraying insecticides as they are found outdoors, whereas the male population can be controlled as they are found indoors. The exact lifetime of the sand-fly is not known. The data obtained in the lab may not reflect the actual time in nature. They fly at a speed of 1

m/s which is below the speed of the mosquitoes, and this limits their dispersal range (Oliveira and de Oliveira 2013; Volf and Volfova 2011; WHO 2010).

1.6 Manifestations of Leishmaniasis:

The Leishmaniasis manifests mainly in four forms and the symptoms are illustrated in fig. 1.6.

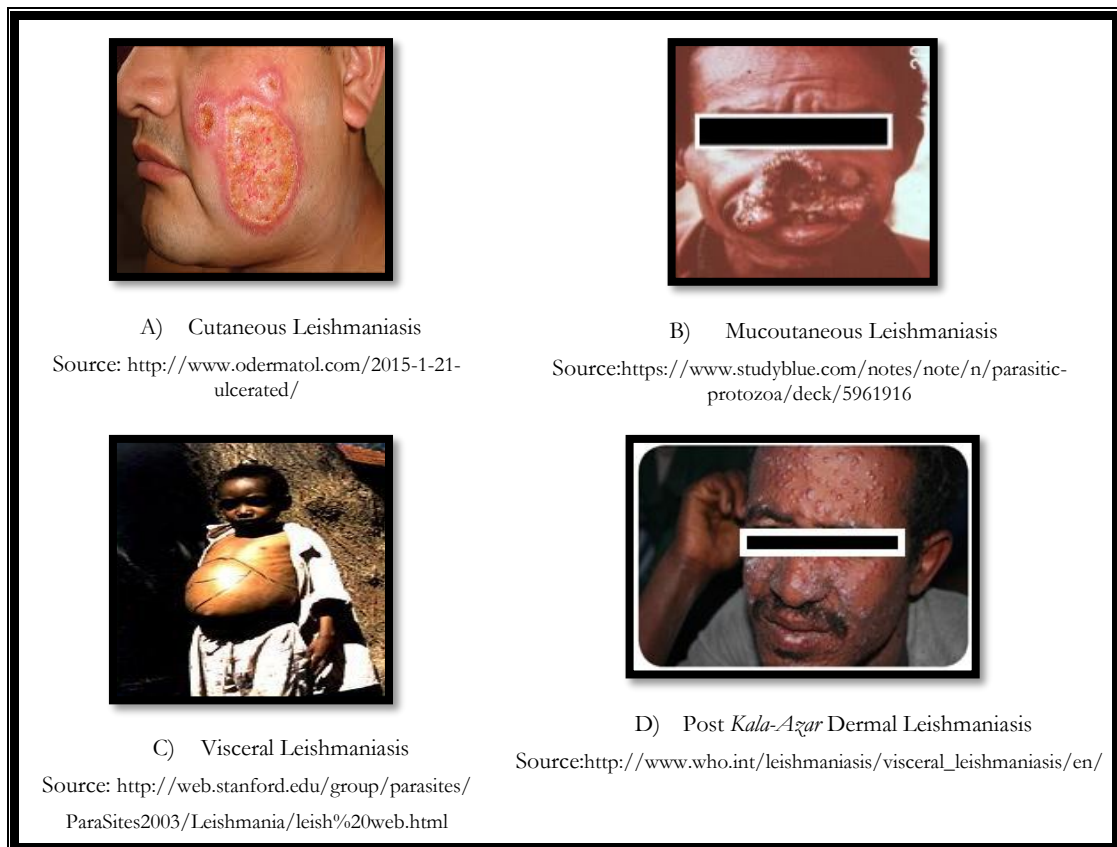


Fig 1.6: Different forms of Leishmaniasis

Cutaneous Leishmaniasis (CL):

CL is triggered by *L. infantum*, *L. tropica*, *L. major*, *L. aethiopica* and *L. donovani* in the old world countries and by *L. Mexicana*, *L. braziliensis*, *L. panamensis*, *L. guyanensis* and *L. peruviana* in the new world countries. It is also called as "Delhi boil, Kandahar sore and Lahore sore". The progress of ulcerative skin lesions with innumerable parasites is the hallmark of CL.

The lesions develop all over the body but typically arise at the infection spot, as a macule, papule or nodule that grows slowly and reaches its peak size in a week. Centrally a crust evolves and exposes an ulcer with a raised edge which meliorates gradually leaving a blister

with refashioned pigmentation. These multiple painless dry ulcers on the skin can evolve after weeks, months or years of the primary infection. Lymphadenitis occurs with the involvement of the lymphatic system. The malady is destructive and disfiguring if left unattended. The oronasal complications occur which distort the nostrils and lips. The spontaneous healing might take place within two to five years leaving a long-lasting ugly scar. CL is similar to the other infectious diseases and cancers, so misdiagnosis and delay in the treatment occur. Some rare cases aggravate to disseminated CL where diffuse, non-ulcerated, non-healing nodular lesions occur which return after the treatment and spread to the entire body with remnant ugly scars leading to death. DCL occurs through *L. mexicana*, *L. amazonensis*, in the South America and *L. aethiopica* in the East Africa and is associated with the HIV co-infection (Reithinger et al. 2007; Vries, Reedijk, and Schallig 2015; WHO 2010)(fig 1.6 A).

Mucocutaneous Leishmaniasis (MCL):

MCL is induced by, *L. major*, *L. infantum*, and *L. donovani* in the immunosuppressed patients in the old world countries and by *L. panamensis*, *L. guyanensis* and *L. braziliensis* in the new world countries (Desjeux 1996). It is called as 'Espundia' in the South America. The mouth and upper respiratory tract mucosal tissues are severely affected with the lymphatic or blood born spreading. After the occurrence of the cutaneous lesion, MCL can manifest from few months to years. The risk group includes mostly adult malnourished men. The Pharynx, palate, larynx, trachea, upper lip, skin on the nose get deformed with lymphadenopathy. The secondary bacterial infections like pneumonia are common. It never heals spontaneously. Severe adversities occur in the patients and are rejected by the society because of their ugly look, and they finally, die due to bronchopneumonia or malnutrition (Goto and Lauletta Lindoso 2012; WHO 2010) (fig 1.6 B) .

Visceral Leishmaniasis (VL):

VL is an infection of the reticulo-endothelial system due to *L. donovani* in India and Africa, *L. infantum* in the Middle East and a few other regions of Asia and *L. chagasi* in the South America. Malnutrition and immune suppression lead to the clinical manifestations. It may be regional, scattered or epidemic with high fatality rate. In India, VL is chronic, infecting infants and youth. The males experience greater threat than the females. The darkening of the skin is observed (*Kala-Azar* - black fever). The common symptoms are fever with chills, drenching sweats and shivering, rapid reduction in weight, profound malaise,

anorexia and uneasiness in the left hypochondrium, hepatomegaly, splenomegaly, and lymphadenopathy. With the progression of the disease, edema, skin and changes in the hair indicating malnutrition are fostered. The complications of severe acute haemolytic anemia, leucopenia, thrombocytopenia, pancytopenia, hemophagocytosis and disseminated intravascular coagulation and hyper-gammaglobinemia, acute renal damage and mucosal hemorrhage can occur. It occurs to non-local people or travelers of any age entering into the endemic areas. The mortality is usually high in acute forms. The risk factors include malnutrition, genetic predisposition, and co-infection due to the other opportunistic pathogens causing the infectious diseases like HIV, Tuberculosis etc. VL is fatal if left untreated within two years of the first appearance of symptoms (Faleiro et al. 2014; Varma and Naseem 2010; WHO 2010) (fig 1.6 C).

Post *Kala-Azar* Dermal Leishmaniasis (PKDL):

The PKDL is an aggravation of VL with peculiar nodules, macules, or maculopapular rashes especially on the face in VL recovered patients. The macules often look like lesions of vitiligo or leprosy. Buccal, genital mucosa and conjunctiva might also get affected. The PKDL emerges after an effective cure from VL and is caused by the immune suppression in the skin to the remaining parasites. The PKDL is seen in India where 10% - 20% of the cases progress within the two to three years of VL treatment, denoted by the gradual enlargement of the facial nodules and dermal black patches instead of ulcers, but the frequency is slowly descending. Apart from causing PKDL in the old world countries, *L. tropica*, *L. donovani*, and *L. infantum* rarely may also produce abnormal viscerotropic disease. *L. chagasi* causes PKDL in the new world countries. The PKDL may appear somewhere between two years to a few decades after VL treatment. A previous history of VL is not necessary for this disease. The PKDL patients serve as the parasite reservoirs and are of epidemiological importance (Faleiro et al. 2014; Ramesh, Singh, and Salotra 2007; WHO 2010; Zijlstra et al. 2003)(fig 1.6 D).

1.7 Hosts for Leishmaniasis:

In Leishmaniasis, the zoonotic infection occurs through the animals and the anthroponotic infection through the humans. The ecosystem in which the *Leishmania* species survive is made of the sand fly vectors and the vertebrate reservoir hosts. Generally, for a given *Leishmania* species, one principal reservoir host exists in a particular focus, but other mammals may get infected, and become the minor and incidental hosts. The response

shown by the infected animals is hard to detect and the symptoms are unnoticeable. VL and CL in the humans are due to *L. donovani* and *L. tropica* respectively. The status of some hosts like fox, jackal, badger, rat, and cat has not been fully established in maintaining the *L. infantum* foci. The domestic cat may be hosting *L. infantum*. VL in dogs is due to *L. infantum*, which are easily available for the sand fly to pick as the viscera and dermis layers of the skin lodge a large number of parasites. *L. panamensis* and *L. peruviana* can also infect the dogs. The transmission of parasites can occur from dog to dog both in the domestic and wild environments. In the Americas, domestic equines like donkeys, mules, and horses are infected by *L. braziliensis*. Both in the old and new world countries, *L. infantum* is found to be infecting wild canine species like fox, jackal, wolf, raccoon dog which acquire the infection from the village dogs. *L. major* in the Central Asian arid regions infects great gerbils. *L. aethiopica* in the East Africa, Namibia and *L. tropica* in the Northern Israel and Saudi Arabia infect hyraxes. *L. guyanensis* in the Brazil and French Guiana infect sloths and anteaters which are nomadic and arboreal and spread the parasite. *L. guyanensis*, *L. mexicana*, and *L. amazonensis* can infect the rodents (WHO 2010).

1.8 Diagnosis of Leishmaniasis:

Observing the amastigotes in the patient-derived splenic aspirates and the skin lesions under the microscope were the original 'gold standard' diagnosis techniques for leishmaniasis. In the 1970s, indirect fluorescent antibody test (IFAT) and Enzyme-Linked Immunosorbent Assay (ELISA) were introduced. In the 1980s, direct agglutination test (DAT) was introduced. In the mid-1990s, immunochromatographic strip test (ICT) was introduced, in which a cloned recombinant K39 antigen (rK39) was detected by the dipstick test. The ICT does not need a laboratory and can be used in the field conditions. In the 1990s, using the PCR, the kinetoplast DNA was detected which was more sensitive and was useful for the diagnosis of species in the tissue specimens and blood. The series of events in the diagnosis of VL are as follows:

- (i) Suspicion based on the clinical features like long-term fever and hepatosplenomegaly, which is the hall mark symptom of VL;
- (ii) Observing the amastigotes from the patient-derived samples like lymph nodes, bone marrow or splenic aspirates under the microscope and later culturing them;
- (iii) Detection based on the immunological tests;
- (iv) Detection at the molecular level using the PCR.

The external and few internal features of VL resemble any of the other systemic infectious diseases like chronic malaria, schistosomiasis etc. Hence the diagnosis is challenging and the confirmation requires *Leishmania*-specific laboratory tests. The *Leishmania* promastigotes in a formalin suspension are used as antigens in the delayed-type hypersensitivity response called the Montenegro skin test. A positive response indicates the CMI whereas a negative response which is observed in an active VL and assumed to be lifelong turns positive after cure and can revert to negative any time. A higher positivity rate is seen in grownups when compared to infants and develops with age in the endemic areas. The classical 'gold standard' confirmatory test for VL is the visualization of amastigotes in the tissue aspirates under a microscope whose sensitivity is 93–99% for the spleen, 53–86% for the bone marrow and 53–65% for the lymph node aspirates but its specificity is high. The drawbacks of microscopy are its invasiveness, poor sensitivity, and unsuitability in the field conditions (Savoia 2015; Singh 2006a; WHO 2010).

The serological tests like IFAT, ELISA or western blotting (WB) are advantageous and have better accuracy but cannot be adapted to the field settings as they can be performed only in the laboratory. As VL occurs among the poor people who live in remote areas, the diagnostic tests should be cheap and suitable for the field conditions like DAT and rK39 antigen-based ICTs. The rK39 based tests being cheap, easy to do, and reproducible, can be used for the early detection. The Latex agglutination test (LAT) which recognizes a heat stable carbohydrate antigen from the patient's urine, has better specificity and moderate sensitivity in the Indian subcontinent. The serological tests suffer from the drawbacks like detection of specific antibodies much longer after cure making the relapse un-diagnosable. Due to the asymptomatic infections, other healthy individuals from the endemic regions with no VL antiquity are detected positive for the antileishmanial antibodies. A problem of possible cross-reactivity with other pathogens like *T. cruzi*, *Mycobacteria*, and the other *Leishmania* species remains. The current, subclinical and past infections are not properly detected by the most serological tests. In the VL-HIV patients' diagnosis by the serological tests is very poor. The quality standards for the diagnostics should be regulated by the government authorities as a number of fake ICTs can be seen in India. The PCR based recognition of *Leishmania* DNA in the patient's blood or bone marrow aspirates is even more quick to detect, but it is found only in the referral hospitals and research centers (Faleiro et al. 2014; Singh 2006b; Tavares, Fernandes, and Melo 2003; WHO 2010).

The rK39 antigen-based ICT is used in the primary care centers and hospitals in rural areas of highly endemic regions. In the district or higher level health facility, the parasitological diagnosis is performed to detect a relapse of VL. The diagnostic tests like PCR and microscopy are required which are more specific in some cases. In the VL-HIV patients, the treatment options and prognosis differ, so all VL patients should be screened for HIV. The other opportunistic infections are also present in them which make the clinical diagnosis more difficult. As the parasite load is advanced in the VL-HIV patients, the diagnosis by microscopy, culturing of parasites, PCR of blood, or bone marrow aspirates is easier to detect than in the immunocompetent individuals. The antigen can be detected in their urine by a highly sensitive LAT (Faleiro et al. 2014; WHO 2010).

1.9 Pathogenesis of Visceral Leishmaniasis:

The host innate and adaptive immune responses regulate the infection. The cell-mediated immunity (CMI) nullifies the infection but the disease worsens when T-cells stop responding to the parasite antigens. The importance of host-specific CMI response against VL is best seen during its disruption in the malnutrition and immunosuppressive conditions like HIV. The clinical manifestation depends on aspects like childhood, deficient IFN- γ cytokines, polymorphism in TNF- α promoter gene and IL-4 coding gene etc. The IL-10 producing CD25⁻T cells are mainly involved in the pathogenesis. The first cells to reach the infection site are the neutrophils and the natural killer (NK) cells influence the course of infection and disease. A blend of Th1 and Th2 immune response is seen in the human VL. The infection primarily affects the liver, spleen, bone marrow and lymph nodes. High load of amastigotes in the bone marrow is observed in the macrophages, neutrophil and eosinophil granulocytes. Granulocytopenia, thrombocytopenia, anemia, and hypoalbuminemia occur. Diarrhea, pneumonia, dysentery and TB cause death in the advanced stages of the disease. The advancement of the disease is related to the absence of lymphocyte proliferation and the IFN γ production. After the treatment the IFN γ , IL-12 increase and the IL-10, TGF- β decrease. The number of CD4⁺CD25⁺ T cells also increase during the active VL and decrease during cure (Faleiro et al. 2014; Nylén and Sacks 2007; WHO 2010).

1.10 Parasites in Host Macrophage:

The parasite contacts, recognizes, binds to the receptors, enters, and then survives in the host cell. Two major parasite surface molecules, the promastigote surface protease (PSP

or 'gp63') and LPG, and a diversity of receptors in the host cell like mannose fucose receptor, CD18 integrins, fibronectin receptor etc., have been identified. The amastigotes survive in the phagolysosomal vacuoles in the host macrophages by adopting escape mechanisms like –

- (i) The presence of active H⁺ pumps to face pH fluctuations;
- (ii) The existence of protective surface molecules like nucleosidase, LPG, gp63 capable of digesting the host enzymes;
- (iii) The ability of silent entry into the host cells;
- (iv) The ability to inhibit the macrophage inducible nitric oxide synthase (iNOS) and in turn the nitric oxide (NO) generation in response to interferon γ (IFN γ);
- (v) The ability to inhibit the phagolysosomal fusion.

The dermal langerhans or dendritic cells are best suited cells for the metacyclic promastigotes to infect and survive. The proliferation and dispersal into the other tissues occur when they are in the macrophages and monocytes. The cytokines are important in deciding the permissiveness of cells to the infection. *Leishmania* influences the cytokine environment by impairing tumor necrosis factor- α (TNF α) or interleukin-12 (IL-12) production or by inducing the production of transforming growth factor β (TGF β) and IL-10 which down-regulate the Th1 response. The resistance or susceptibility is dictated by the host's genetic aspects and its immunity. *Lsh* gene, recently renamed *Wmp1* or 'natural resistance associated macrophage protein' gene is responsible for controlling the preliminary phases of the susceptibility or resistance, whereas the major histocompatibility complex (MHC) controls the subsequent events involving the immune mechanisms. The genetic factors in humans, which make them susceptible to the disease are being probed into, but the proof for the pathological control by the genetic factors of the host has not been found in VL (Faleiro et al. 2014; Handman and Bullen 2002). The pathophysiology of VL in the humans has many unanswered questions:

- (i) Why does the disease not manifest symptoms in many patients for prolonged durations and establish as a clinical form in only a few individuals?
- (ii) Why the disease does occur many times only in infants or youngsters? (80% of VL cases occur in infants of 10 years or below)
- (iii) Why are men predominantly affected than women? (6:1 ratio in India)
- (iv) Which factors other than malnutrition, stress, and immunosuppression caused VL?

(v) Why is PKDL established in a few VL treated patients after considerable time interval?

1.11 Immune Responses in Visceral Leishmaniasis:

Innate Immunity:

The Innate immunity is the primary protective response mediated by the lymphocytes, NK cells, phagocytes, and the dendritic cells (DCs) that restrain the parasite infection, replication and produce the immunoregulatory cytokines. *Leishmania*, being an opportunistic pathogen, hijacks many host factors for its intracellular survival. After entering the skin, it is phagocytosed by the host DCs and macrophages. The neutrophilic and eosinophilic granulocytes accumulate locally to show inflammation which clears injured tissue and inflammatory macrophages start healing the wound. The complement protein C3b, a potent immune opsonin, binds to the *Leishmania* gp63 and converts into iC3b, the inactive form, which helps in the pathogen clearance by phagocytosis rather than lysis. Various chemokines like the monocyte chemotactic protein (MCP), induced protein (IP)-10, and lymphotactin, also activate the NK cells. The FasL-mediated apoptosis in the infected macrophages is another remarkable attribute of the innate immunity. In the first 16-24 hours of infection the lymph node cells, B cells increase and the CD4⁺ cells decrease. The DCs which play a key role in the innate immunity are classified as myeloid (mDC) and plasmacytoid (pDC). The IL-12, via TLR-9 signaling, is produced by the myeloid DCs. The NK cells which generate IFN- γ , show their impact on IL-12 which kills the parasite. Even though pDCs are unable to show phagocytosis property they produce IL-12. The active VL patients show low IL-8 and Th2 response distinguished by increased IL-4⁺ neutrophils and IL-10⁺ eosinophils and diminished IFN γ ⁺ and IL-12⁺ eosinophils (Liew and O'Donnell 1993; H W Murray and Nathan 1999).

Adaptive Immunity:

For the efficient elimination of the pathogens, the protective immune response needs a presentation of the antigens by APCs, active CD4⁺ Th1 cells, and the macrophages. The Th1 cells initiate cytotoxic CD8⁺ T cells, NK cells, and macrophages. The Th2 cells activate eosinophils and induce the B cells to produce antibodies. The CD8⁺ T cells produce the same cytokines for Th1 and Th2 cells which work in feedback association i.e., they can reciprocally inhibit each other's activity. The polarization towards Th1 or Th2 is itself influenced by the early cytokines. The IFN- γ , IL-12 favors Th1 response whereas the IL-4, IL-10 favors Th2 response. The CMI by Th1 cells is through secretion of the IL-12,

a potent immune activating cytokine, by the macrophages and DCs. The B lymphocytes start generating antibodies once they are incited by the immune cytokines secreted by Th2 cells. The TGF- β , an immune cytokine which induces IgA antibody dissemination, Th2 response and Th1 inhibition is secreted by Th3 cells. The active VL shows a hike in the TGF- β mRNA levels and the plasma concentration. The cathepsin-B, a parasite cysteine protease, triggers TGF- β which decreases the NO production by the host macrophages. The release of IL-12 by the macrophages is shut off by TGF- β and IL-10. The IFN- γ inhibits release of IL-10. The deprivation of Th1 response makes the host more susceptible to VL than the presence of Th2 response. The raised titers of proinflammatory cytokines and chemokines like IL-1, IL-4, IL-6, IL-8, IL-10, IL-12, IL-13, IL-15, IFN γ , monokines induced by IFN γ , and TNF α , which are indicators of the authoritative Th2 response are common in VL. During the chronic disease, IL-10, a crucial immunosuppressive cytokine, evokes harmful inflammatory responses like disruption of the antigen presentation in the macrophages and DCs, T cell initiation and cytokine generation which favor constancy of the parasite in the host. The bone marrow, lymph nodes, and spleen tissue show a hike in the serum IL-10 concentration and mRNA levels in the VL patients. But there is no direct evidence that IL-10 retardation advocates the parasite evacuation. The plasma antibodies form an immune complex and attach to the Fc receptors on the host macrophages which triggers the IL-10 production and benefits the parasite (Faleiro et al. 2014; Gautam et al. 2011; Liew and O'Donnell 1993).

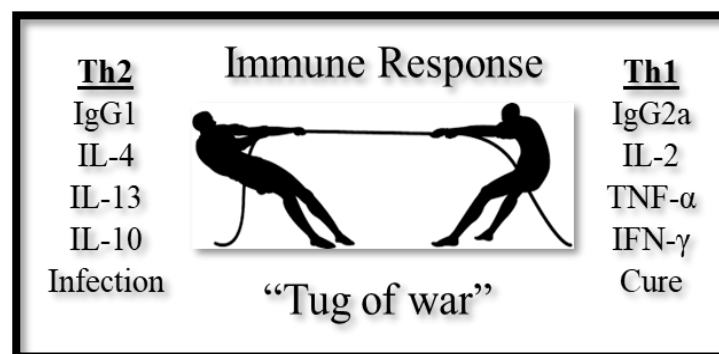


Fig 1.7 The Resistance or susceptibility to disease is decided by the tug of war between cytokines

At the early stages of infection, the low IFN- γ drives the disease progression while the high IFN- γ protects. The IFN- γ mediated activation of macrophages to generate toxic NO through augmented NOS expression and a Th1 response can eliminate the pathogen and diminish the infection. The NO pathway is a common channel to kill *Leishmania*. The

TNF- α and IFN- γ activate infected macrophages to produce ROIs, RNIs, and NO to kill the intracellular amastigotes. The NOS which occurs as the constitutive i.e. cNOS found in many cells and the inducible i.e. iNOS found only in the activated macrophages generates the NO from L-arginine by the oxidative deamination reaction. The suppression of parasite DNA synthesis and respiration through the inhibition of Fe-containing enzymes is the general mechanism in which the NO and its other free radicals like NO² and OH[•] show their potent antimicrobial activity. In the infected macrophages, IFN- γ , TNF- α , and MIF induce NOS whereas IL-3, IL-4, TGF- β , and IL-10 hinder its expression. So the Th1 response favors and the Th2 response inhibits NO. The parasite induces arginase enzyme which acts on the NO and cleverly escapes the iNOS dependent killing in the host macrophages. The parasite containing the polymorphonuclear leukocytes show oxidative burst to eliminate the infection.

The antigen-specific antibodies are produced through the humoral response. The *Leishmania* antigen-specific IgG, IgM, and IgE are elevated in the active VL. A high IL-10 and low IFN- γ along with high IgG1 and IgG3 are seen in VL patients. During the CMI, T-cells produce different cytokines. The *Leishmania*-specific antigens bind to the lymphocytes and make them incompetent to produce cytokines. Both the CD4⁺ effector T-cells and the CD8⁺ memory T-cells safeguard the host. The CD4⁺ cells are involved in the hepatic granuloma formation initially but are later restored by the CD8⁺ cells. The enzymes like granzyme, granulysin, and perforin, secreted by the CD8⁺ cells lyse the macrophages infected with the parasites. The resistance or susceptibility is decided by the 'Tug of War' between Th1 cytokines (IFN- γ , IL-2, TNF- α , and IL-12) and Th2 cytokines (IL-4, IL-5, IL-6, and IL-10) (fig 1.7). The IL-12 and NK cell-mediated differentiation of Th cells to Th1 cells is performed by the IFN- γ , a strong macrophage activator. So the protection is mediated by the Th1 polarization and the IFN- γ generation. The CD4⁺CD25⁺ regulatory T-cells are activated by IL-10. The successful treatment lowers the IFN- γ , IL-4, IL-10 and IL-13 levels which are usually found to be high during VL. The resistance of infection is suppressed by the neutralization of IL-2, which does not affect the granuloma formation. The IL-10 or IL-12 levels decide the bend of immunity towards the pathogen or protection. The IL-10⁺ IFN γ ⁺ producing antigen-specific T cells mediate reoccurrence of the disease. The IL-4, a Th2 cytokine, is usually affiliated with the hampered treatment (Faleiro et al. 2014; H. Goto and Lindoso 2004).

1.12 Chemotherapy against Leishmaniasis and Treatment Options for VL:

Pentavalent antimonials, AmB, Liposomal AmB, Pentamidine, Miltefosine, and Paromomycin are few drugs for leishmaniasis. A detailed note on the Chemotherapy against Leishmaniasis has been given under the review of literature section.

An ideal drug should cure the patient; for VL in particular, it should diminish the danger of relapse, transmittal of the resistant parasites and the occurrence of PKDL. The standard first-line VL drugs are pentavalent antimonials from the past 70 years. AmB deoxycholate and Pentamidine are the second-line drugs. AmB lipid formulations, Miltefosine and Paromomycin are being used from the past 10 years. Malnutrition, renal and hepatic complications, collateral infections like pneumonia, TB, HIV and other immune-compromising conditions hamper treatment. After the successful treatment, the general condition of the patient improves, fever resolves, splenomegaly regresses and the blood count comes to normal. The absence of clinical relapse even after six months indicates a definitive cure. However, the resistance to the drugs is of extreme concern in Bihar, and Nepal. The threat of congenital transmission is more hazardous than the drug adverse effects. AmB deoxycholate, and its lipid formulations are the best drugs to treat VL. The detrimental conditions like abortions or vertical transmissions are not reported in case of liposomal AmB. The risk of abortion and premature delivery in the pregnant mothers prevails due to pentavalent antimonials. Paromomycin has risk of ototoxicity. Pentamidine is inadvisable during initial three months of pregnancy. Miltefosine being likely fetocidal and teratogenic is advised to discontinue during the pregnancy. The expected mothers need to be evaluated for pregnancy before the chemotherapy and avail efficacious birth-preventive pills for a minimum of three months after the therapy. As VL itself decreases CD4⁺ cell count, the HIV-VL patients have a much lower CD4⁺ count and high parasite loads. So it is extremely difficult to cure them. Extensive mortality rate, adverse effects of chemotherapy, low clinical response, and high recurrence rate are common in them. The antimonials are more toxic in the HIV patients. The first drugs to be tried are AmB and its lipid formulations (Faleiro et al. 2014; Tiunan et al. 2011; WHO 2010).

1.13 Vaccines for Leishmaniasis:

There is no vaccine for Leishmaniasis. The rehabilitation from infection is followed by a strong immune response. The protection from *L. major* infection was demonstrated earlier through the Leishmanization process, where the live virulent promastigotes from a fresh

culture were administered through an *i.d* injection. The whole killed parasites or extracts were used in the first-generation candidate vaccines.

Till date, three vaccines have been tested namely, Mayrink vaccine, Convit vaccine, and Razi Institute vaccine. The Mayrink vaccine is *L. amazonensis* based vaccine obtained from the previous pentavalent vaccine in Brazil followed by parasite alone. The Convit vaccine from Venezuela is an inoculation of *L. mexicana* with the BCG (Bacillus Calmette–Guérin). The Razi Institute vaccine from Iran is an inoculation of *L. major* with the BCG. The second generation vaccines were made out of the recombinant proteins and the genetic vaccines. A combination of adjuvants and antigens can protect the experimental animals. The ‘Leish-111f + MPL-SE’ vaccine is under clinical trials. The protective response against the live challenge in the mice was shown by Genetically Modified (GM) *Leishmania* that causes little disease or infection. The method of stimulating immune response during the chemotherapy is used which is important in the recovery of patients (WHO 2010).

VL has been neglected in terms of vaccination as a solid proof of acquired protective immunity in humans after recovery from the VL is lacking. Moreover, a majority of human infections remain sub-clinical or asymptomatic, and there is no reliable laboratory animal model resembling the human disease.

Three types of vaccines are currently being developed which are (i) live-attenuated or heat-killed parasite vaccines (ii) vaccines with the GM parasites, recombinant proteins generated by virus or bacteria and subunit vaccines (iii) vaccines with the plasmid DNA and immunogenic proteins generated by the virus. An incomplete knowledge about the pathogen inhibitory immune mechanism has been one of the serious obstacles for generating vaccines for VL. The present knowledge of host immune response during VL comes from the mice models as complicated invasive techniques are needed in the humans (Faleiro et al. 2014). The vaccines are safer, cost much less than the chemotherapy, and do not show any adverse effects. The immunomodulators can have therapeutic role hereafter but presently they are not in use (Jain and Jain 2015; Kumar and Engwerda 2014; Modabber 2010; WHO 2010).

1.14 Different Approaches for Novel Antileishmanial Compounds:

The emergence of resistance to standard antileishmanial drugs along with problems associated with the treatment of immunosuppressed patients in whom drugs do not work

well have provoked the interest in developing novel antileishmanial drugs and new methods of treatment in following approaches:

- (i) Better knowledge of *Leishmania* biochemistry and the identification of unique metabolic pathways will be helpful in identifying novel drugs;
- (ii) A systematic search for the antileishmanial compounds from the natural sources;
- (iii) Further development of some promising compounds identified earlier;
- (iv) Using immunotherapy along with the chemotherapy.

Chapter II

Review of Literature

2.1 Chemotherapy against Leishmaniasis- a review:

In 1912, Vianna introduced the trivalent antimonials for the treatment of CL and MCL in Brazil. In 1915, Di Cristina and Caronia introduced them for VL in Italy. In 1922, Brahmachari introduced the first safer pentavalent antimonial, urea stibamine, which remained the first option to treat leishmaniasis. During the 1980s in Bihar, clinical isolates proved resistant to antimonials as VL cases failed to respond to the treatment. The conventional drugs like pentavalent antimonials, AmB, and pentamidine had high toxicity, high cost and drug resistance. The Liposomal AmB (1996), Miltefosine (2004) and Paromomycin (2006) were registered for VL. The immediate necessity for safe, effective drugs will lead to the discovery of new compounds (WHO 2010).

Pentavalent Antimonials:

Meglumine antimoniate as Glucantime[®] and sodium stibogluconate as Pentostam[®] are the pentavalent antimonials, remained as the first-line therapy since the 1940s but are toxic. The dosage ranges between 20 mg/kg BW/day to a limit of 1275 mg, for 20 to 30 days delivered by an *i.m* injection. For CL treatment, the other routes of delivery are *i.l* and *i.v* injections. The inhibition of trypanothione and various bioenergetic pathways in the parasite by an active intracellular reduced trivalent form of the drug has been reported (Ephros et al. 1999). Anorexia, abdominal pain, anemia, arthralgia, acute pancreatitis, cardiac arrhythmia, elevated liver enzyme concentrations, headache, lethargy, leukopenia, malaise, myalgia, metallic taste, nausea, thrombopenia, and vomiting are the common side effects. The serum chemistry, complete blood picture and electrocardiography of the patients are routinely monitored. The course is altered in case of serious side effects like hepato-cardiotoxicity (Frézard, Demicheli, and Ribeiro 2009; WHO 2010)(fig.2.1).

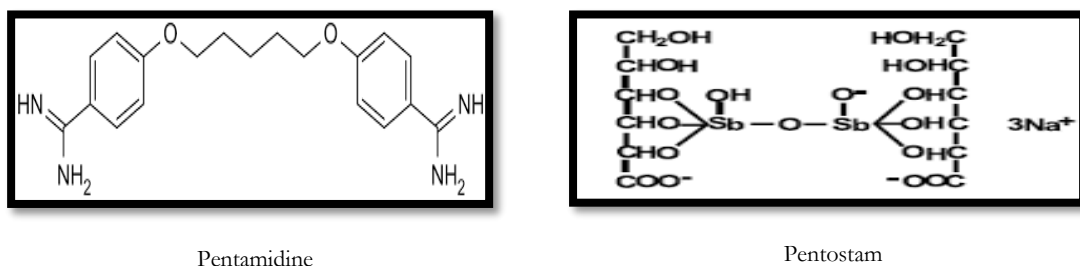


Fig 2.1 The chemical structures of Pentamidine and Pentostam

The second-line of treatment is Pentamidine isothionate, an aromatic diamidine, whose mode of action is unknown. It is delivered by an *i.m*. or *i.v*. injection. It has severe toxicity and adverse side effects like diabetes mellitus, myocarditis, renal toxicity, severe

hypoglycemia, and shock may occur. It might be disrupting the mitochondria membrane potential (Ψ_m) and polyamine biosynthesis by competitive inhibition of arginine transport and non-competitive inhibition of putrescine and spermidine. The antimonial resistant patients were administered 4 mg/kg BW pentamidine alternatively for 20 days. Because of its extreme price and declining efficacy, it was banned in India (Shyam Sundar and Chatterjee 2006). Use of antimonials was hampered by the emergence of resistant strains because of the widespread misuse of the drug. In India, these drugs were freely accessible and inappropriate dosages were recommended by local unqualified medical practitioners, which led to the emergence of resistance. As the parasites were exposed consistently to the drug, tolerance has emerged (S Sundar et al. 1994).

Amphotericin B (AmB) and its Lipid Formulations:

AmB, a polyene fungal antibiotic, which interacts with the ergosterol (abundantly present in the cell membrane of *Leishmania*) by altering ion balance, by forming pores and finally leading to the cell death (Roberts et al. 2003). A dose of 1 mg/kg BW on alternate days for 15 days is recommended. In India, in spite of its high cost, AmB is the first-line drug in the endemic regions where the pentavalent antimonial resistance is seen. AmB is used as the first-line therapeutic in Bihar where antimonials were unsuccessful in more than 60% of the cases. High fever, rigor and chills are common. Nephrotoxicity interrupts the therapy in a few cases. Other rare but major adverse reactions are hypokalaemia and myocarditis. Sufficient water and extra amounts of potassium should be given to the patients (Balasegaram et al. 2012)(fig.2.2).

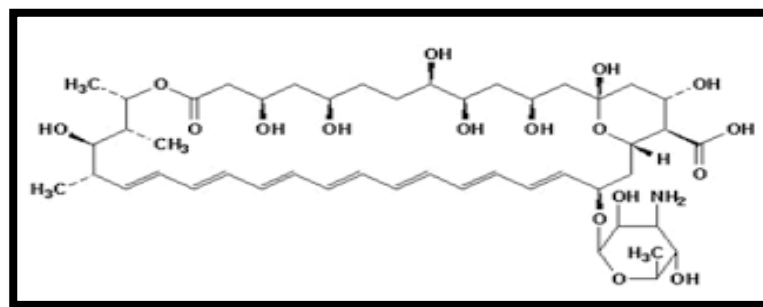


Fig 2.2 The chemical structure of Amphotericin B

Lipid Formulations of AmB:

The Liposomal AmB available as AmBisome[®], AmB lipid complex available as Abelcet[®] and AmB colloidal dispersion available as Amphocil[®] are the three lipid formulations which have similar efficacy and less toxicity when compared to the AmB deoxycholate.

The development of lipid formulations has enhanced the efficacy of AmB. An *i.v.* infusion over 2 hours is recommended. In a few patients, back pain, fever, chills, and rigor might occur, and mild nephrotoxicity or thrombocytopenia might be seen. The AmBisome[®] kills parasites rapidly, so the patients with resistance have not been observed in spite of its extensive usage. It is accumulated in the tissues, slowly released and expelled as it has a long half-life (Bekersky et al. 2002). It increases the solubility and thermal stability and decreases the toxicity of AmB. It has many advantages over the conventional AmB, like increased cure rate, minimal relapse in the patients, better comfort in usage by the patients, and hiked efficacy but costs high. However, under the National Leishmaniasis Elimination Program, WHO has reduced its cost by 10%. About 91% cure rate is reported on the usage of a single dose of 5 mg/kg BW. Abelcet[®] and Amphocil[®] are being used at a dosage of 1-5 mg/kg BW/day and 1 mg/kg BW/day respectively (Shyam Sundar et al. 2010).

Paromomycin:

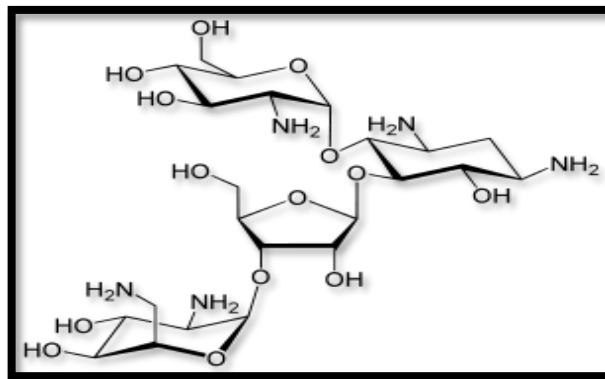


Fig 2.3 The chemical structure of Paromomycin

Paromomycin is available as an *i.m.* injection with the trade name Aminosidine[®]. It is a broad spectrum aminoglycoside antibiotic. In Kenya, in the 1980s, it was successfully used against the human VL for the first time (Chunge et al. 1990). It was registered as an antileishmanial drug in India in 2006. It is effective at a dose of 15 mg/kg BW by an *i.m.* injection for 21 days in India (S Sundar et al. 2007). Tetany, reversible ototoxicity, renal, and hepatotoxicity are rare but seen in a few patients. A skin cream is available for CL (WHO 2010). It is suggested to be used in association with the other drugs, as single drug treatment might show low efficacy. Even though its cost is less (US\$ 5–10 per treatment), and effective against a vast range of parasites, its production was banned due to unknown reasons (Shyam Sundar et al. 2007)(fig.2.3).

Miltefosine:

Miltefosine or (hexadecyl 2- (trimethylazaniumyl) ethyl phosphate) or hexadecylphosphocholine (C₂₁H₄₆NO₄P), is an alkyl phospholipid, an analog of the phosphatidylcholine (PC). It is amphiphilic and zwitterionic due to the presence of positively charged amino and negatively charged phosphoryl groups, having a molecular weight (MW) of 407.57 g/mol. It is white crystalline hygroscopic powder quickly soluble in water and organic solvents. It was lodged in India for VL therapy in 2002, which costs about US\$ 125–200 per course. The typical side effects are anorexia, diarrhea, nausea, and vomiting. Skin allergy, increased liver transaminase levels, and renal insufficiency may be rarely seen. It is prohibited for the pregnant women as it is fetocidal and teratogenic. It is effective if taken after the meals (Berman 2005; Sundar et al. 2002; WHO 2010)(fig.2.4).

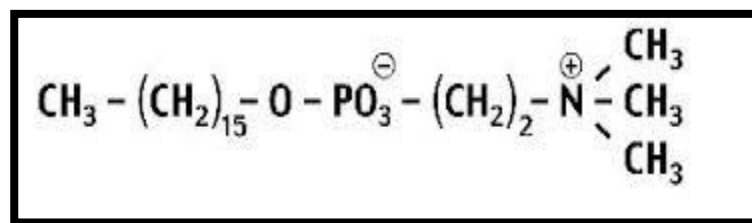


Fig 2.4 The Chemical structure of Miltefosine

Two research groups from the United Kingdom and Germany synthesized miltefosine initially as an anticancer drug for the cutaneous lymphomas and breast cancer. The researchers have probed into its antileishmanial activity *in vitro* and *in vivo* and later performed the phase III clinical studies against the human VL in India. ASTA Medica, the WHO Special Program for research and training in tropical diseases, in collaboration with the Indian government approved it as the first and the only oral drug in VL therapy in 2002. This has opened the doors for the outpatient management in the hospitals in the endemic areas. Later it has been lodged in Germany and Colombia. It has high bioavailability, a long half-life of 160 hrs and is easy for oral administration, but it is teratogenic and harmful for the pregnant mothers. Its recommended dosage is 100-150 mg/day or 2.5 mg/kg BW for 28 days. A relapse after 9-12 months of successive treatment with the miltefosine is reported (Dorlo et al. 2014; Shyam Sundar et al. 2002, 2012).

Within a short span of time, *Leishmania*, has developed resistance to this drug in India. Two transporters in the parasite, namely, LdMT and β -subunit LdROS3, a P-type ATPase of aminophospholipid translocase family, regulate the intracellular accumulation of

miltefosine (Pérez-Victoria et al. 2006; Pérez-Victoria, Castanys, and Gamarro 2003). The endocytic vesicles at the flagellar pocket, internalize miltefosine monomers. Even though the drug is internalized rapidly, it is metabolized very slowly due to its equilibration in the internal organelle membranes as it is water soluble. The probable reasons for the emergence of resistance are as follows:

- (1) A single point mutation in LdMT and/or LdROS3 might have caused a decreased intracellular drug accumulation due to the decreased influx;
- (2) Overexpression of the multidrug-resistant MDR1 gene which encodes for a glycoprotein;
- (3) Reduced content of unsaturated phospholipid alkyl chains in the parasites;
- (4) Its long half-life; and
- (5) Uncontrolled and improper use in the endemic countries like India.

The exact mode of the antileishmanial activity of miltefosine is not known but it is reported to cause apoptotic like action on the *L. donovani* promastigotes causing nuclear condensation, DNA fragmentation, mitochondrial dysfunction, a decrease in the Ψ_m and inhibition of Cytochrome-C oxidase (Paris et al. 2004). It inhibits the acyl-CoA acyl transferase enzyme involved in the ether lipid remodeling which arrests *L. mexicana* (Lux et al. 2000). It is evident that miltefosine has multiple mechanisms of action. As miltefosine is a lipid-based drug it probably targets the fatty acid, phospholipid and sterol metabolism in the parasites. It alters the lipid content in the membranes i.e., decreases phosphatidyl choline and increases phosphatidyl ethanolamine which indicates partial inhibition of the phosphatidyl ethanolamine-N-methyl transferase enzyme of the parasite. It also inhibits the entry of exogenous choline into the parasite (Verma and Dey 2004). It is reported that miltefosine shows immunomodulatory effects on the *Leishmania* infected host macrophages. It enhances IFN- γ , induces IL-12 and skews immune response towards Th1 type (Wadhone et al. 2009).

Sitamaquine:

Sitamaquine (8-aminoquinoline) is an oral medicine for VL for the past 20 years. The fact that it has antileishmanial effects was discovered at the synthetic chemistry department of the Walter Reed Army Institute for Research, USA. In India, after 180 days of treatment, its cure rate was 87%. The general undesirable effects like abdominal pain, headache, vomiting, dyspepsia, and cyanosis can be seen. Methemoglobinemia was only reported in

the Indian patients. In humans, the half-life was evaluated to be 26.1 hours (Schrevel and Loiseau 2016)(fig.2.5).

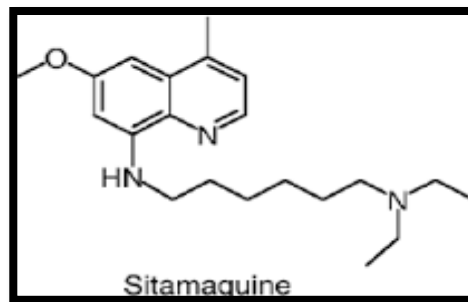


Fig 2.5 The Chemical structure of Sitamaquine

Azoles medicines:

A few oral antifungal drugs like ketoconazole, fluconazole, itraconazole show considerable antileishmanial activity (El-Hajj et al. 2001).

2.2 Combination Trials in Leishmaniasis – a review:

As individual treatment with the existing antileishmanial drugs have drawbacks like high toxicity, the emergence of resistance, the combinations among existing antileishmanial drugs, a combination of antileishmanial drugs with the plant compounds, other natural products, antibiotics, antifungals, antivirals, anticancer drugs and novel synthetic molecules have been tried earlier *in vitro*, *in vivo* and in the patients. The earlier combination trials are being reviewed here.

The *in vitro* antileishmanial activity of Nicotinamide (NAm) or Vitamin B3 has been reported. A combination trial of NAm and trivalent antimony on *L. infantum* axenic amastigotes showed that NAm in synergy with the trivalent antimony considerably improved the antileishmanial activity. NAm in combination with AmB showed an additive activity and with pentamidine slightly showed an antagonistic activity. NAm together with the pentavalent antimony remarkably decreased the burden of *L. infantum*, *L. amazonensis* and *L. braziliensis* (Gazanion et al. 2011). Pam3Cys which is an inbuilt immunoadjuvant and TLR2 ligand in fusion with miltefosine notably inhibited the parasites in BALB/c mice in comparison to the individual drugs. An increased phagocytosis index, Th1 cytokines, ROS, RNS and H₂O₂ were observed (Shakya, Sane, Vishwakarma, et al. 2012). The diminazene and chloroquine were at least nine times less efficient in killing *L. donovani* promastigotes *in vitro* than their combination, which was safer and remarkably decreased

the parasite burden in spleen (Mwololo et al. 2015). An *in vitro* and *in vivo* evaluation of the combinations of pure compounds of essential oil *Chenopodium ambrosioides* (ascaridole, carvacrol, and caryophyllene oxide) was performed. A mixture of ascaridole–carvacrol showed a synergistic effect *in vitro* against *L. amazonensis*, while a moderate action was seen for ascaridole–caryophyllene oxide and carvacrol–caryophyllene oxide mixtures. Ascaridole–carvacrol was mixed in 1:4 ratios by a fixed ratio method which killed the promastigotes and the intracellular amastigotes in a synergistic manner and lowered cytotoxicity. When compared to control, Ascaridole–carvacrol mixture demonstrated a significant difference in the lesion dimensions and the parasite population in the infected BALB/c mice (Pastor et.al 2015). An *in vitro* assessment of the antileishmanial effect of antiretrovirals namely darunavir and atazanavir (protease inhibitors) and tenofovir, efavirenz, nevirapine and delavirdine mesylate (reverse transcriptase inhibitors) on *L. infantum* was performed. Various antiretroviral combinations and antiretroviral + miltefosine combination were evaluated. Efavirenz demonstrated the best leishmanicidal action followed by delavirdine mesylate. Efavirenz + miltefosine showed a better leishmanicidal action (Costa et al. 2016). DB766 and antifungal azoles were used in combination against the intracellular *L. donovani in vitro*. The combination trial in swiss webster mice used as the control showed that high doses of posaconazole and ketoconazole increase DB766 exposure. DB766-posaconazole combinations showed an increased efficacy than DB766 or posaconazole alone in the *L. donovani* infected BALB/c mice (April C et al. 2018).

A ketoconazole and miltefosine mixture with picroliv, a potent immunomodulator agent was used against *L. donovani in vitro and in vivo*. The mixture showed a greater efficacy which was enhanced further with the addition of picroliv, in hamsters than the individual compounds. The ketoconazole and miltefosine mixture showed a noteworthy hike in ROS, RNS, H₂O₂, and phagocytosis in the animals, but after adding picroliv to this mixture no change in phagocytosis and metabolites levels was observed due to its anti-oxidative and non-leishmanicidal characteristics, respectively (Shakya et al. 2011). ODN-2006, an immuno-stimulating class B bacterial oligodeoxynucleotide (CpG-ODN) was delivered along with miltefosine in an *in vivo* trial on mice. The liposomal CpG-ODN + miltefosine mixture ultimately inhibited the parasites in comparison to free CpG-ODN + miltefosine mixture, only miltefosine, only CpG-ODN, and liposomal CpG-ODN individually. Also in the hamsters, a remarkable decrease in the parasite burden was observed with liposomal

CpG-ODN mixture (Gupta et al. 2011). The *in vitro* combination activity of Nitazoxanide, an anti-protozoan agent with amphotericin B, Glucantime®, miltefosine and sitamaquine on *L. infantum* amastigotes showed additive interaction (Mesquita, Tempone, and Reimo 2014).

The BALB/c mice in to which *L. donovani* parasites were injected were administered with (i) Oral atovaquone for 7 days which reduced the liver parasite population and (ii) Suboptimal dose of antimony + full-dose atovaquone (100 mg/kg BW) which converted the pentavalent antimony's effect from partially leishmanistatic to leishmanicidal. The study suggests that atovaquone can be an adjunct to the conventional antimony treatment as it increases the efficiency and reduces the dose and duration of initial antimony treatment (Henry W. Murray and Hariprashad 1996). A combination of indolylquinoline derivative A and SAG showed an absolute removal of the liver and spleen parasite numbers in *L. donovani* infected hamsters. The reduction was lower in the individual treatments (Pal et al. 2002). Thalidomide + Glucantime combination in *L. major* infected BALB/c mice has greater efficacy than the mono therapies as the foot pad swelling in the combination group was remarkably reduced in contrast to the mice administered with either of the drug. Thalidomide increased IFN- γ and decreased IL-10 secretion (Solgi et al. 2006). A mix of AmB in low dose and stearylamine (SA) containing cationic liposomes which are leishmanicidal in suboptimum dose cleared the liver and spleen parasite load in the BALB/c mice. The mixture was better than free AmB in preventing relapse and reinfection, maintaining an immunomodulatory action of free AmB on the CD4⁺ and CD8⁺ T cells for IFN γ generation, reducing drug toxic effects demonstrated by a decrease in TNF α . Decreased IL-10, increased IL-12 and NO levels in the spleen culture supernatants, indicated cure better than free AmB (A. Banerjee, De, and Ali 2008). A combination of amiodarone, an antiarrhythmic drug and miltefosine showed a synergistic effect on the increase of intracellular amastigotes and cured murine models of leishmaniasis infected with *L. mexicana* (Serrano-Martín et al. 2009). *In vivo* evaluation of diminazene, artesunate and their mixture against *L. donovani* indicated that drug combination significantly mitigated the spleen parasite burden in comparison to the individual therapy at same dosages (Joshua et al 2011).

Paromomycin sulfate (PM) + stearylamine (SA) containing phosphatidylcholine (PC) liposomes were assessed for *in vitro* and *in vivo* leishmanicidal action at low-doses. The combination showed a significant synergism towards cure by showing immunomodulatory

action on the CD4⁺ and CD8⁺ T cells for IFN γ generation and down-regulated IL-10 and TGF- β . In Spleen the effect was additive (Antara Banerjee, De, and Ali 2011). The combination therapy with plumbagin from *Plumbago capensis*, triterpenoid saponin extract, and herbicides like acriflavine, trifluralin removed the intra lesional parasites totally and appreciably minimised the spleen and hepatic *L. major* population in the BALB/c mice injected with parasites, in comparison to the untreated controls, which indicates a synergism between the drug combinations and a greater efficacy and superiority of the combination over individual doses. Saponin and acriflavine mixture followed by the various combinations of saponin, plumbagin, trifluralin, acriflavine did not effectively reduce the lesion size and the parasite load. The uptake of other drugs was instigated by the saponin. The prolonged effect of these compounds indicates their low catabolism, slow clearance and long biological half-life (Makwali et al. 2012). The antileishmanial activity of miltefosine + free/liposomal palmitoyl tuftsins (p-tuftsins) was assessed in the *L. donovani* infected BALB/c mice. The parasitic inhibition by miltefosine + free p-tuftsins was significant which was further enhanced by the liposomal encapsulation of p-tuftsins. The parasitic clearance was significantly enhanced by the liposomal p-tuftsins + miltefosine combination which increased Th1 cytokine production (IL-12, TNF- α , and IFN- γ), ROS and RNS and phagocytosis index (Shakya, Sane, Haq, et al. 2012). In a combination trial with miltefosine and pentoxifylline, on 27 isogenic, *L. amazonensis* infected C57BL/6 mice, the combination group significantly decreased the paw diameter and reduced the parasite burden when compared to either of the drugs administered alone (Angélica et al. 2014). To treat murine VL, the green propolis water extract (WEP) and its combination with free or liposomal meglumine antimoniate (MA) was evaluated. The oral WEP alone, oral WEP + *i.p* liposomal MA was given to the *L. infantum* infected mice. The WEP alone decreased the liver parasite population. The liposomal MA alone decreased the liver and spleen parasite population. In the combination no synergism was observed in the reducing parasite burden which was not so remarkable. WEP, liposomal MA, and the combination guarded the liver and spleen from lesions (Ferreira et al. 2014). In the *L. donovani* infected BALB/c mice, *Tinospora cordifolia* pure herb + Cisplatin combination was used, as only cisplatin decreased the parasite burden but damaged and induced morphological changes in the liver and kidney. The combination has neutralised these effects and augmented the Th1 immune response by enhancing the IgG2a, IFN γ and IL-2 and declining the Th2 cytokines IL-4 and IL-10 (Sachdeva, Sehgal, and Kaur 2014). The combination of allicin and AmB was used on *L. infantum* infected hamsters and no clinical symptoms or liver and kidney

changes were observed. AmB alone did not clear the parasite and zero parasite detection was observed in two mice treated with allicin. Allicin alone significantly reduced the spleen and liver parasite burden. The combination reduced parasite burden, which was comparable to the standard AmB. The combination reduced the spleen and liver parasite burden through a partial additive effect (Corral et al. 2014). Nano Curcumin alone showed notable antileishmanial effect both *in vitro* and *in vivo*. Nano Curcumin + miltefosine showed synergism on the parasite *in vitro*. The combination demonstrated augmented *in vivo* antileishmanial effect escorted by hiked ROS, RNS, phagocytic activity and lymphocyte proliferation (Tiwari et al. 2017). Paromomycin + miltefosine combination in hamsters infected with *L. infantum*, reduced the liver, spleen and bone marrow parasite population. The combination showed a progressive efficacy but not a remarkable decline in the susceptibility (Hendrickx et al. 2017).

In a trial on dogs in Italy, a polymer matrix collar with 10% imidacloprid + 4.5% flumethrin was used as a new method to prevent *L. infantum* infection as the control against both human and canine leishmaniasis. 124 young dogs were divided into two groups, 63 with collar and 61 without. At the end of the trial, none out of 63 with collars proved positive for *L. infantum*, whereas 22 dogs out of 61 without collars were infected; the combination demonstrated 100% efficacy. The use of combination collars bestowed prolonged security to dogs and reducing the chances of infection to the humans (Otranto et al. 2013). *L. infantum* infected mongrel dogs were treated with a combination of liposomal meglumine antimoniate (LMA) + allopurinol. The combination clinically improved dogs and significantly reduced the bone marrow and spleen parasite load. The combined treatment showed negative results in the liver qPCR in all dogs. Both xenodiagnosis and diagnosis of the persistence of the parasite in the skin by qPCR indicated that the combination blocked transfer of the skin parasites to the sand flies. Based on the parasitological tests 50% cure rate was observed in the combined treatment (Da Silva et al. 2012).

A mixed therapy with paromomycin and antimonials cured the VL patients in Bihar effectively than antimonials alone (van Griensven et al. 2010). In an *i.v* ambisome and oral miltefosine combination treatment to 135 Indian *Kala-Azar* patients, 124 of 127 were cured. The ambisome shows side effects like fever, body pains and rigors, whereas miltefosine shows gastro intestinal adverse effects, but the combination was very well tolerated and has good efficacy and feasibility of administration (Shyam Sundar et al.

2011). In a trial in the East Africa, PM, SSG and PM + SSG combination was used for treatment of VL. The efficacy of PM *vs.* SSG, PM+SSG *vs.* SSG was compared. SSG was more efficacious than PM. The ability of SSG + PM composition is safe and almost same as the standard SSG (Musa et al. 2012). In a clinical trial, three PKDL cases were administered with AmB-miltefosine combination which showed greater efficacy of combination over individual drugs. When given alone, AmB caused renal damage, and Milt caused gastrointestinal side effects. The combination therapy showed advantages like better tolerance and compliance, reduction in the dose and duration of both the drugs when compared with the mono-drug therapy. The chance of emergence of resistance to either of the drugs can be reduced by the combination therapy (Venkat Ramesh et al. 2014). In a trial in Bihar on 102 confirmed HIV-VL coinfecting patients', *i.v.* liposomal AmB + oral miltefosine was administered. The antiretroviral therapy (ART) was not discontinued. The combination was well tolerated, safe, and effective (Mahajan et al. 2015). From 2002 to 2008, out of 422 treated PKDL cases in South Sudan, 343 received Sodium stibogluconate (SSG) and 79 SSG/ paromomycin combinations. The combination treatment (97%) had better cure rate than mono therapy (90%), shorter duration and with low cost. Thus, the combination therapy demonstrated remarkably better results than only SSG treatment (Abongomera et al. 2016). In a trial in Sudan and Kenya, AmB + SSG, AmB + miltefosine and miltefosine alone were used which showed a cure rate of 87%, 77%, and 72% respectively. No major safety concerns were identified (Wasunna et al. 2016). In a study on 3126 VL patients in the Eastern Africa, SSG + PM was used as the first-line treatment, which showed an early cure of 95.1%. The HIV-VL cases and the patients more than 50 years of age showed early cure of 56% and 81.4%, respectively, while 1063 cases in the study showed at least one adverse event; 60 cases showed a serious adverse event; and 30 died. Overall, the SSG-PM dual was efficacious and safe excluding the HIV-VL cases and older patients (Kimutai et al. 2017). The safety and ability of AmB + miltefosine, AmB + paromomycin, and paromomycin + miltefosine were compared with a standard AmB in a trial in Bangladesh. Out of 601 patients, 158 got AmB monotherapy, 159 got AmB + paromomycin, 142 got AmB + miltefosine and 142 got paromomycin + miltefosine and the final cure rates after 6 months of treatment were 98.1%, 99.4%, 94.4% and 97.9% respectively. Overall the complete therapy was efficacious, received well with no side effects. Miltefosine + paromomycin showed adverse events more frequently (Rahman et al. 2017).

2.3 Natural Products for Leishmaniasis Treatment:

Ayurveda (*Ayu*=Life, *Veda*=Science or Knowledge) is a living ancient Indian system of traditional medicine with a history of more than 5000 years. The Ayurvedic system of medicine is based on the fact that the universe is made of five elements (*Panchabhuta*: earth, water, fire, air and ether) and a holistic treatment to cure the human diseases is achieved through the inception of equilibrium among the five elements of human life, body, mind, and soul. Various Ayurvedic texts like *Ashtanga Hridayam*, *Ashtanga Sangraha*, *Charaka Sambita* and *Susruta Sambita* describe a set of rejuvenative formulas to not just cure but to prevent many diseases. These are called as ‘*Rasayanas*’ which are organ and tissue-specific. The traditional ayurvedic practices have been modernized and are being considered as a complementary or alternative medicine. According to the Ayurveda, *Tri-Doshas* (three basic energy complexes) - *Vata*, *Pitta* and *Kapha*, characterise the humans in relation to their nature and hence the diseases. A healthy individual has an equilibrium state (*sāmatva*) of the *tri-doshas*, while a diseased individual has an inequality (*visamatva*). The individuals who predominantly are of *Pitta* type tend to have inflammations, infectious diseases and ulcers. The treatments for bodily diseases are characterized under the ‘*Kayachikitsa*’ component of *Ayurveda* (Kaul and Wadhwa 2017) (<https://en.wikipedia.org/wiki/Ayurveda>).

Ayurvedic Treatment for VL:

Ayurvedic Name: *Kala Jwara*, *Vishama Jwara*

Prescription: 60 mg *Shuddha nilanjan* (pure antimony), 60 mg *Mukta bhasma*, 120mg *Tamra bhasma*, (copper powder), 120 mg *Praval bhasma* (calcium), 120mg *Shankha bhasma* (conch powder), 120 mg *Shuddha swar nagairika*, 120 mg *Yakritplibodaradilauba*, (*Yakrit*- liver; *Pleeba* – spleen; *Udara*- stomach; *Aadi*- etc; *Lauha* – metal), Tulasi Leaves, *Geloy Satwa*, *Faulaad Lauha*.

Directions: Above concoction with honey (drug carrier) is advised four times a day.

Diet: Nutritious and protein-rich food along with milk, fruits, vegetables, eggs etc. are to be fed to the patient.

Other regimen: The patient is advised to abstain from laborious physical work.

(<http://ayurvedichawa.blogspot.in/2010/03/leishmaniasis.html>);

(<http://www.dramitdutta.com/Leishmaniasis-ayurvedic-skin-treatment.aspx>).

The treatment in traditional systems is always a combination of many ingredients - multiple drugs which have multiple targets and exert multiple actions and trigger “butterfly effect” in the patient’s body. Different molecules or sometimes the same molecule acts as an immune booster for the host and an inhibitor for the parasite. The multiple drug constituents being natural in origin, have better compatibility with the human body. So they have relatively minimal side effects and are easily consumable and have greater efficacy. As for centuries, various natural compounds are being consumed as part of the regular diet and ayurvedic medicine, they are safe (Kaul and Wadhwa 2017).

Ashwagandha for Leishmaniasis:

Ashwagandha (*Withania somnifera*) - also called as the “Queen of Ayurveda”, “Winter cherry” or “Indian ginseng” - is a sub-tropical herb, largely cultivated in Madhya Pradesh, Uttar Pradesh, Punjab, Gujarat, Rajasthan, and also found in Africa. *Ashwagandha* is among top 32 significant plants with medicinal values, identified by the National Medicinal Plant Board of India (<http://www.nmpb.nic.in>) because of its high requirement at the local and international level. With various trade names its extract is available over the counter even in many European countries and in the United States as a dietary supplement. It belongs to the *Solanaceae* family. The name *Ashwagandha* signifies odor of its roots and leaves that resemble the horse smell (*Ashwa* - horse *gandha* - smell). It is a *Medhya Rasayana*. Its scientific name indicates its sleep inducing activity which is related to its anti-stress activity (*somnifera* – sleep-inducing). The genus *Withania* comprises of 26 species of which two (*W. somnifera* and *W. coagulans*) occur in India. It belongs to the GRASE (Generally Recognized as Safe and Effective) family of herbs. It is an upright, greyish, moderately hairy evergreen shrub with long tuberous roots. Almost every part of the plant is used for various health advantages. Its antioxidant, antiinflammatory, antistress, antidiabetic, cardio and neuroprotective activities, and many other activities have been reported earlier (Kaul and Wadhwa 2017; Mir et al. 2012; Singh et al. 2011; Winters 2006).

Withanolides are the main reason for the diverse pharmacological and therapeutic attribute of *Withania somnifera*. Withanolides are an aggregation of C₂₈-steroidal lactone triterpenoid compounds created on an unbroken or reshuffled ergostane platform in which C-22 and C-26 are properly oxidized to make a δ -lactone ring on ninth carbon side chain and a six-membered lactone ring. The fundamental frame is a withanolide skeleton described as a 22-hydroxyergostan-26-oic acid-26, 22-lactone. Over 1000 withanolides have been

identified in the past 50 years from the *Solanaceae*, *Leguminosae*, *Labiatae*, *Myrtaceae*, and *Taccaceae* families and over 40 withanolides have been isolated. They are structurally divergent in various genera like, *Jaborosa*, *Dunalia*, *Lycium*, *Datura*, *Acnistus Physalis* etc., apart from the *Withania*. They have antitumor, antimicrobial, antibacterial, antiinflammatory, antidepressant, antioxidant, antiulcer, antineoplastic and cytotoxic, antineurodegenerative, antileishmanial, antitrypanosomal, antistress, immunomodulating, immune mitigating, cognition augmenting and memory-boosting effects, quinone reductase induction, hypotensive, bradycardic, respiratory inciting action, radiosensitizing, cardiogenic, and insect antifeedant properties (Kaul and Wadhwa 2017). The metabolic contents of a plant depend on its age, the environment in which it is grown etc. About 48 primary and secondary metabolites from the roots and 62 from the leaves have been described. Leaves mainly harbor WA and Withanone, whereas root has WA. As the plant grows from the young (6 weeks) to mature (12–18 weeks) stage, WA content increases in the leaves and roots. However, accumulation declines at the maturation stage (Kaul and Wadhwa 2017). Research on the *Ashwagandha* has revealed the potential benefits of root extracts or their active components instead of the leaf extracts. Many studies in the past have probed the effect of leaves extracts for their benefits as leaf extracts are advantageous over the root extracts by being environment friendly. The complete sacrifice of the plant to make the extract is not needed, unlike for the root extracts. A few recent reports have used water extracts of the leaves instead of alcoholic root extracts. The leaf powder or water extract is safe and uncomplicated to make without the use of organic solvents for the extraction (Kaul and Wadhwa 2017).

Withaferin A:

Withaferin A (4 β , 5 β , 6 β , 22R)-4, 27-dihydroxy-5, 6-22, 26-diepoxyergosta-2, 24-diene-1, 26-dione) (C₂₈H₃₈O₆) is a cell-permeable bioactive steroidal lactone and is the first pharmacologically active withanolide isolated from the *Withania somnifera* (fig. 2.6).

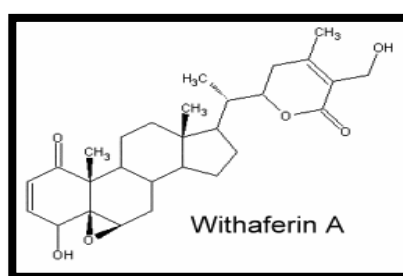


Fig 2.6 The molecular structure of Withaferin A

The major amount of WA is seen in the shoot tips, later in the leaves, nodes, internodes, roots, flowers, and seeds of the *Withania somnifera*. WA is a major secondary metabolite and has many pharmacological activities but its primary molecular target is unknown in the *Leishmania* infection. WA has shown antileishmanial activities possibly by inhibiting DNA topoisomerase-I (Sen et al. 2007), Protein kinase C (Grover et al. 2012), Pteridine Reductase-1 (Chandrasekaran et al. 2016). WA has anti-inflammatory (Al-Hindawi, Al-Khafaji, and Abdul-Nabi 1992), antitumor (Widodo et al. 2007), antibacterial (Owais et al. 2005), antioxidant, anticonvulsive, and immunosuppressive properties (Sharma et al. 2011; G Singh et al. 2010). WA was first isolated by Kurup (1956) from the leaves of the Indian variety. Subramanian and Sethi (1969) proposed an extraction and isolation method of WA from the *Withania somnifera* root powder. Sangwan and Sangwan (2013) have described a better way of isolating WA.

2.4 Need for Combination Therapy:

The Ayurvedic formulations or natural products can be used along with the available drugs in absence of any detrimental drug-drug cross reactions. High costs, increased adverse reactions of synthetic drugs, dearth of rehabilitative medication for many persistent diseases, and the advent of resistance are some of the major reasons for re-popularising complementary and alternative medicines. The natural/herbal products are being widely used throughout the world as a substitute for modern medicine due to their capacity to attack many sites simultaneously. The herbal products are promising candidates to treat several infectious diseases as their formulations are in the single delivery system and they have fewer side effects. The combination treatment has significant advantages. It reduces the risk of emergence of resistance to the existing and novel drugs. It shortens the duration of medication, heightens the compliance, mitigates the comprehensive quantity of medicines, reduces their adverse effects and price, prolongs the effective life of available medicines (Nisha Singh et al. 2014). The combination of a powerful and safe immunostimulant with a decreased dose of the antileishmanial drug is a rational method which would be efficacious than the immunotherapy or the drug therapy alone. Currently one of the most rational approaches is a combination of a natural compound with an existing antileishmanial drug. An ideal combination of drugs would be of a fast acting short half-life drug and slow acting longer half-life drug to clear the persisting parasites preferably with distinct modes of action (Kaul and Wadhwa 2017).

2.5 Drug Discovery Approaches for VL:

As an effective vaccine for leishmaniasis does not exist till date, the chemotherapy is the only control strategy. The existing antileishmanial drugs are limited and the emergence of resistance towards them is a major challenge. The existing antileishmanial drugs are the repurposed drugs. AmB deoxycholate and its lipid formulations, ketoconazole, fluconazole, itraconazole are originally antifungals. Paromomycin is an antibiotic. Pentamidine isothionate is an antiglycemic agent. Miltefosine is an anticancer drug. The antileishmanial potency of these drugs have been tested and repurposed as antileishmanial drugs. Yet unfortunately, very soon, patients in the endemic areas have stopped responding to a few of these drugs, as the parasite developed resistance against them. More over these drugs are costly and toxic. So the antiparasitic drug discovery has become a thrust area of research and organizations like Institute of One World Health (IOWH), Drugs for Neglected Diseases Initiative (DNDi), Bill and Melinda Gates foundation and others are funding for this purpose. The inflow of funds for drug development for tropical diseases is hastening the research and has enabled technological advances.

The drug discovery process is a multi-disciplinary approach. The first and foremost step in the antiparasitic drug discovery is the identification of a suitable drug target from a biological pathway specific to the parasite. Theoretically, the target in the parasite should be missing in the host or sufficiently distinctive from the host homolog (Drews 2000). *Leishmania* belongs to the order Kinetoplastidae which emerged from the primordial Eukaryotic clan. As *Trypanosomatids*, phylogenetically, branched out primitively from the higher Eukaryotes, there are a few targets that are exclusive to these parasites. The target should be crucial for the parasite's growth, and the stage of life-cycle in which the target gene is manifested should be considered. The target should have a binding cleft so that exact inhibitors can be constructed, and if it is an enzyme then its hindrance should be fatal to the parasite. The target should be inexpensively assayable and suitable for the high throughput screening. Conventionally the drug targets were identified basing on the biochemical and physiological variations between the host and parasite. This approach has changed now due to the accessibility of the integrated genome sequences of *Leishmania* species like *L. donovani*, *L. major*, *L. infantum*, and *L. braziliensis*. It is now possible to identify the novel parasite specific drug targets. With the genome sequence information microarrays and proteome analysis can be applied to find the parasite-specific genes. The bioinformatics approaches like computer aided drug discovery tools (CADD) etc., have

contributed enormously in hastening the antiparasitic drug discovery (Chandra et al. 2010; Chawla and Madhubala 2010; Drummelsmith et al. 2003; Duncan et al. 2011; Monte-Alegre, Ouaiissi, and Sereno 2006; Naula, Parsons, and Mottram 2005; Gaganmeet Singh, Jayanarayan, and Dey 2008).

Folate Biosynthesis Pathway:

One of the metabolic pathways in *Leishmania* species which is crucial for its survival is the folate biosynthesis pathway (fig. 2.7). It is a drug target in the anticancer and antimalarial treatment. The enzymes of this pathway namely, Thymidylate synthase (TS) (EC 2.1.1.45) and Dihydrofolate reductase (DHFR) (EC 1.5.1.3) are potential drug targets.

The folates are utilized as cofactors in the DNA, RNA synthesis, and the amino acid metabolism. *Leishmania* utilizes an exogenous source of folate/biopterin as they are pteridine auxotrophs conversely to their vertebrate hosts (Beck and Ullman 1990; Lemley et al. 1999). The folates and biopterins function as cofactors only in their absolute reduced tetrahydro forms. In general, the tetrahydro folate is produced from folate and dihydro folate by the NADPH-dependent DHFR enzyme (Blakley RL 1984). However, in *Leishmania*, the DHFR exists as a bifunctional enzyme, along with TS forming the DHFR-TS complex (Beverley, Ellenberger, and Cordingley 1986; Cruz and Beverley 1990; Ferone and Roland 1980; Ivanetich and Santi 1990). The DHFR and TS are found on one polypeptide in the *Trypanosomatids*, with the DHFR on amino and the TS domain on carboxy termini. In contrast to the mammalian cells, in *Leishmania*, the *de novo* biopterin synthesis pathway is missing (Beck and Ullman 1990; Kaur et al. 1988; Scott, Coombs, and Sanderson 1987; Thöny, Auerbach, and Blau 2000) and the DHFR-TS shows no activity with biopterin or dihydro biopterin (Nare, Hardy, and Beverley 1997). Instead, reduced biopterin is produced by the Pteridine reductase 1 (PTR 1) (1.5.1.33), which, step by step, reduces oxidized biopterin to dihydrobiopterin and tetrahydrobiopterin. PTR1 is an important enzyme in the pteridine salvage pathway and is indispensable for the parasite's maturation and survival (Bello et al. 1994; Luba et al. 1998; Nare, Hardy, and Beverley 1997). This NADPH-dependent enzyme is structurally dissimilar to the DHFR and corresponds to the short-chain dehydrogenase family (Wang et al. 1997; Whiteley JM, Xuong NH 1993). PTR1 displays an extensive selectivity for pteridine substrate and also reduces folate to dihydro and tetrahydro forms (Bello et al. 1994; Nare, Hardy, and Beverley 1997). The parasite uses the host folates and reduces them to active tetrahydro forms utilizing its DHFR-TS and PTR1 enzymes.

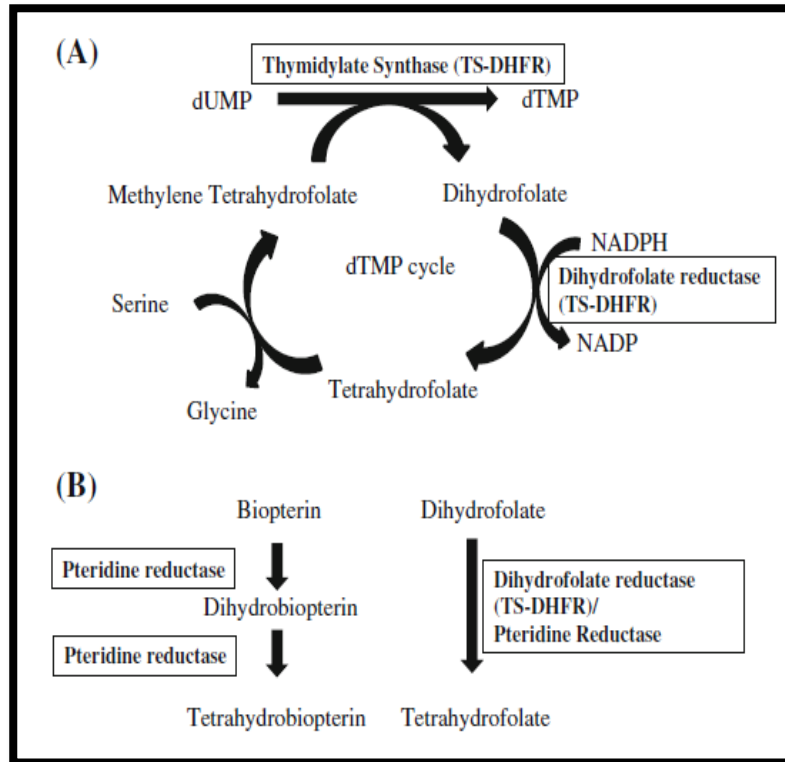


Fig: 2.7: Folate synthesis pathway (A) TS synthesizes dTMP converting Methylene THF to DHF which is converted back to THF by DHFR. (B) Pteridine reductase (PTR1) reduces pterins and folates. (Source: Chawla and Madhubala 2010)

The DHFR-TS reduces 7, 8-dihydrofolate (DHF) to 5, 6, 7, 8-tetrahydrofolate (THF), a prerequisite cofactor in the *de novo* synthesis of thymidylate in *Leishmania* (Ivanetich and Santi 1990). The *L. major* DHFR-TS enzyme has been characterized. Interestingly, *Leishmania* parasites are unable to survive in the animals lacking DHFR-TS (Veras et al. 1999). The *dhfrts*⁻ mutants of *Leishmania* could not survive long in the mammalian host unless high and near toxic levels of thymidine were provided (Cruz and Beverley 1990). PTR1 gene deletion is fatal to the promastigotes but can be neutralized by catering reduced pterins but not folates, illustrating a cardinal responsibility for unconjugated pteridines (Bello et al. 1994; Nare, Hardy, and Beverley 1997; Wang et al. 1997).

The standard inhibitors of DHFR like methotrexate were inefficient towards *Leishmania*. The *dhfr-ts* mutants of *Leishmania* were resistant to methotrexate as the gene for PTR1 was present. PTR1 is least inhibited by antifolates and can be a diversion for the DHFR-TS. Many molecules were evaluated in contrary to PTR1 in *L. major* out of which a few hindered both DHFR-TS and PTR1. So an inhibitor that targets both the enzymes at a time or a combo of two inhibitors precisely inhibiting both the enzymes is required. The

inhibition of any of these two enzymes decreases dTMP for the DNA synthesis thus inhibiting the replication as well as the parasite's viability (Chawla and Madhubala 2010).

The previous *in silico* studies describe that WA inhibits the protein kinase, which instigates apoptosis through the Topoisomerase I - DNA complex (Sen et al. 2007) and the Withanolides from *Withania somnifera* inhibit the protein kinase C signaling pathway in *L. major* (Grover et al. 2012). The studies reveal that in *L. major* promastigotes, PTR1 expression provides a plausible 'metabolic by-pass' of DHFR-TS blockage, granting a restricted or absolute retraction of anti-pteridine inhibition confiding upon the corresponding levels of PTR1 expression (Bello et al. 1994; Nare, Hardy, and Beverley 1997). PTR1 activity in *L. major* promastigotes is 10 to 17 fold reduced than in *L. major* and *L. mexicana*, and *L. major* is substantially more susceptible to MTX. This implies that PTR1's role as a metabolic-bypass is even more significant in *L. major* and *L. mexicana* than in *L. donovani* (Cunningham and Beverley 2001; Kaur et al. 1988; Scott, Coombs, and Sanderson 1987). Moreover, the DHFR-TS is low in *L. mexicana* amastigotes comparative to the promastigotes implying that PTR1-dependent effects were more intensified in the amastigote compared to the promastigotes. Thus, to be an efficacious antifolate therapeutic, targeting macrophage-resident amastigotes needs to consider, the capacity of PTR1 to by-pass inhibitors targeted opposed to the DHFR-TS. One prospect is recognizing molecules which can shun both PTR1 and DHFR-TS separately or simultaneously. Initial research has recognized many lead molecules which hinder both PTR1 and DHFR enzymes *in vitro* and hinder the promastigotes at sub-micro molar levels, and one compound inhibited *L. major* amastigotes in the cultured macrophages (Nare, Hardy, and Beverley 1997).

2.6 Hypothesis:

The Withanolides have been extracted, identified from *Withania somnifera* leaves and their *in vitro* antileishmanial activity was reported. In Withanolide treated parasites apoptotic markers like morphological changes, phosphatidyl serine externalization, generation of ROS, mitochondrial membrane potential's depolarization, DNA fragmentation, the prevention of cell cycle at sub G₀/G₁ phase were observed (Chandrasekaran et.al 2013). The leaf extract of *Withania somnifera* (alcoholic fractions F5, F6) and the purified WA's antileishmanial and immunomodulatory activities were checked both *in vitro* and *in vivo*. Compared to the control, reduced number of amastigotes in the mouse peritoneal macrophages, reduced IL-10 mRNA expression and induction of ROS were observed in

the F5 (15 µg/mL), F6 (10 µg/mL), and WA (1.5 µM) treated groups *in vitro*. Upon treating the mice with the F5 (25 and 50 mg/kg BW), F6 (25 and 50 mg/kg BW) orally, and WA (2 mg/kg BW) intraperitoneally (*i.p*) for 10 days, a reduced spleen and liver parasite population, decreased mRNA expression of IL-4, IL-10, and TGF-β and elevated ratio of IFN-γ/IL-10 mRNA expression, and enhanced IgG2a titres in comparison to IgG1 were observed (Chandrasekaran et.al 2017). To probe into the mode of antileishmanial activity of WA, PTR1, a parasite-specific enzyme from the folate biosynthesis pathway was chosen as the drug target which salvages the pteridine and is crucial for the growth. Molecular docking to know the binding mode of WA with PTR1 was performed after which, PTR1 gene was cloned, the recombinant protein was expressed, purified and the enzyme kinetics (using Michaelis–Menten equation) and the inhibition studies with WA (by plotting Line weaver–Burk graph) were performed. The Enzyme’s inhibition in the crude lysate of treated parasites was also performed. It was observed that WA inhibits *Ld* PTR1 in an un-competitive mode (Chandrasekaran et.al 2015). Based on the previous findings the following has been hypothesized.

WA has Multiple Targets:

Earlier it has been demonstrated that WA inhibits *Ld* PTR1. It is possible that ‘WA may inhibit *Ld* DHFR-TS, the other crucial enzyme in the folate biosynthesis pathway.

WA can act in Combination with Existing Antileishmanial Drugs:

The natural products act in an additive or synergistic way. As existing drugs have severe side effects, a combination of the natural compound with an existing drug might show greater efficacy. An ideal combination is of a fast-acting short half-life drug with a slow-acting longer half-life drug to remove the leftover parasites. Hence the hypothesis is that WA + Milt combination might improve the efficiency, reduce the duration and lower the treatment failure.

2.7 Objectives of the Study:

Based on the above hypothesis the following objectives have been framed.

1. *In silico* prediction of the drug-like properties of WA and Miltefosine (positive control)
2. *In silico* and *in vitro* inhibition studies of WA on *Ld* DHFR-TS, the other potential enzyme in the Folate Biosynthesis Pathway
3. The Determination of the additive effect of WA and Milt in the treatment of experimental VL.

Chapter III

Materials

and

Methods

Objective I

In silico Prediction of Drug-like Properties of Withaferin A and Miltefosine (positive control)

3.1 Drug Likeness of Withaferin A:

The SMILES (simplified molecular input line entry system) formula of WA {O=C/1O[C@H](CC(=C\1CO)\C)[C@@H](C)[C@H]6CC[C@@H]4[C@]6(C)CC[C@@H]3[C@]5(C(=O)\C=C/[C@H](O)[C@]52O[C@@H]2C[C@H]34)C} was submitted in the query box in molsoft server (<http://molsoft.com/mprop/>) to obtain drug-likeness properties of WA.

The drug-likeness of a molecule can be evaluated from its molecular structure much before it is synthesized. It is a qualitative concept used in the drug designing to check out "how much a given compound is like a drug" keeping in view properties like solubility, bioavailability, ligand efficiency, lipophilic efficiency, and potency at the biological target. It can be estimated for any compound and does not reflect its actual biological activity. It is not relevant to many biological molecules like proteins, as they are digested after consumption (Leeson and Springthorpe 2007; Lipinski 2004).

The ideal drugs should have following qualities:

- Molecular weight (MW): Smaller the better, as it affects the diffusion. Many commercially available drugs have MW between 200-600 Da (Lipinski 2004).
- Solubility in water and fat: An oral drug should be water and fat-soluble as it has to pass through the intestinal lining, move in the blood and pass through the lipidicous cell membrane to get into it. An exemplary to the lipidicous cell membrane is 1-octanol (a lipophilic hydrocarbon). The logarithm of octanol/water partition coefficient, LogP (experimentally measured) or cLogP (computationally predicted) forecasts the solubility of a possible oral drug (Leo, Hansch, and Elkins 1971). The water solubility of a drug is calculated from the number of hydrogen bond donors (HBD) vs. alkyl side chains. A low water solubility value reflects in slow absorption and action and a high value in fat solubility and thus drug can't permeate the cell membrane to get into the cell.

- Potency at biological target: Drugs should have high potency i.e. high pIC_{50} value at a given concentration, to reduce the danger of non-specific, adverse effect. A drug with high potency and low clearance requires less total dose, which mitigates the risk of individual therapeutic adverse reactions.
- Substructures like alkyl nitro compounds, alkylating agents etc., are irritants, mutagenic and carcinogenic, so it is better to avoid these functional groups.

Christopher A. Lipinski in 1997 formulated a generalization which later was popularized as the 'Lipinski's Rule of Five', 'Pfizer's Rule of Five' or 'Rule of Five' (RO5). It is called so because all the numbers are multiples of five. It evaluates the drug-likeness and determines if a given compound has qualities that would make it a likely bioactive oral therapeutic suitable for the human consumption (Lipinski 2004). Including absorption, distribution, metabolism, and excretion (ADME) properties, other molecular attributes crucial for a drug's pharmacokinetic activity in human system are stated by the rule. It cannot predict the pharmacological activity of a compound. As per the rule, an orally active drug should have ≤ 5 HBDs (total number of NH and OH bonds), ≤ 10 hydrogen bond acceptors (HBA) (all N or O atoms), $MW < 500$ daltons, $\log P \leq 5$. Later a few variations were made like $\log P$ value should be between -0.4 to $+5.6$, molar refractivity between 40-130, MW between 180–500, number of atoms between 20–70, and polar surface area (sum of surfaces of O's, N's and attached H's) $\leq 140 \text{ \AA}^2$. The compounds which satisfy the above conditions are predicted to have good oral bioavailability (Ghose, Viswanadhan, and Wendoloski 1999; Lipinski 2004). Most of the chemical molecules satisfy the Rule of Five; however, a few natural products are exceptions.

3.2 Prediction of Gastrointestinal Absorption and Blood-Brain Barrier Penetration Capacity of Withaferin A using BOILED-Egg model:

The GI absorption and BBB penetration capacity of WA were predicted using the BOILED-Egg model. These are very important pharmacokinetic properties to calculate at various stages of the drug discovery because many drugs fail due to poor pharmacokinetics and bioavailability, apart from efficacy and toxicity. Pharmacokinetics is the fate of a drug in the body, whereas bioavailability is the fraction of dose that reaches bloodstream after the oral administration. The oral bioavailability, whose early estimation is crucial in drug discovery, depends on many factors but primarily on the gastrointestinal absorption. The

BBB is a physical and biochemical shield protecting the brain. The tight junctions on the endothelial cells prevent the paracellular perforations by different molecules and act as physical barrier whereas P-glycoprotein pumps out the substrates from the central nervous system (CNS) and acts as a biochemical barrier. The drugs which need to access the brain enter through passive diffusion. Thus, the BBB selectively allows the central acting molecules and limits the unwanted peripheral drugs.

Due to the rapid advances in the drug discovery process, many lead clinical compounds are being identified. The small sample amount of compounds and need for the animal testing are a few practical problems being encountered which have enhanced the need for computational models which can predict the pharmacokinetic parameters like bioavailability. Brain Or Intestinal Estimated permeation method or BOILED-Egg is one such precise predictive model that calculates the lipophilicity and polarity of compounds and predicts both the BBB and intestinal permeation capacity of drugs and translates into molecular design speedily, simply with a clear graphical output and is simple in concept and interpretation. It is a swift, intuitive, easily reproducible, statistically robust model to forecast the passive GI absorption and BBB penetration of compounds useful for the drug discovery, development, and helps in the lead optimization. The 2D graphical nature of the model gives an indication of how distant a molecular structure is from the perfect physicochemical area for proper absorption. Egan et al., (Egan, Merz, and Baldwin 2000) based on the n-octanol/water partition coefficient ($\log P$) and polar surface area (PSA) developed a model to differentiate between properly absorbed and poorly absorbed small molecules. The model is called 'egg' as the area most occupied by well absorbed compounds is elliptical. The model has been built on the basis of recent human intestinal absorption data which includes 660 small molecular structures which were subjected to WLOGP (n-octanol/water partition coefficient) vs tPSA (topological polar surface area) computation. So the model is a plot of WLOGP vs tPSA. If a small molecule is located at a point in the yolk/yellow region in the model it probably permeates through the BBB. The points located in the white region are molecules anticipated to be passively absorbed by the GI tract. The molecules predicted to be effluated from the CNS by the P-glycoprotein are shown as blue dots and those which are not to be effluated as red dots. The model is widely used in the industrial and academic contexts. Many commercial packages like Discovery studio, Dassault Systemes, BIOVIA use the model. It has been successfully used in the discovery of Telaprevir, a drug for Hepatitis C (Daina and Zoete 2016).

3.3 Prediction of Oral Bio-Availability for Withaferin A:

For the specific biological effect of a potent drug to occur, it must extend to its target in the body in required amounts, and be available in a bioactive form for a required time. The bioavailability is the fraction of drug dose that reaches the bloodstream after the oral administration. The oral bioavailability depends on many factors but primarily on the GI absorption. Generally, drugs are available as tablets and capsules which cannot pass through the membranes; so they have to be dissolved in the aqueous digestive fluids and diffuse across the intestinal wall into the hepatic portal vein for transport through the liver before they reach the circulation. An oral drug to be bio-available should be water and fat-soluble as it has to pass through the intestinal lining, move in the blood and permeate the lipidicous cell membrane to get into the cell. If a drug is low in water solubility it is absorbed slowly and if it is low in fat solubility it cannot permeate the cell membrane to get into it. It is very difficult to test the dissolution of a drug *in vivo* due to the absence of the standardized methods. It is costly and time-consuming to get the diffusion rate data of drugs from the animal experiments, assuming that the absorption process in the animals (i.e., rat) is identical to humans (Zhao et al. 2002). The *in silico* models are a valid accurate reliable alternative to experimental methods to predict the bioavailability. The bioavailability of WA was obtained from the Swiss ADME tool by uploading the SMILES notation. It is calculated based on the following properties:

Lipophilicity: $-0.7 < \text{XLogP3} < 5.0$

Size: $150 \text{ g/mol} < \text{MV} < 500 \text{ g/mol}$

Polarity: $20 \text{ \AA} < \text{TPSA} < 130 \text{ \AA}$

Solubility: $0 < \text{LogS (ESOL)} < 6$

Saturation: $0.25 < \text{Fraction of Carbons in sp3} < 1$

Flexibility: $0 < \text{Number of Rotatable Bonds} < 9$

A physicochemical scope on each axis is determined by the above physicochemical properties and the server generates a pink coloured hexagon which is the physicochemical space available for the oral bioavailability of the drug, in which the radar plot of the molecule has to completely fall to be assessed as orally bioavailable. The oral bioavailability of WA was determined using the following formula ‘% Absorption = $109 - (0.345 \times \text{TPSA})$ ’ where TPSA is the topological polar surface area (Vishwanathan, Gurupadayya, and Venkata Sairam 2016).

3.4 Prediction of Cardiac Toxicity of Withaferin A:

The cardiac toxicity of WA, based on the hERG (human ether-à-go-go related gene) ion channel blocking capacity was anticipated using the 'Pred-hERG 4.0' web server which has a simpler intuitive user interface. Using this tool, the chemical libraries containing thousands of potential drug compounds can be screened to identify at an early stage whether they are hERG blockers or non-blockers. The tool has a data set of 5,984 compounds and is available at <http://labmol.com.br/predherg/>. The SMILES string of WA was submitted and an outcome as a probability map was obtained.

The 'hERG is an ion channel well appreciated for its participation in the hearts' electrical activity and synchronization of the heartbeat. The lethal cardiac arrest as a side effect of a few drugs is due to stoppage of the hERG K⁺ channels. It is most important to check whether a potential drug compound blocks this channel or not. In early stages of the drug development process, this channel is one of the most important anti-targets to be considered. For the USFDA (United States Food and Drug Administration) to give the clearance, testing a novel bioactive compound for the hERG safety is compulsory. Earlier non-cardiovascular drugs like cisapride, sertindole, terfenadine were released but later revoked from the market because of their hERG K⁺ channel blocking capacity with adverse cardiac complications, leading to the patient's death.

The *in vitro* patch-clamp electrophysiology technique and *in vivo* zebra fish model tests are the experiments to evaluate the binding capacity of drugs to the hERG K⁺ channel. But these are time taking, laborious, expensive and need technical expertise to perform. The computational tools have been developed based on the existing data which can accurately, reliably identify the potential hERG blockers (Braga.et.al 2015).

3.5 Prediction of Absorption, Distribution, Metabolism, and Excretion (ADME) Properties for Withaferin A:

The assessment of ADME properties prematurely during the drug discovery is essential to prevent the pharmacokinetics-related failures later in the clinical trials. The databases have many chemical compounds which are being evaluated, taking various parameters into consideration to select the best ones so that they can be synthesized, tested, and promoted as safe and effective medicines for the patients. The drug molecules must be less toxic and show high target specific biological activity. The body's metabolism acts as one of the

crucial protective mechanisms against destructive molecules by changing them into the excretory products. The natural products tend to escape the metabolic excretion as they have evolved along with the humans. So they have inherent benefits over the chemically synthesised molecules and may not have the drug likeness properties. Understanding the metabolic fate of the natural products and their derivatives is crucial to know about the active molecules and the mechanisms involved.

To know the metabolic fate of drugs, both experimental and computational approaches are applied to understand their cross reactions with the enzymes of metabolic pathways like Cytochrome P450, Dehydrogenases, Hydrolases, Peroxidases, Glutathione S transferases etc. The experimental methods need expertise, laborious, and time taking and expensive to carry out, whereas the computational tools predict the drug metabolism with high throughput, lower cost, lesser time. The Swiss ADME, designed by the molecular modeling division of the Swiss Institute of Bioinformatics is a fast predictive web tool having intuitive interpretation with statistical significance and can be translated into molecular design. It predicts physicochemical, drug-likeness, medicinal chemistry, water solubility, pharmacokinetics and lipophilicity properties of compounds. The SMILES string of WA was submitted as an input, and the information on the following properties was obtained as the output.

Physicochemical Properties:

The molecular formula, molecular weight, number of heavy atoms, number of aromatic heavy atoms, the fraction of carbons with sp³ hybridisation, number of rotatable bonds, number of H-bond acceptors, number of H-bond donors, molar refractivity and topological polar surface area were obtained. All these parameters indicate the physicochemical properties of given compound.

Drug-likeness Properties:

The given compound is checked for its drug-likeness by five different rule-based filters given by five different researchers from five different pharmaceutical companies. They are Lipinski (Pfizer), Ghose (Amgen), Veber (GSK), Egan (Pharmacia) and Muegge (Bayer) filter methods. The Abbot Bioavailability score is generated based on the compound's probability of having minimum 10% oral bioavailability in rats and measurable CaCO₂ permeability.

- ✓ Lipinski filter: According to this filter a compound is drug-like if it has $MW \leq 500$; $MLOGP \leq 4.15$; $N \text{ or } O \leq 10$; $NH \text{ or } OH \leq 5$ (Lipinski et al. 2012).
- ✓ Ghose filter: According to this filter a compound is drug-like if it has MW between $160 \leq MW \leq 480$; $WLOGP$ between $-0.4 \leq WLOGP \leq 5.6$; molecular refractivity between $40 \leq MR \leq 130$; and the number of atoms between $20 \leq \text{atoms} \leq 70$ (Ghose, Viswanadhan, and Wendoloski 1999).
- ✓ Veber filter: According to this filter a compound is drug-like if it has the number of rotatable bonds ≤ 10 , and the topological polar surface area $TPSA \leq 140$ (Veber et al. 2002).
- ✓ Egan filter: According to this filter a compound is drug-like if it has $WLOGP \leq 5.88$; and $TPSA \leq 131.6$ (Egan, Merz, and Baldwin 2000).
- ✓ Muegge filter: According to this filter a compound is drug-like if it has MW between $200 \leq MW \leq 600$; $XLOGP$ between $-2 \leq XLOGP \leq 5$; $TPSA \leq 150$; Number of rings ≤ 7 ; Number of carbons > 4 ; Number of hetero atoms > 1 ; Number of rotatable bonds ≤ 15 ; Number of H-bond acceptors ≤ 10 ; and Number of H-bond donors ≤ 5 (Muegge, Heald, and Brittelli 2001).
- ✓ Abbott Bioavailability Score: According to this filter a compound is drug-like if it has the probability of permeability and bioavailability (F) $> 10\%$ in rats (Martin 2005).

Medicinal Chemistry Properties:

The prediction of medicinal chemistry properties like PAINS, Brenk structural alert, lead likeness and synthetic accessibility will be very useful for the medicinal chemists in their drug discovery process.

- ✓ PAINS or Pan Assay INterference Compounds: These are recurrent hitters or random chemical compounds which are false positives in high throughput drug screening. The compounds under this category react non-specifically with any biological target instead of one specific target (Baell and Holloway 2010). It is very important to predict whether a given compound is a PAINS compound or not before synthesizing it.
- ✓ Brenk Structural Alert: This alert is given if the compound contains chemical moieties which are unstable and potentially toxic (Brenk et al. 2008). So it is

important to predict if the given compound has toxic moieties so that they can be replaced with safer groups.

- ✓ Lead Likeness: A good lead like compound is generally small, less hydrophobic than the drug-like compounds, shows a non-covalent high affinity ligand binding, monoionic, hydrophobic, hydrogen bonding, time-independent reversible competitive binding. A good lead like compound binds accurately to its protein target in the biochemical assay and shows a viable structure-activity relationship (SAR). Ultimately it helps in identifying potential compounds to further optimize and synthesize by medicinal chemistry (Rishton 2003; Teague et al. 1999).
- ✓ Synthetic Accessibility: This parameter indicates how much a given compound is accessible to synthesize it chemically by the medicinal chemists. It is indicated as a score based on the analysis of molecular fragments of more than 13 million chemical compounds. The range of the score is between 1 (very easy) to 10 (very difficult). The compound having a molecular fragment which is more frequent is easier to synthesize, while the one which is rare is very difficult to synthesize (Ertl and Schuffenhauer 2009).

Water Solubility:

It is of utmost importance for a compound to be soluble in order to be orally bioavailable and in turn be an effective drug. A compound can be handled easily and formulated as a tablet/capsule/tonic/injection only if it is soluble. The solubility class logarithmic scale (Log S scale) for a compound is

Insoluble < -10 < Poorly < -6 < Moderately < -4 Soluble < -2 Very < 0 < Highly

The water solubility of a compound can be predicted based on the following topological methods

- ✓ ESOL (Estimated SOLubility): The physical methods of aqueous solubility estimation like accurate equilibrium solubility determination are time-consuming experiments. This quantitative structure-property relationship (QSPR) based computer prediction is a simple, swift and robust method to predict the water solubility of a given molecule based on its structure. The model is built on the basis

of a linear regression of the dataset containing 2874 measured solubilities against the parameters like calculated logP (clogP), molecular weight, rotatable bonds, aromatic proportion, non-carbon proportions, H-bond donors, H-bond acceptors and polar surface areas. The final model considers only four properties namely clogP, molecular weight, aromatic proportions and the number of rotatable bonds as they contribute enormously to the solubility of a compound. The clogP or octanol-water partition coefficient is a direct estimate of solubility. The low molecular weight compounds tend to solubilize earlier. The aromatic rings and number of rotatable bonds in the compound increase flexibility, entropy and in turn the solubility (Delaney 2004).

- ✓ Log S (Ali method): This model considers the effect of phenol and phenol like groups in hiking the solubility of a compound. The model is based on a dataset of 1265 molecules and its accuracy of predicting aqueous solubility is ± 1 log unit (Jogoth et al. 2012).
- ✓ Log S (SILICOS-IT): This is a fragmental method calculated by FILTER-IT program, version 1.0.2, of the SILICOS-IT (<http://www.silicos-it.com>).

Pharmacokinetic properties:

The BBB permeation, skin permeability coefficient (Log K_p) and interaction of molecules with the cytochromes P450 and P-glycoprotein are the pharmacokinetic properties which can be predicted using the tool. The BBB permeation is based on the BOILED-Egg model. If the skin permeability coefficient (Log K_p in cm/s) value is more negative it means that the given compound is less skin permeable.

It is crucial in the drug discovery process to assess whether a given compound is a substrate of permeability-glycoprotein (P-gp) or an inhibitor of the cytochromes P450 (CYP) superfamily of isoenzymes. P-gp is an ATP-dependent efflux pump on the cell membranes that pumps out the xenobiotics. Many drugs have been reported which accidentally inhibit the P-gp but not as specific target. So it is crucial to predicting whether a given compound is a substrate for P-gp. The Cytochromes P450 (CYP) superfamily of isoenzymes has five important isoforms (CYP1A2, CYP2C19, CYP2C9, CYP2D6, CYP3A4) which are crucial for the xenobiotic elimination by metabolic biotransformation. If any drug molecule inhibits CYPs, it may lead to decreased clearance and increased accumulation of the drug in the body which leads to adverse drug-drug interactions. It is

estimated that about 50-90% of the chemotherapeutic small molecules inhibit the CYP isoforms. So it is very important to check whether a given compound inhibits the CYP isoforms.

Lipophilicity Properties:

The lipophilicity of a given compound depends on its n-octanol and water partition coefficient ($\log P_{o/w}$). Using the tool, this property is calculated by five predictive models like XLOGP3, WLOGP, MLOGP, SILICOS-IT, and iLOGP. Later consensus $\log P_{o/w}$, an arithmetic mean of above five values, is automatically calculated (Daina, Michielin, and Zoete 2017; Lipinski et al. 2012; Moriguchi et al. 1994; Wildman and Crippen 1999).

3.6 Prediction of Target Class for Withaferin A:

The Swiss Target prediction tool was used for the ‘Target Class’ prediction of WA, which is an online tool for the computer-aided drug design offered by the Swiss Institute of Bioinformatics. The tool accurately predicts new reliable targets in diverse species, for bioactive small molecules which can be used in the follow-up experiments. A table of probable targets ranked according to their score in relation to the query molecule and a pie chart showing the percentage of different target classes is obtained.

The proteins evolving from a common predecessor have similar structure and function, and in most cases similar bioactive small molecules bind to these similar proteins, modulating their activity, and showing phenotypic effects. The actual molecular target of chemical compounds and their possible off-target effects are not known in the routine phenotypic assays. Many compounds might be having more than one target but are not known. Probing into the mechanism of action of small bioactive molecules helps in knowing the expressed phenotypes, forecasting their probable adverse effects or cross-reactivity and the possibility of repositioning/repurposing for new applications. The target for a new query compound can be forecasted by pointing out proteins bound to the familiar ligands which are a look-alike to it. In the modern-day drug discovery, chemical compounds are screened against arrays of protein targets and computational predictions narrow the group of potential targets and suggest the consequential targets for known compounds. The databases like ChEMBL, DrugBank, PubChem, ZINC contain large datasets of interactions between the proteins and small molecules.

The SMILES notation of WA was provided into the box in the web interface which is freely accessible at <http://www.swisstargetprediction.ch>. The server, using the 2D and 3D similarity properties in coordination, differentiates the query molecule to a library of 2,80,381 compounds combining with 2,686 targets of human, mice, rat, cow, and horse (Gfeller et al. 2014; Gfeller, Michielin, and Zoete 2013).

Objective II

In silico and *in vitro* Inhibition Studies of Withaferin A on *Ld* DHFR-TS, the Other Potential Enzyme in The Folate Biosynthesis Pathway

3.7 Similarity Search between PTR1 and DHFR-TS of *L. donovani*:

The amino acid sequences of PTR1 (accession no. CBZ34227.1) and DHFR-TS (accession no. CBZ31672.1) of *L. donovani* were acquired from the GenBank, National Center for Biotechnology Information database (NCBI) (<http://www.ncbi.nlm.nih.gov>). The similarity between the enzymes was identified using the Clustal Omega online tool (<https://www.ebi.ac.uk/Tools/msa/clustalo/>).

3.8 Interaction between PTR1 and DHFR-TS of *L. donovani*:

The amino acid sequences of PTR1 and DHFR-TS were submitted in the STRING online protein-protein interaction prediction tool (<https://string-db.org/>) to forecast if there is any kind of interaction between these two enzymes. The STRING is a library of familiar and forecasted physical and functional protein-protein interactions which are from the computational predictions and interactions clustered from the other libraries. These interactions are acquired from the genomic predictions, cutting edge lab experiments, conserved co-expression, programmed text mining, and the existing information from databases. It presently covers 96,43,763 proteins from 2,031 organisms (Szklarczyk et al. 2015).

3.9 Comparison of Similarity between *Ld* DHFR-TS and Other *Leishmania* Species:

The *L. donovani*, *L. chagasi*, *L. infantum*, *L. major* DHFR-TS protein sequences, (accession no. CBZ31672.1, AAM88576.1, AAM82248.1, and CAJ02132.1) (520 amino acids) were obtained from the GenBank NCBI in the Fast Alignment (FASTA) format and the similarity search was performed in the Clustal Omega online tool to observe the intra-species similarity of DHFR-TS enzyme.

3.10 Comparison of Similarity between *Ld* DHFR-TS and Human DHFR and TS Genes and Proteins:

The nucleotide sequences of *Ld* DHFR-TS (accession no. AY123971.1), Hu DHFR (accession no. AH002819.2) and Hu TS (accession no. NM_001071) genes, amino acid sequences of *Ld* DHFR-TS, Hu DHFR (accession no. AAH71996.1) and Hu TS (accession no. NP_001062.1) proteins were obtained from the GenBank, NCBI database. The similarity between the host and the parasite genes and proteins was examined using the Clustal Omega online tool. The secondary structure details between the host and the parasite enzymes were compared.

3.11 Homology Modeling of *L. donovani* DHFR-TS:

The 3D structures of proteins greatly help in understanding their function. Many protein and protein-ligand complexes have been solved by the biophysical advancements like X-ray Crystallography, NMR Spectroscopy and Electron Microscopy. The Protein Data Bank (PDB: <http://www.rcsb.org/pdb>) is a protein 3D structure database with nearly 1,10,777 experimentally resolved structures. The 3D structure of target compound can be retrieved from the PDB. If not, it can be modelled using the computational methods by performing a homology or comparative modeling, which is the most accurate and efficient for construction of the 3D structure of proteins and yields good models convenient for an extensive range of operations, including the structure-based drug designing and virtual screening (Kopp and Schwede 2004). Generally, the proteins with matching amino acid sequences have related 3D structures and the homology modeling based protein structure prediction depends on an already available experimentally determined structure of a related protein from the same or different species. The homology modeling builds a 3D structure of a protein for which a 3D structure does not exist, from its primary structures by comparing with different established protein structures. A protein which lacks a 3D structure, for which a model is to be generated, is called the target. An experimentally established protein 3D structure is called the template, using which a model can be generated. To generate a model, both the target and the template should have at least 30% or more sequence or structure similarity (Cavasotto and Phatak 2009). The homology modeling involves several steps like template identification, multiple sequence alignment, backbone generation, loop modeling, side-chain modeling, model optimization and verification. The 3D structures of ligands can be accessed from the databases like Pub

Chem (<http://pubchem.ncbi.nlm.nih.gov/>). Later, the ligand is pre-processed to get a clear structure with right molecular mechanical specifications and atom types. Many soft wares perform the ligand preparation and optimization which generate active conformations appropriate to study the interaction with the target molecules. Most software's apply following steps for the ligand optimization a) removal of counter-ions from the parent molecule b) protonation of the ligand, neutralisation of the charged groups followed by ionisation and c) generation of tautomeric or stereoisomeric states of the ligand. The ligand structures are generated based on the number of chiral carbons present and are minimized to relax in the 3D space. The formal charge and bond order of nitrogen is checked before performing the docking. The virtual screening is a novel sophisticated automation in the drug discovery, which is correlative to the laboratory high throughput screening (HTS). Here the computational docking of molecules into the active site of receptors can be performed to identify the potential lead structures (Lyne 2002).

A sequence similarity search was performed between *Ld* DHFR-TS and *T. cruzi* DHFR-TS in the Swiss model (<http://swissmodel.expasy.org/interactive#alignment>) (Biasini et al. 2014) and identified it as the best suited template sequence. The target-template sequence identity was computed using the BLOSUM62 substitution matrix. The template for structural modeling was confirmed using the PDB-BLAST in the PDB. As *Ld* DHFR-TS has no 3D structure in the PDB, the crystal structure of *T. cruzi* DHFR-TS with NADPH, dUMP and C-448 antifolate (PDB ID: 3INV) were employed as the template to build the homology model of *Ld* DHFR TS. The full-length protein sequence in the FASTA format and the 3D structure in the .pdb format of *T. cruzi* DHFR-TS protein were acquired from RCSB PDB (<http://www.rcsb.org/pdb/home/home.do>). The ligands were removed and only, enzyme was selected by the software before the homology modeling. The protein model was constructed using the SWISS Model (<https://swissmodel.expasy.org/>) (Arnold et al. 2006; Bordoli et al. 2008; Guex and Peitsch 1997; Schwede et al. 2003) and checked with the Ramachandran plot, prot param, PROCHECK analysis, Global Model Quality Estimation (GMQE) and Qualitative Model Energy Analysis (QMEAN) scores (Benkert, Tosatto, and Schomburg 2008). The global and per-residue model quality has been evaluated with QMEAN scoring function. The generated model was further verified by the PROCHECK and PDB sum online server. The accuracy of the back bone torsion angles Φ (phi), φ (psi) of the modeled protein was inspected by the PROCHECK, and the Ramachandran plot was generated. Various physical and chemical specifications of the

modeled protein like molecular weight, theoretical pI, amino acid composition, extinction coefficient, aliphatic index and grand average of hydropathicity etc. were checked with prot param tool (<http://web.expasy.org/protparam/>). The secondary structure details between the target and the template were compared.

3.12 Molecular Docking of Enzyme and Ligand:

The 3D structures of the ligands WA, MTX and DHFA (PubChem CID 265237, 126941, 98792, respectively) were acquired from the PubChem database (<https://pubchem.ncbi.nlm.nih.gov/>). The open Babel (http://openbabel.org/wiki/Main_Page) was used to convert the parameters into the .pdbqt format. The docking was performed in Auto Dock Vina, which is the most extensively used freely available docking software (Trott and Olson 2010). Initially, the blind docking, i.e., a random search for binding sites on the protein, followed by docking within the restricted search space around the possible binding sites for the refined docking was performed. The best conformations were selected based on the binding affinity and the binding energy values. Pymol (<https://www.pymol.org/>) was used for the visualization and the graphical representations. The DHFA, substrate for DHFR-TS enzyme, MTX, the competitive inhibitor and WA, the ligand were docked. Later, the amino acid environment around the binding pocket was compared between all the three ligands. All the three ligands were docked with Hu DHFR and Hu TS (Kaul and Wadhwa 2017).

3.13 Molecular Dynamic Simulations:

The 3D structures available on databases are snapshots of the highly stationary spatial conformation. The protein complexes generated through the homology modeling and the docking are also snapshots. These stationary snapshots give detailed spatial information regarding the molecular structures and the protein-ligand interactions but do not pin point the molecule's dynamic properties and their interactions temporally. The molecular dynamics simulations (MDS) are utilized to analyze the dynamics of molecules. The MDS is useful in testing and developing the theoretical models using a more reliable depiction, give freedom to jump the barriers to testing theories, and give novel perceptions on the mechanisms and processes.

The MDS of *Ld* DHFR-TS, Hu DHFR, and Hu TS and their WA complexes were performed in the Gromacs 5.0(<http://www.gromacs.org/>) (Abraham et al. 2015). The topological parameter of the ligand was obtained from the ATB server (<https://atb.uq.edu.au/>) (Malde et al. 2011). Initially, the protein or its complex was kept in a cubic box and filled with water using the SPC/E water models. The system was energy minimized using the GROMOS54a7 force field (Huang, Lin, and Van Gunsteren 2011) and equilibrated at 300 K using V-rescale for 200 ps as NVT ensemble followed by the equilibration at 1atm pressure using the Parrinello–Rahman algorithm as NPT ensemble for 200ps. The equilibrated conformation was further extended for the production simulation for 25 ns. The LINCS algorithm was applied for the bond constraints with distance cut-off using the Verlet during simulation. The results were analyzed using the Gromacs tools and the binding energy (B.E) was calculated using the MM-PBSA tool (Genheden and Ryde 2015).

3.14 Cloning, Expression, and Purification of *L. donovani* DHFR-TS:

DNA Isolation:

For the nuclear DNA isolation, 10–15 ml of *L. donovani* promastigote culture was taken and the parasites were harvested at 4000 rpm for 15 min at 4°C. The DNA was obtained by employing the DNA extraction kit (Machery-Nagel, Deer Park, NY). Later the extracted DNA was pelleted and stored at -20°C for further use.

Media for Culturing of Bacterial Cells:

Luria Bertani (LB) liquid media:

To a few ml of doubled distilled water, 5 gm of yeast extract powder (HiMedia), 10 gm of peptone (HiMedia), and 5 gm of NaCl (HiMedia) were added and dissolved. Later the solution was diluted to 1000 ml, and the liquid media was autoclaved for 20 min at 121 lbs. pressure.

LB agar plates

For every one litre of the above LB Liquid media, 15 gm of agar-agar (HiMedia) was added before autoclaving. When the media is luke warm, kanamycin antibiotic solution (50 µg/ml) (HiMedia) was added and agar media was poured into 100 mm plates (Corning) and allowed to solidify under the laminar hood (Sambrook, et al., 1989).

Cloning of DHFR-TS gene:

The genomic DNA was employed as the template to extend the DHFR-TS coding region. The Phusion high-fidelity DNA polymerase (NEB) was employed to amplify, in a Veriti 96 well thermal cycler (Applied Biosystems). A set of primers were designed for *L. donovani* DHFR-TS gene sequence obtained from the GenBank, NCBI database (Accession no.: AY123971.1). The ORF was amplified using the forward / sense primer 5' AAT **CAT ATG** TCC AGG GCA GCT GCG AGG3' containing the restriction site Nde I and the reverse/antisense primer 5' TTT **AAG CTT** CTA TAC GGC CAT CTC CAT CTT GAT 3' containing the restriction site Hind III. The PCR amplification reaction contained 0.5 µg of the genomic DNA, 5X Phusion HF reaction buffer, 10 mM dNTP mixture, 10 picomoles each of DHFR-TS specific forward and reverse primers (Xcelris Labs Ltd) and 0.05 U/µl of Phusion DNA polymerase in 20 µl of final volume. The PCR reaction had an initial denaturation at 98°C for 30 sec, denaturation at 98°C for 10 sec, then annealing at 70°C for 30 sec, extension at 72°C for 1min, for a total of 35 cycles, succeeded by the extension at 72°C for 10 min. The augmented PCR product as a DNA band was visualized under the UV transilluminator after performing the 1% agarose (Lonza) gel electrophoresis. The amplified DHFR-TS PCR product was extracted with the gel extraction kit (Machery-Nagel). The eluted PCR product and the pET28a vector (Novagen) were double-digested with the restriction enzymes Nde I and Hind III (Thermo Fisher Scientific) in 20 µl final volume reaction mixture, for 3 hrs at 37°C and ligated with the T4 DNA ligase (Thermo Fisher Scientific) at 16°C overnight. The 20 µl final volume of ligation reaction mixture contained 10X Ligation buffer (Thermo Fisher Scientific), pET28a vector (Novagen), insert DNA (DHFR-TS PCR product), T4 DNA ligase and Milli Q water. The recombinant plasmid was transformed into the *E. coli* DH5α competent cells and the positive colonies were selected using the kanamycin resistance marker. A few hand-picked colonies from the master plate were grown in 300 µl of fresh culture for 4 hours. Later a colony PCR was performed to authenticate the existence of the gene of interest in the plasmid. The PCR positive colonies were grown in 10 ml of fresh LB media from which the plasmid was isolated and double-digested with the Nde I and Hind III restriction enzymes to release the insert.

Preparation of Competent Bacterial cells:

Briefly, an isolated colony was picked and dropped into 5 ml LB medium (without antibiotic) and was allowed to grow overnight at 37°C in a shaking incubator. This is called

primary culture. A secondary culture was grown by adding 500 μ l of overnight grown primary culture into 50 ml fresh LB medium (without antibiotic) in a shaking incubator at 37°C till the absorbance at 600 nm (OD_{600}) reached to 0.4-0.5. The culture was spun at 2000 x g for 5 min at 4°C. The pellet was dissolved in 2 ml of 0.1 M $MgCl_2$ (Sigma-Aldrich) centrifuged and the supernatant was removed. The pellet was dissolved in 5 ml 0.1 M $CaCl_2$ (Sigma-Aldrich) and incubated on the ice for 1-2 hrs. The cells were spun 2000 x g for 5 min at 4°C and the supernatant was removed. The pellet was dissolved in 2 ml of chilled 0.1 M $CaCl_2$ with 15% glycerol solution (HiMedia). The competent cells were aliquoted in volumes of 100 μ l and stored at -80°C until future use.

Transformation:

Briefly, 100 μ l of frozen competent cells were thawed on ice for few mins, 20 ng of the plasmid DNA was mixed and incubated on ice for 30 min. Later a heat shock was given to the cells at 42°C for 90s in the water bath after which the microtubes were immediately kept on ice for 5 min. 1 ml of fresh LB media (without antibiotic) was added to the above mixture and kept in a shaking incubator of 1 hour at 37°C. The cells were spun at 2000 rpm and the supernatant was removed and the pellet was dissolved in 100 μ l of fresh LB medium (without antibiotic) and this was spread on to an agar plate containing the kanamycin antibiotic and incubated overnight in the incubator at 37°C to obtain the transformed colonies.

Expression of Recombinant DHFR-TS protein:

The recombinant plasmid was transformed into *E. coli* BL21 cells and plated for further protein expression studies. An isolated colony was harvested from the plate and 10 ml of culture was grown over night. Later, the secondary culture was grown until the OD at 600 nm reached 0.5 – 0.6. The DHFR-TS protein expression was induced in the logarithmic phase culture (at OD_{600} of 0.5–0.6) for 4 hours with 1 mM IPTG (Sigma-Aldrich). Both the un-induced and induced cells were harvested and lysed in the 2 X sample buffer (100 mM Tris-HCl pH-8, 20% glycerol, 4% SDS (HiMedia), 2% β -ME (SRL), and 0.2% bromophenol blue (SRL)) and separated on a 12% SDS-PAGE (Laemmli, 1970).

SDS–Polyacrylamide Gel Electrophoresis (SDS–PAGE) and Western Blotting:

The uninduced and induced cell lysates were run on a 12% SDS–PAGE and the band was transferred onto a nitrocellulose membrane (Pall Life Sciences) using the transblot SD semidry transfer cell apparatus (BioRad). The membrane was blocked with the blocking

buffer (5% (w/v) skimmed milk powder (HiMedia) in 1 X TBS- 0.1% Tween20 (HiMedia)) for 1 h at RT. It was incubated for 1 h with the HRP conjugated his-tag mouse mAb (Cell Signalling Technology) (1:5000) in 1 X blocking buffer. Later, the blot was washed thrice with 1 X TBS-T (10 min each). Finally, the membrane was developed with the ECL™ prime western blotting detection kit containing luminol and peroxide solutions (GE health care) for visualization of the band using the ChemiDoc™ MP Imaging system (BioRad).

Purification of Recombinant DHFR-TS Protein:

The harvested induced cell pellet was dissolved in the lysis buffer (50 mM Tris pH 8.0, 0.25 M NaCl, 5 mM βME, 10 mM Imidazole (Sigma-Aldrich), 1 mM PMSF (SRL), and 0.2 mg/ml lysozyme (HiMedia)) and sonicated on the ice at 35 W with 5 pulses for 30 s each. The cell lysate was centrifuged at 12000 rpm for 15 min at 4°C and the supernatant and the pellet were used to perform the SDS-PAGE to visualize the recombinant protein in the inclusion bodies (pellet) but not in the soluble fraction (supernatant).

Purification of Recombinant Protein from Inclusion Bodies:

The BL21 cell culture pellet was dissolved in the lysis buffer (50 mM Tris-HCl (HiMedia), pH 8.0, 10 mM EDTA (SRL), 5% (v/v) Glycerol (HiMedia), 1 mM DTT (HiMedia), 50 mM NaCl (HiMedia), 1 mM PMSF (SRL), 0.2% (w/v) Sodium deoxycholate (NaDOC) (SRL) and 200 µg/mL lysozyme(HiMedia)) and was incubated on the ice for 30 minutes. Later it was sonicated on ice for 3 X 30 sec bursts and then centrifuged at 12500 rpm, for 15 mins at 4°C. The supernatant was removed and the pellet was washed with 20 mL wash buffer (50 mM Tris-HCl, pH 8.0, 0.1 mM EDTA, 5% (v/v) Glycerol, 0.1 mM DTT, 50 mM NaCl, and 2% (w/v) Sodium deoxycholate (NaDOC)) for 1 h by stirring at 4°C on a magnetic stirrer at 500 rpm. The sonication was repeated and centrifuged at 12500 rpm for 20 min at 4°C. The washing step was repeated twice. Later, the pellet was dissolved in the solubilization buffer (5M Guanidinium hydrochloride (SRL), 50 mM Tris-HCl pH 8.5 and 400 mM L-Arginine (SRL)) for 1 h by stirring at 4°C on a magnetic stirrer at 500 rpm. It was spun at 15000 rpm for 30 min at 4°C to remove the un-solubilized protein. The pellet was discarded and the supernatant was preserved in which the solubilized protein was present. This was added drop by drop into the refolding buffer (50 mM Tris- HCl, pH: 8.0, 200 mM L-Arginine). The protein was kept in the refolding buffer at 4°C for 24 h to allow the proper refolding. Later it was spun at 12500 rpm at 4°C for 30 min to expel the

protein aggregates and concentrated using a protein concentrator (Amicon[®] ultra filter Merk Millipore) to obtain a clear protein solution.

Gene sequencing:

The recombinant plasmid containing the cloned gene was sequenced utilizing gene specific primers to match similarity with *L. donovani* DHFR-TS sequence. The gel electrophoresis was performed to see the plasmid's purity and integrity. The recombinant plasmid containing the cloned gene and gene specific forward and reverse primers were sent to Xcelris Labs Ltd. Ahmedabad for the Sanger sequencing.

3.15 Enzyme Assay:

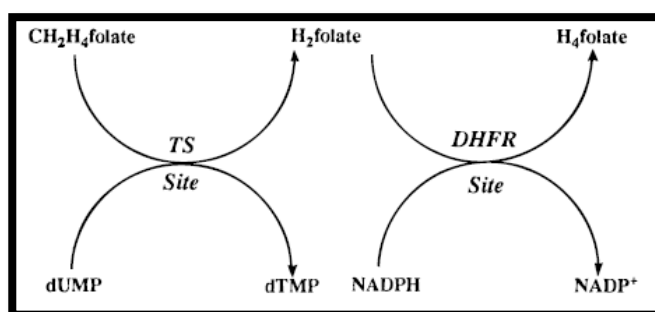


Fig 3.1: Conversion of NADPH to NADP⁺ by DHFR enzyme (Po-Huang Liang et al. 1998)

The DHFR activity was resolved spectrophotometrically by observing a decline in the OD at 340 nm that follows switching of the substrates NADPH and dihydrofolate to products the NADP⁺ and tetrahydrofolate. The standard assay mixture (1.0 ml) included 50 mM Tris buffer, pH 7.4, 5 mM DTT, 0.1 mM EDTA, 1 mg/ml BSA, 0.1mM NADPH (Sigma-Aldrich), 0.1 mM Dihydrofolate (Sigma-Aldrich), and 0.6 μM enzyme. The blanks contained all other reagents except NADPH as the reaction was initiated with the NADPH and a decline in the OD of NADPH at 340 nm was quantified spectrophotometrically (UV1800 Shimadzu Corporation Japan) (Pak-Lam et al. 1996, Po-Huang Liang et al. 1998).

Inhibition by Methotrexate:

The DHFR enzyme was inhibited by competitive inhibitor MTX. The standard assay mixture (1.0 ml) contained all the reagents, 0.1 mM dihydrofolate, and 0.6 μM enzyme along with 2 μM MTX (Sigma-Aldrich). The reaction was initiated with NADPH and a decline in the OD at 340 nm was quantified spectrophotometrically.

Inhibition by Withaferin A:

The DHFR enzyme was inhibited by WA. The standard assay mixture (1.0 ml) contained all the reagents, 0.1 mM dihydrofolate, and 0.6 μ M enzyme along with 1.2 μ M WA (Sigma-Aldrich). The reaction was initiated with NADPH and a decline in the OD at 340 nm was quantified spectrophotometrically.

Objective III

Determination of the Additive Effect of WA on Milt in the Treatment of Experimental VL

3.16 Parasites:

The *L. donovani* DD8 (MH0M/IN/80/DD8) parasites were procured from the American Type Culture Collection (ATCC, USA) and were cultured in the complete M-199 Medium, complemented with 15% heat-inactivated FBS (Sigma-Aldrich), 4 mM NaHCO₃ (Sigma-Aldrich), penicillin (100 U/ml) and streptomycin (100 mg/ml) (Sigma-Aldrich) pH 7.4 at 25°C in BOD Incubator.

3.17 Culture media:

To culture the *L. donovani* parasites M199 media has been used. Briefly, one litre of autoclaved Milli Q water was taken and 0.35 gm. of NaHCO₃ (Sigma-Aldrich) was added in the sterile conditions (under the hood). One bottle containing 10.6 gm. of M199 media powder (Sigma-Aldrich) was added in the above solution to make incomplete media. 15% Heat inactivated fetal bovine serum (FBS) (Sigma-Aldrich) and 1% penicillin, streptomycin (100 U/ml penicillin and 100 µg/ml streptomycin) (Sigma-Aldrich) were added to the incomplete media and percolated through the 0.22 µm sterile filter (Merk Millipore) under vacuum to make the complete media which was stored in the refrigerator (4°C) for further use.

To culture the mouse peritoneal macrophages and cell lines like J774.A1 and THP1 etc. the RPMI1640 media (Roswell Park Memorial Institute) is used. Briefly, one litre of autoclaved Milli Q water was taken and 2 gm. of NaHCO₃ was added in the sterile conditions (under the hood). One bottle containing 16.4 gm. of RPMI media powder (Sigma-Aldrich) was added in the above solution to make incomplete media. 10% Heat inactivated fetal bovine serum (FBS) and 1% penicillin, streptomycin (100 U/ml penicillin & 100 µg/ml streptomycin) were added to the incomplete media and filtered through the 0.22 µm sterile filter under vacuum to make the complete media which was stored in the refrigerator (4°C) for further use.

To culture, the *ex vivo* cells and various cell lines, the DMEM media (Dulbecco's Modified Eagle's Medium) is also used. Briefly, one litre of autoclaved Milli Q water was taken and

3.7 gm. of NaHCO₃ was added in the sterile conditions (under the hood). One bottle containing 10 gm of DMEM media powder (Sigma-Aldrich) was added in the above solution to make the incomplete media. 10% Heat inactivated fetal bovine serum (FBS) and 1% penicillin, streptomycin (100 U/ml penicillin & 100 µg/ml streptomycin) were added to the incomplete media and filtered through the 0.22 µm sterile filter under vacuum to make the complete media which was stored in the refrigerator (4°C) for further use.

3.18 Experimental Animals:

The inbred female BALB/c mice of 40-50 days age and 20-30 gm. weight used for the study were procured from Sainath agencies, Hyderabad and maintained in the animal house. All the experiments were done as per the institutional animal ethics committee (IAEC) guidelines. During the study, animals were kept at room temperature and uncontrolled natural photoperiod. They were given standard rodent pellets and drinking water *ad-libitum*.

3.19 Infection of Female BALB/C mice with *L. donovani* and the Drug Treatment:

The metacyclic promastigotes (the infective stage of the parasite) were isolated from the stationary phase promastigote culture by the ficoll gradient centrifugation method. The mice were injected with 1×10^7 *L. donovani* metacyclic promastigotes in 100 µl of phosphate buffer saline (PBS) via the tail vein injection under the aseptic conditions. After 5 weeks, the infected mice were divided into 5 groups, apart from the control mice.

- (i) Control (uninfected)
- (ii) Infected
- (iii) Infected and Milt alone treated (5 mg/kg BW/day, oral)
- (iv) Infected and WA alone treated (2 mg/kg BW/day, *i.p*)
- (v) Infected and treated with Combination I (2.5 mg/kg BW Milt + 2 mg/kg BW WA) by oral route
- (vi) Infected and treated with Combination II (2.5 mg/kg BW Milt oral + 2 mg/kg BW WA *i.p*)

The mice were weighed group wise, the average weight of each group was identified and the drug concentration was calculated accordingly. WA powder (Sigma-Aldrich) was dissolved in methanol, diluted with PBS and was given by an *i.p* injection in a final volume of 400 µl. Milt powder (Cayman Chemicals) was dissolved in milli pore water, diluted with

PBS and was given by an oral gavage in a final volume of 300 μ l. In one of the combination groups, both drugs were given by oral route and in the other group, each drug was given in their respective routes. In the respective routes combination group, first an *i.p* injection of WA and after 30 minutes, an oral dose of Milt was given. 7-weeks post infection/ 2-weeks after treatment, the mice were sacrificed. Before sacrificing the mice, the blood was collected through the retro-orbital method; it was allowed to clot at RT for 30 mins and was spun at 1000 rpm for 10 mins to obtain the serum which was stored at -80°C. The spleen and liver were collected for further study.

3.20 Weight parameters in mice:

The whole body weights of mice before and after treatment were measured by placing the mice on a sensitive balance. The spleen weight, after dissection was measured using the sensitive balance.

3.21 Preparation of Spleen cells:

The spleen was collected after dissecting the mice through the aseptic procedure and was kept in cold sterile cRPMI media. The spleen was homogenized under the aseptic condition using 100-micron cell strainers (BD Biosciences) and a micro pestle, by adding cRPMI media. The cells were centrifuged at 1500 rpm for 10 mins. The supernatant was removed and the pellet was dissolved in the RBC lysis buffer (15 mM NH₄Cl (SRL), 12 mM NaHCO₃ (Sigma-Aldrich) and 0.1 mM EDTA) and incubated on ice for 15 mins. The cells were washed and re-suspended in cRPMI media and were counted using the hemocytometer. The serial dilution was performed in a 96 well culture plate. 200 μ l of cRPMI media was taken in all the 96 wells. In the first well, 50 μ l of the spleen cells were added. Then 50 μ l from the first well was added in the second well and the serial dilution was continued till the last column. 50 μ l of the last column was discarded. The plate was placed in the BOD Incubator and was monitored for the parasite growth.

3.22 Preparation of Soluble Antigen (SLA) from *L. donovani* promastigotes:

The *L. donovani* promastigote culture was aliquoted into a 50 ml falcon and spun at 4000 rpm at 4°C for 15 mins. The supernatant was discarded and the pellet was washed thrice with PBS. The pellet was dissolved in 180 μ l of autoclaved Milli-Q water followed by freeze-thawing for 5 times in -80°C freezer. 20 μ l of the PIC (protein inhibitor cocktail) (Sigma-Aldrich) was added and vortexed. Sonication at 20% amplitude for 45 secs, 5 times with 1 min gap was performed. Later it was spun at 9980 rpm for 15 mins at 4°C. The

supernatant was gathered into another tube. The protein concentration was measured as 5 µg/µl using the Thermo Scientific™ NanoDrop 2000 UV-Vis spectrophotometer.

3.23 Estimation of IgG2a and IgG1 Titres in Serum by Indirect ELISA:

An indirect ELISA was performed to determine the IgG2a and IgG1 antibody titers in the sera of infected and treated mice. Briefly, the soluble leishmania antigen (SLA) of *L. donovani* was diluted in the coating buffer (PBS, pH 7.2) at 250 ng/100 µl/well and was adsorbed to 96 well plates at 4°C overnight. Later the plate was washed with the washing buffer (PBS containing Tween-20 (PBS-T) and blocked with the blocking buffer (1% BSA in PBS) for 2 hours at 37°C. The serum (1:100) from the control and the treated mice diluted in the dilution buffer were appended to the plate and incubated for 1 hr at 37°C. The plate was washed and incubated with 100 µl of anti-mouse IgG1 conjugated to the HRP and IgG2a (1:10,000) (abcam) for 1 hr at 37°C in the dilution buffer. Later, the plate was washed with the washing buffer and each well was incubated with 100 µl of TMB/H₂O₂ (Sigma-Aldrich) for 30 mins at RT. By adding 50 µl of 2 M H₂SO₄ (Fischer Scientific), the reaction was interrupted and the OD was quantified at 450 nm in an ELISA plate reader (TECAN).

3.24 Determination of Spleen Parasite Load:

The Mice were sacrificed and touch biopsies of the spleen were taken on the glass slides, fixed with methanol, stained with Giemsa stain (HiMedia) and visualized under the microscope (Leica). The Leishman-Donovan units (LDU) were quantified to estimate the intensity of infection as (No. of amastigotes/No. of organ nuclei) X weight of organ in grams.

Giemsa Staining

Briefly, thin smears of the parasite culture on glass slides are made, air dry and fixed with methanol for 5 mins. Later the slide is flooded with diluted Giemsa Stain (1 vol of stain: 9 vols of Dis. H₂O) for 30 mins. The stain is washed away gently with distilled water keeping the slide in a slanting position and after drying it is observed under the microscope.

3.25 Histopathological Examination of Liver Tissue:

The mice were sacrificed. The control and the treated group mice liver sections were stored in 10% formalin saline (9 gm NaCl, 100 ml of 40% formaldehyde, 900 ml water). The tissues were sent to Sridevi histology center, Hyderabad for Haematoxylin-Eosin staining

to estimate the granuloma formation. After the H-E staining was performed, the number of granulomas per 50 fields was estimated under the microscope.

3.26 Estimation of Different Biochemical Parameters in Serum:

Before sacrificing the mice, the blood was obtained by the retro-orbital method and the serum was extracted within 30 mins by spinning at 1500 rpm for 10 mins.

3.27 Estimation of Serum Glucose:

The serum glucose concentration was estimated using the blood glucose monitoring device ACCU-CHEK® Active (Roche). 10 µl of serum of the healthy, infected and treated mice was placed on the test strip and the concentration was visualized on the screen as numbers.

3.28 Estimation of Serum Cholesterol:

The quantitative determination of the serum cholesterol concentration by the photometric method was performed using the CHOLESTEROL-SR® *invitro* diagnostic kit (Prism Diagnostic Pvt Ltd). The blank, standard and the unknown samples (healthy, infected and treated) were mixed with the reagent provided in the kit, incubated for 15 mins at RT and then the absorbance was measured using the spectrophotometer (UV1800 Shimadzu Corporation Japan) at 505 nm. The Serum cholesterol concentration (mg/dl) was determined using the formula: absorbance of sample/ absorbance of standard X standard concentration. The normal range of the cholesterol concentration is 200 mg/dl.

3.29 Estimation of Serum Triglycerides:

The Quantitative determination of the serum triglyceride concentration by the photometric method was performed using the *in vitro* diagnostic kit (Prism Diagnostic Pvt Ltd). The blank, standard and the unknown samples (healthy, infected and treated) were mixed with the reagent provided in the kit, incubated for 15 mins at RT and then OD was measured in the spectrophotometer at 505 nm. The serum triglyceride concentration (mg/dl) was determined using the formula absorbance of sample/ absorbance of standard X standard concentration. The normal value of the triglyceride concentration ranges from 30 to 150 mg/dl.

Chapter IV

Results

and

Discussion

Objective I

In-silico Prediction of Drug-like Properties of Withaferin A and Miltefosine (positive control)

4.1 Withaferin A is 'Drug-Like' molecule:

As per the prediction of the molsoft tool, WA has drug-like properties which are very much comparable to Milt. All the parameters like MF, MW, HBA, HBD, Mol Log P, Mol Log S, Mol PSA, Mol Vol, No. of Stereo centers are within the scope of the Lipinski's Rule of Five (table 4.1).

Table 4.1: Drug likeness properties of WA and Milt as analyzed by Molsoft

Molecular properties	Withaferin A	Miltefosine
MF (Molecular Formula)	C ₂₈ H ₃₈ O ₆	C ₂₁ H ₄₆ NO ₄ P
MW (Molecular Weight)	470.27g/mol	407.32g/mol
HBA (No. of Hydrogen Bond Acceptors)	6	4
HBD (No. of Hydrogen Bond Donors)	2	0
Mol Log P (Octanol/water partition coefficient)	3.21	6.50
Mol Log S (Water solubility)	-4.07(in Log(moles/L)) 39.60 (in mg/L)	-4 (in Log(moles/L)) 40.31 (in mg/L)
Mol PSA (Molecular Polar Surface Area)	75.66 A ²	45.06 A ²
Mol Vol (Molecular Volume)	564.08 A ³	457.31 A ³
No. of Stereo centers	11	0

As per the drug-likeness plots, the score was 0.36 for WA and 0.03 for Milt (fig.4.1).

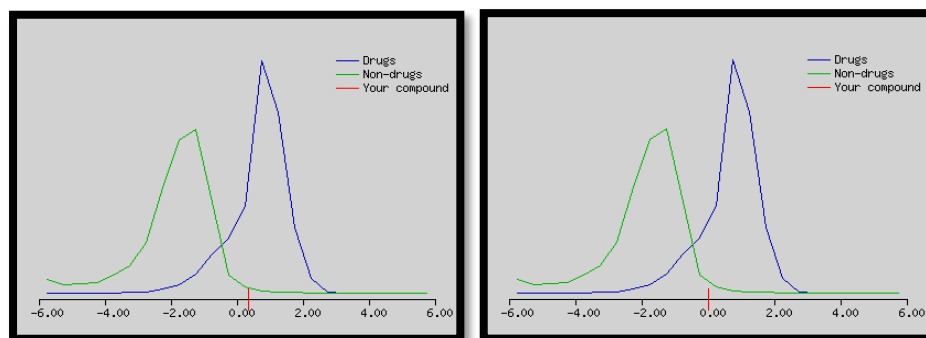


Fig 4.1: Drug likeness plots and scores of WA and Milt.

4.2 Withaferin A is Absorbed in the GI Tract:

As per the prediction of the BOILED-Egg model, WA is being absorbed in the GI tract and does not cross the BBB. It does not affect the CNS as it is effluxed out by the P glycoprotein. WA is shown as a point in the white region in the model, so it probably is absorbed passively by the GI tract. The molecules predicted to be effluated from the CNS by the P-glycoprotein are shown as blue dots. Both WA and Milt are comparable in these properties, as both are being absorbed in the GI tract and effluxed out by the CNS (fig.4.2).

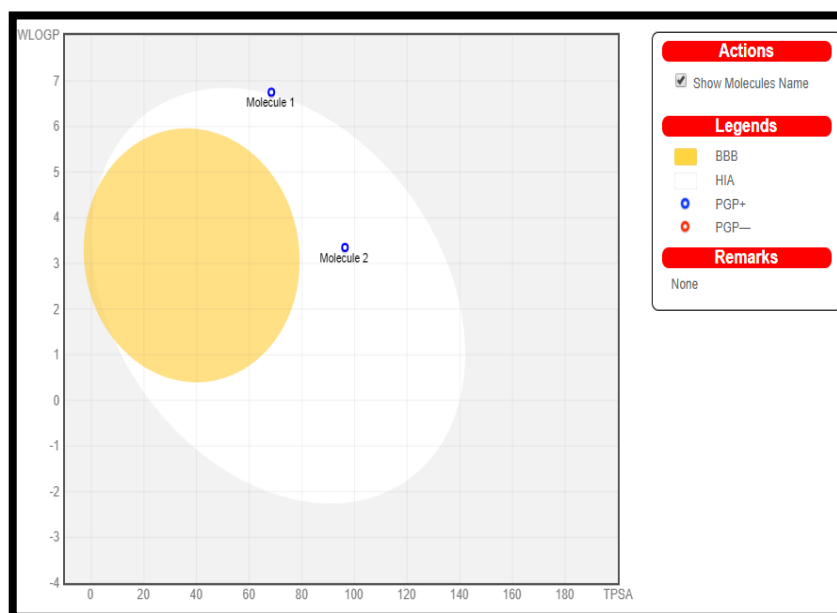


Fig 4.2: WLOGP versus TPSA plot; Prediction of the Gastrointestinal Absorption and the Blood Brain Barrier Penetration Capacity of WA and Milt using the BOILED-Egg model; BBB: the points located in the yolk are the molecules predicted to passively permeate through the Blood Brain Barrier; HIA: the points located in the white are molecules predicted to passively absorbed by the gastrointestinal tract; PGP+: the blue dots are for the molecules predicted to be effluated from the CNS by the P- Glycoprotein; PGP-: the red dots are for the molecules predicted to be effluated from the CNS by the P- Glycoprotein; Wlog P - n-octanol/water partition coefficient by Wildman & Crippen; TPSA -topological polar surface area.

4.3 Withaferin A has Oral Bio-Availability:

The oral bioavailability for WA was calculated as 75.75% and for Milt as 85.38% which are comparable to each other. The radar plot of WA and Milt is falling within the pink colored hexagon, generated by the server, which is the physicochemical space available for the oral bioavailability (fig 4.3).

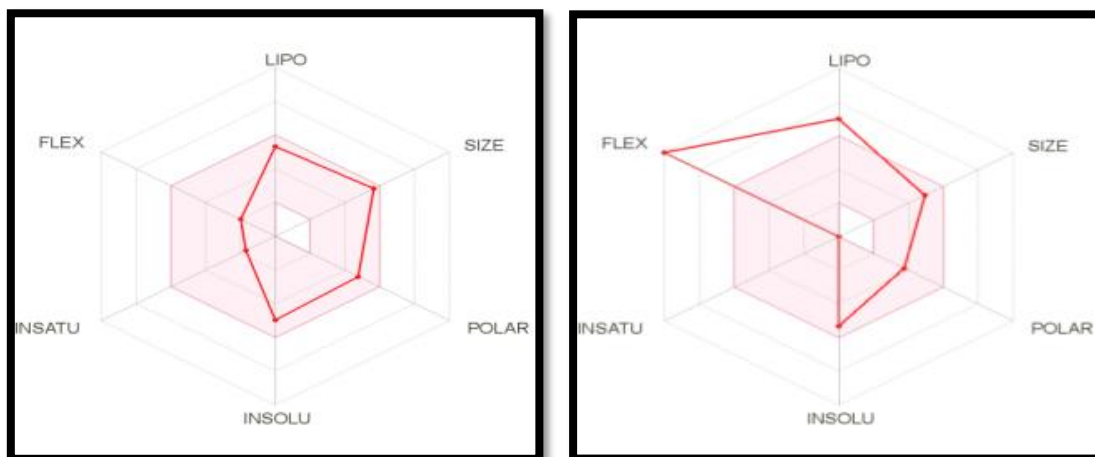


Fig 4.3: Prediction of Oral Bio-Availability for WA and Milt.

4.4 Withaferin A is not Cardio-toxic:

According to the prediction of the 'Pred-hERG 4.0', WA has no cardiac toxicity and does not block the hERG ion channel on the heart tissue (fig 4.4).

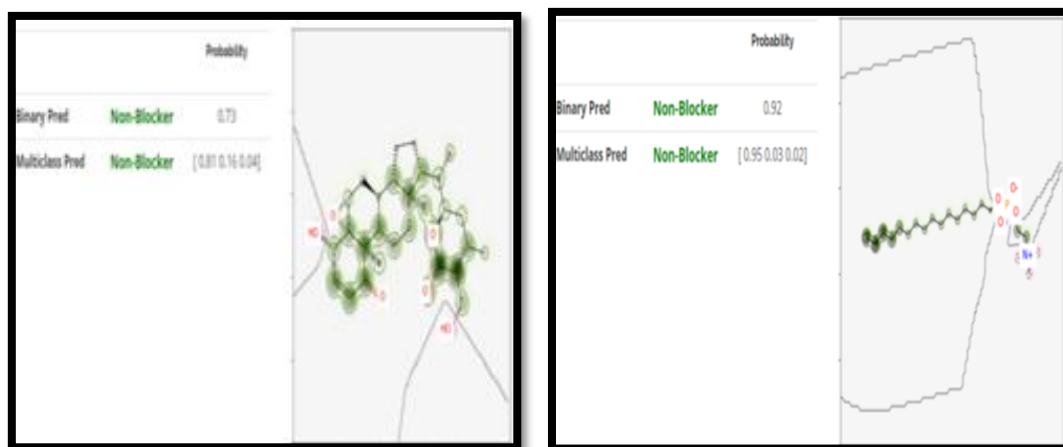


Fig 4.4: Prediction of Cardiac toxicity for WA and Milt

4.5 Withaferin A has Good ADME Properties:

All the parameters indicating the ADME properties of WA and Milt like physicochemical, drug-likeness, lipophilicity, medicinal chemistry, water solubility and pharmacokinetic

properties are indicated in the tables 4.2 to 4.7. WA does not inhibit the Cytochromes P450 (CYP) superfamily of isoenzymes. The synthetic accessibility score of WA suggests that the chemical synthesis of WA in its present form is little difficult. But the unwanted and bulky groups, which are only of structural importance, can be removed and a smaller structure can be synthesized with those groups which are of functional importance and involved in the binding to the target.

Table 4.2: Medicinal Chemistry Properties

Property	Withaferin A	Miltefosine
PAINS	0 alert	0 alert
Brenk	1 alert: Three-membered heterocycle	2 alerts: phosphor,aternary_nitrogen_2
Lead likeness	No; 2 violations: MW>350, XLOGP3>3.5	No; 3 violations: MW>350, Rotors>7, XLOGP3>3.5
Synthetic Accessibility	6.83	4.67

Table 4.3: Physicochemical Properties

Property	Withaferin A	Miltefosine
Formula	C ₂₈ H ₃₈ O ₆	C ₂₁ H ₄₆ NO ₄ P
Molecular weight	470.60 g/mol	407.57 g/mol
Num. heavy atoms	34	27
Num. aromatic heavy atoms	0	0
Fraction C sp ³	0.79	1
Num. rotatable bonds	3	20
Num. H-bond acceptors	6	4
Num. H-bond donors	2	0
Molar Refractivity	127.49	115.90
TPSA	96.36 Å ²	68.40 Å ²

Table 4.4: Drug-likeness Properties

Property	Withaferin A	Miltefosine
Lipinski	Yes; 0 violation	Yes; 0 violation
Ghose	No; 1 violation: #atoms>70	No; 2 violations: WLOGP>5.6, #atoms>70
Veber	Yes	No; 1 violation: Rotors>10
Egan	Yes	No; 1 violation: WLOGP>5.88
Muegge	Yes	No; 2 violations: XLOGP3>5, Rotors>15
Bioavailability Score	0.55	0.55

Table 4.5: Lipophilicity Properties

Property	WA	Milt	Property	WA	Milt
Log $P_{o/w}$ (iLOGP)	3.24	0.26	Log $P_{o/w}$ (MLOGP)	2.75	-0.08
Log $P_{o/w}$ (XLOGP3)	3.83	6.79	Log $P_{o/w}$ (SILICOS-IT)	3.93	5.45
Log $P_{o/w}$ (WLOGP)	3.35	6.75	Consensus Log $P_{o/w}$	3.42	3.83

Table 4.6: Water Solubility Properties

Property	Withaferin A	Miltefosine
Log S (ESOL)	-4.97	-5.32
Solubility	5.01e-03mg/ml;1.07e-05 mol/l	1.93e-03mg/ml;4.74e-06 mol/l
Class	Moderately soluble	Moderately soluble
Log S (Ali)	-5.55	-8.03
Solubility	1.33e-03mg/ml;2.82e-06 mol/l	3.77e-06mg/ml;9.26e-09 mol/l
Class	Moderately soluble	Poorly soluble
Log S (SILICOS-IT)	-3.79	-7.20
Solubility	7.54e-02mg/ml;1.60e-04 mol/l	2.55e-05mg/ml;6.25e-08 mol/l
Class	Soluble	Poorly soluble

Table 4.7: Pharmacokinetic Properties

Property	WA	Milt	Property	WA	Milt
GI Absorption	High	High	CYP2C19 inhibitor	No	No
BBB Permeation	No	No	CYP2C9 inhibitor	No	No
P-gp substrate	Yes	Yes	CYP2D6 inhibitor	No	No
CYP1A2 inhibitor	No	No	CYP3A4 inhibitor	No	No
Log K_p (skin permeation)	-6.45cm/s	-3.97cm/s			

4.6 Withaferin A Targets Enzymes:

As per the prediction by the Swiss Target prediction tool, the ‘target class’ for WA is ‘enzymes’ which is true for Milt. For WA, the probability of enzymes being the target is 70% and for Milt, it is 60% (figs. 4.5 and 4.6).

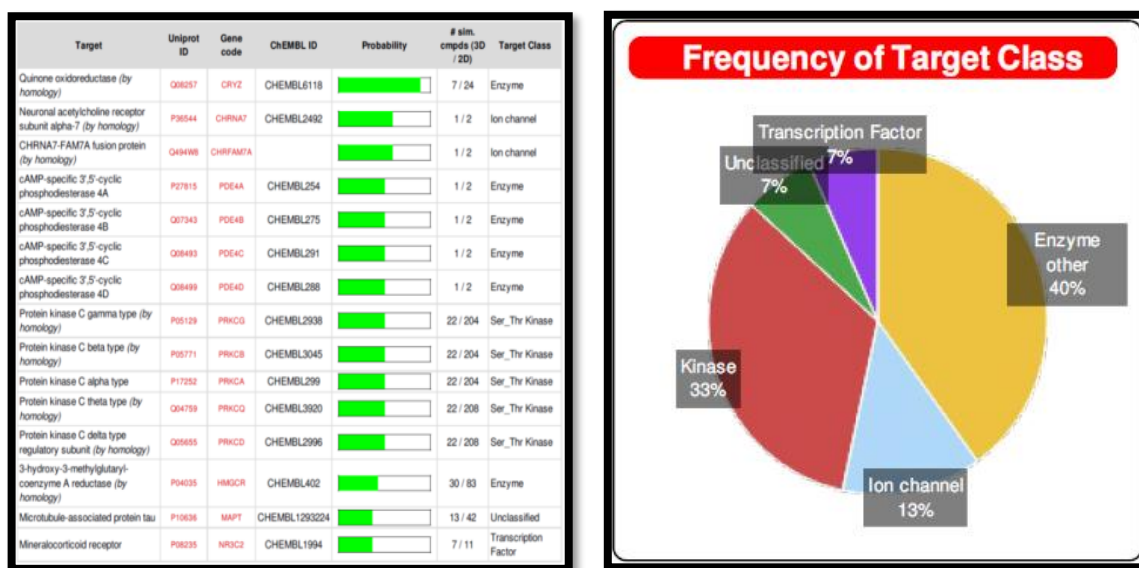


Fig 4.5: Prediction of the Target class for Withaferin A using the Swiss Target

Target	Uniprot ID	Gene code	CHEMBL ID	Probability	# sim. compds (3D / 2D)	Target Class
Camitine O-palmitoyltransferase 1, liver isoform (by homology)	P16416	CPT1A	CHEMBL1293194		0 / 1	Enzyme
Camitine O-palmitoyltransferase 1, brain isoform (by homology)	Q8TCD5	CPT1C			0 / 1	Enzyme
Camitine O-palmitoyltransferase 1, muscle isoform (by homology)	Q82523	CPT1B	CHEMBL2216739		0 / 1	Enzyme
Phospholipase A2, membrane associated	P14505	PLA2G6A	CHEMBL3474		0 / 5	Enzyme
Calcium-dependent phospholipase A2 (by homology)	P39877	PLA2G3	CHEMBL4323		0 / 5	Enzyme
Group IIF secretory phospholipase A2 (by homology)	Q862M2	PLA2G2F	CHEMBL4278		0 / 5	Enzyme
Group IIE secretory phospholipase A2 (by homology)	Q8N257	PLA2G2E	CHEMBL2154		0 / 5	Enzyme
Group IID secretory phospholipase A2 (by homology)	Q9JN94	PLA2G2D	CHEMBL4281		0 / 5	Enzyme
γ-lysophosphatidic acid receptor 1	Q82533	LPAR1	CHEMBL3819		0 / 10	Membrane receptor
γ-lysophosphatidic acid receptor 3	Q9J8Y5	LPAR3	CHEMBL3250		0 / 10	Membrane receptor
γ-lysophosphatidic acid receptor 2 (by homology)	Q9H890	LPAR2	CHEMBL3724		0 / 10	Membrane receptor
Phospholipase A2	P04054	PLA2G1B	CHEMBL4426		0 / 1	Enzyme
M-phase inducer phosphatase 1	P39304	CDG25A	CHEMBL3775		0 / 5	Ser_Thr_Tyr Phosphatase
M-phase inducer phosphatase 2	P39305	CDG25B	CHEMBL4804		0 / 5	Ser_Thr_Tyr Phosphatase
Platelet-activating factor receptor	P25105	PTAFR	CHEMBL250		0 / 1	Membrane receptor

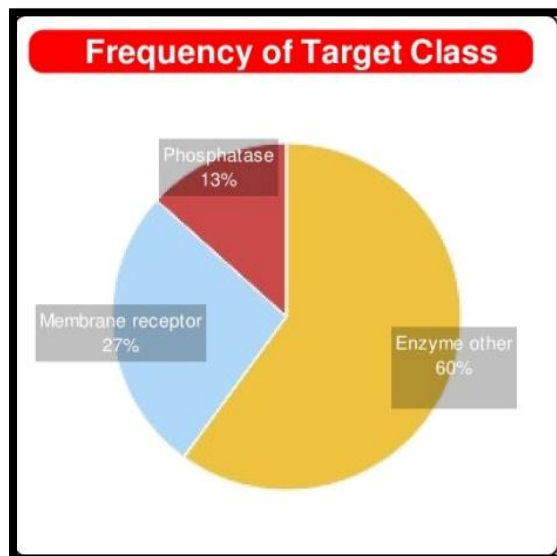


Fig 4.6: Prediction of the Target class for Miltefosine using the Swiss Target

Objective II

In-silico and *In-vitro* Inhibition Studies of Withaferin A on *Ld* DHFR-TS, the Other Potential Enzyme in the Folate Biosynthesis Pathway

4.7 PTR1 and DHFR-TS of *L. donovani* are Not Similar:

The PTR1 and DHFR-TS proteins (enzymes) of *L. donovani* have only 13.5% similarity. On the same lines, the 3D structures of these two proteins do not overlap with each other indicating the low structural similarity (fig. 4.7).



Fig 4.7: The multiple sequence alignment and the 3D structures of PTR1 (up) and DHFR-TS (down).

4.8 PTR1 and DHFR-TS of *L. donovani* do not Interact Physically:

As per the prediction by the STRING 4.0, PTR1 and DHFR-TS do not physically bind each other but they have a relation called ‘Gene Neighborhood’ (fig 4.8).

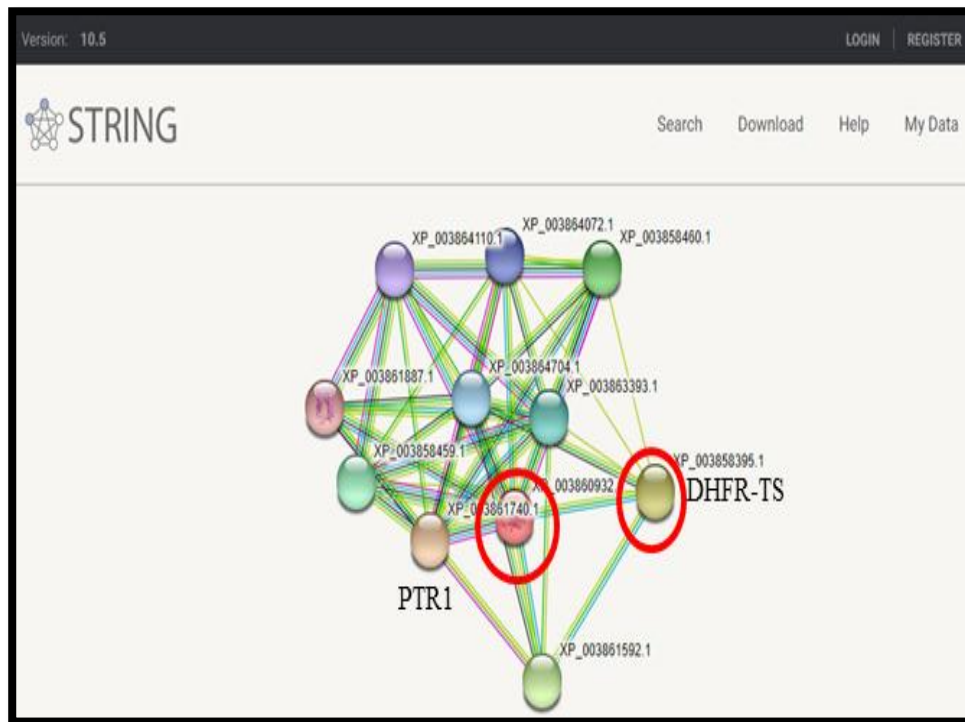


Fig 4.8: The interaction between PTR1 and DHFR-TS.

4.9 DHFR-TS is Highly Conserved among *Leishmania* species:

The percent similarity of DHFR-TS from *L. chagasi*, *L. infantum*, *L. major* with DHFR-TS of *L. donovani* is 99.2%, 99.8%, 95.7% respectively. This suggests that DHFR-TS is a highly conserved enzyme across the *Leishmania* species. So theoretically an inhibitor working in one species should also work on the other species (fig 4.9).



Fig 4.9: The multiple sequence alignment between different leishmania species.

4.10 *Ld* DHFR-TS and Human DHFR Genes and Proteins are Dissimilar:

The similarity between *Ld* DHFR-TS (1563 bp, 520aa) and Human DHFR (564 bp, 187aa) was 24.29% at the gene level where as it was 25.13% at the protein level (fig. 4.10).

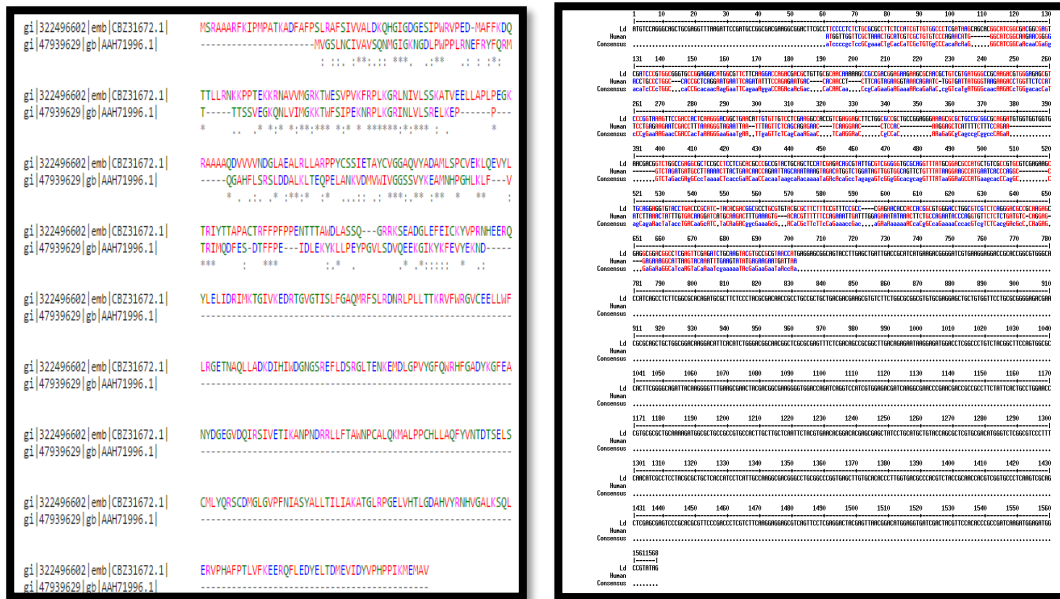


Fig 4.10: The multiple sequence alignment between *Leishmania* DHFR-TS and human DHFR gene and protein sequence.

4.11 *Ld* DHFR-TS and Human TS Genes and Proteins are Similar:

The *Ld* DHFR-TS (1563 bp, 520aa) and Hu TS (942 bp, 313aa) are 51.38% similar at gene and 54.63% at protein level (fig. 4.11).



Fig 4.11: The multiple sequence alignment between *Leishmania* DHFR-TS and human TS gene and protein sequence.

4.12 *Ld* DHFR-TS Model is Valid and Reliable:

The amino acid sequence of *Ld* DHFR-TS was blasted against the PDB-BLAST database for identifying a template. *T.cruzi* DHFR-TS has 67.32% identity with the *Ld* DHFR-TS and was

selected as the template (fig.4.12). The quality of the model generated by the Swiss-Model was verified using different tools (fig 4.13 and 4.14). The model with better scores in all measures was chosen which showed 0.2% of the residues in the disallowed regions of the Ramachandran plot with GMQE score of 0.82 and QMEAN score of -2.25 (table 4.8, fig 4.15). The Φ and Ψ backbone torsion angles of most of the non-glycine residues are within the allowed regions of which 86.2 % are in the energetically most favored area. Only 12.7% of residues are found in the additional allowed regions and 0.9% in the generously allowed region (table 4.9). The Prot Param results show that the protein model has MW of 58.7 kDa, pI is 7.13, has 65 negatively and 65 positively charged residues, the extinction coefficient is 67840, the aliphatic index is 85.37 and the grand average of hydropathicity (GRAVY) is -0.243 (table 4.10). The generated model is a homodimer of $\alpha+\beta$ class and the protein consists of 4 β sheets, 3 β α β units, 5 β hairpins, 11 β bulges, 19 β strands, 21 α helices, 14 helix-helix interactions, 57 β turns and 9 γ turns. Similar numbers of secondary structural elements were found in the *T. cruzi* DHFR-TS indicating that both the proteins belong to the class $\alpha + \beta$ and the RMSD between the template and the generated model was calculated to be 0.625Å (fig 4.14). All quality check results showed that the model is valid and reliable.



Fig 4.12: Sequence identity between *Ld* DHFR-TS and *T. cruzi* chain A. Asterisks indicate identical amino acids. Dots and colons indicate conserved amino acid substitutions. Dashes indicate gaps.

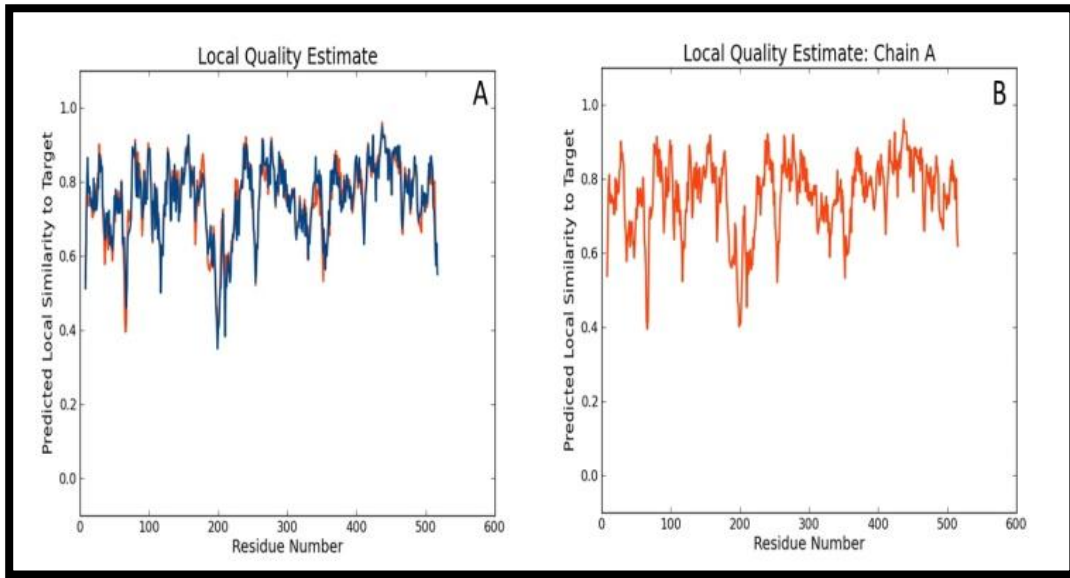


Fig 4.13: A local quality estimate of (A) modeled *Ld* DHFR-TS and (B) reference *T.cruzi* DHFR-TS obtained from Swiss model.

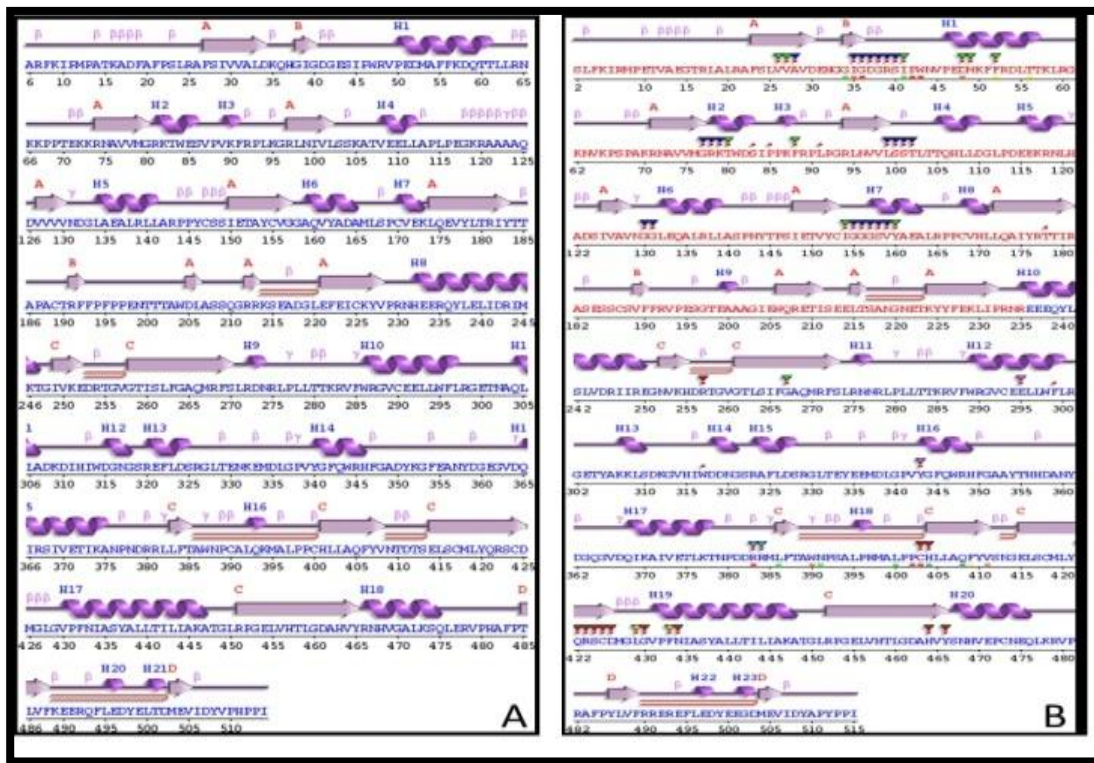


Fig 4.14: Secondary structures of (A) modeled *Ld* DHFR-TS and (B) reference *T.cruzi* DHFR-TS obtained from PDB sum.

Table 4.8: Features of the generated *Ld* DHFR-TS model from the Swiss model

Template	3inv.1.A	Resolution	2.37Å
Seq. Identity	67.32%	Seq. Similarity	0.50
Oligostate	Homodimer	GMQE	0.82
Coverage	0.99	QMEAN4	-2.25
Found by	user alignment	Description	Bifunctional Dihydrofolate reductase thymidylate synthase
Method	X ray		

Table 4.9: Ramachandran plot Statistics from the PROCHECK results for modeled *Ld* DHFR-TS protein and reference *T. cruzi* DHFR-TS protein

	No. of Residues		Percentage	
	Modelled <i>Ld</i> DHFR-TS	Reference <i>T. cruzi</i> DHFR-TS	Modelled <i>Ld</i> DHFR-TS	Reference <i>T. cruzi</i> DHFR-TS
Most favoured regions [A, B, L]	763	791	86.2%	89.4%
Additional allowed regions [a, b, l, p]	112	90	12.7%	10.2%
Generously allowed regions [~a, ~b, ~l, ~p]	8	4	0.9%	0.5%
Disallowed regions [XX]	2	0	0.2%	0.0%
Non-glycine and non- proline residues	885	885	100%	100%
End-residues (excl. Gly, Pro)	4	4		
Glycine residues	64	76		
Proline residues	64	62		
Total number of residues	1017	1027		

Table 4.10: Physical and chemical parameters of modeled protein from the Prot-Param tool

Number of amino acids	520		
Molecular weight	58703.6		
Theoretical pI	7.13		
Amino acid composition	Ala (A) 46- 8.8% Arg (R) 37- 7.1% Asn (N) 17- 3.3% Asp (D) 28- 5.4% Cys (C) 10- 1.9% Gln (Q) 16- 3.1% Glu (E) 37- 7.1% Gly (G) 32- 6.2%	His (H) 10- 1.9% Ile (I) 22- .2% Leu (L) 54- 0.4% Lys (K) 28- 5.4% Met (M) 14-2.7% Phe (F) 25- 4.8% Pro (P) 32- 6.2% Ser (S) 23- 4.4%	Thr (T) 30- 5.8% Trp (W) 8- 1.5% Tyr (Y) 16- 3.1% Val (V) 35- 6.7% Pyl (O) 0- 0.0% Sec (U) 0- 0.0% (B) 0 0.0% (Z) 0 0.0% (X) 0 0.0%
Total number of negatively charged residues (Asp + Glu)	65		
Total number of positively charged residues (Arg + Lys)	65		
Atomic composition	Carbon C 2634 Nitrogen N 720 Sulfur S 024	Hydrogen H 4132 Oxygen O 753	
Formula	C ₂₆₃₄ H ₄₁₃₂ N ₇₂₀ O ₇₅₃ S ₂₄		
Total number of atoms	8263		
Extinction coefficients (in units of M ⁻¹ cm ⁻¹ , at 280 nm measured in water)	Ext. coefficient- 68465 Abs 0.1% (=1 g/l) 1.166, assuming all pairs of Cys residues form Cystines Ext. coefficient- 67840 Abs 0.1% (=1 g/l) 1.156, assuming all Cys residues are reduced		
Estimated half-life (N-terminal of sequence considered is Met)	30 hrs (mammalian reticulocytes, <i>in vitro</i>). >20 hrs (yeast, <i>in vivo</i>). >10 hrs (E.coli, <i>in vivo</i>).		
Instability index	46.57 (Classifies protein as unstable)		
Aliphatic index	85.37		
Grand average of hydropathicity (GRAVY)	-0.243		

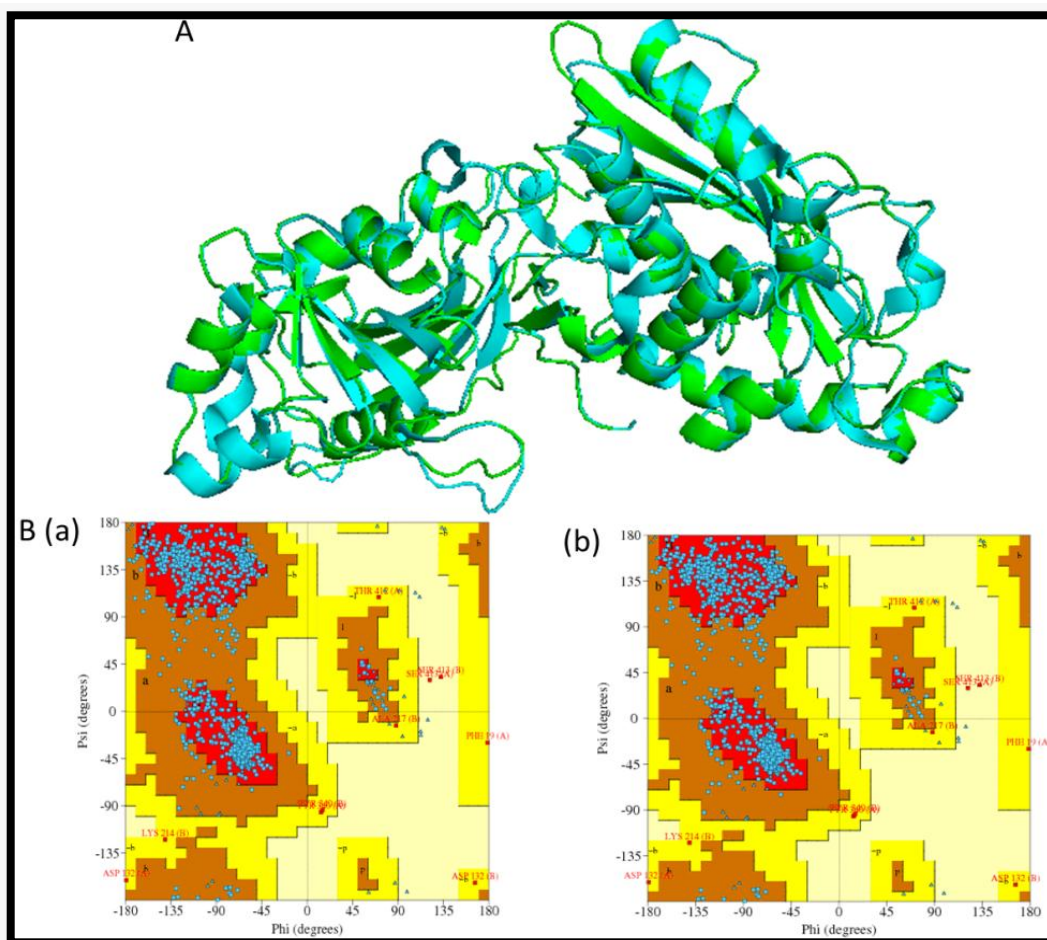


Fig 4.15: (A) Superimposed image of the template *T. cruzi* DHFR-TS chain A (PDB ID: 3INV) shown in blue and the modeled *Ld* DHFR-TS shown in green. (B) Ramachandran plot of a) modelled *Ld* DHFR-TS and reference *T. cruzi* DHFR-TS obtained using the PROCHECK.

4.13 Molecular Docking of Enzyme and Ligand:

To find the active site of *Ld* DHFR-TS, it was first docked with the substrate DHFA and found that DHFA binds at two active sites, one in the DHFR and one in the TS domain (fig 4.17). It is reported that an electrostatic channel is present connecting the two active sites and the substrate channeling, a phenomenon where a metabolite or intermediate is directly transported from one active site to another without being leaked into the solution occurs. The TS active site is situated 40Å from the DHFR active site (Elcock et al. 1996; Grumont et al. 1986; Liang and Anderson 1998). Asp 52, Arg 97 and Thr 180 of the DHFR domain form H-bonds with the DHFA and the B.E is -7 Kcal/mol. Arg 283, His 401, Gln 421, and Asn 433 of the TS domain form H-bonds with the DHFA and the B.E is -7.6 Kcal/mol.

As MTX is a competitive inhibitor of DHFR, the *Ld* DHFR-TS was docked with MTX to confirm the active sites. MTX is also binding at two active sites competing with the

substrate for the active site. Ser 86 of the DHFR domain forms H-bond with MTX and the B.E is -7.9 Kcal/mol. Arg 283, Glu 292, His 401, Gln 421 and Asn 433 of the TS domain form H-bonds with MTX and the B.E -7.6 Kcal/mol. The binding site for MTX was compared with the 3D crystal structure of the bifunctional *Tc* DHFR-TS in complex with MTX (3CL9), by superimposing on *Ld* DHFR-TS docked with MTX and the RMSD of the ligand was found to be 0.625Å. Likewise, the crystal structure of the mouse TS in ternary complex with N(4)-hydroxy-2'-deoxycytidine-5'-monophosphate and cofactor product, DHFA (4EZ8), the crystal structure of the Hu TS ternary complex with dUMP and tomudex (1i00) and Hu TS in complex with dUMP and MTX (5x66) were also used for superimposing and confirming the respective ligand positions. The RMSD values were 0.768Å, 0.806Å and 0.669Å respectively (fig 4.17).

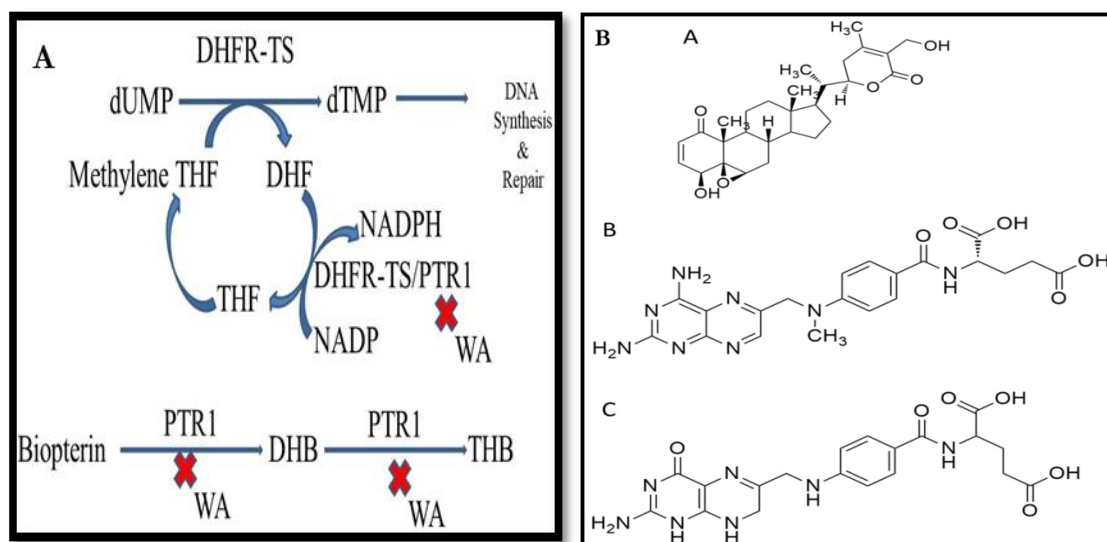


Fig 4.16: A) Folate biosynthesis pathway: DHFR-TS synthesizes dTMP while converting the methylene THF to DHF which is converted back to THF by the DHFR-TS. PTR1 converts dihydrobiopterin to tetrahydrobiopterin. PTR can reduce both pterins and folates. WA inhibits both PTR1 and DHFR-TS enzymes. B) 2D structures of ligands a) WA b) MTX c) DHFA drew using the ChemDraw ultra version 12.0 software.

Further, *Ld* DHFR-TS was docked with WA. Lys 173 forms H-bond with WA and the B.E of WA is -10.3kcal/mol. It was observed that WA is binding to the enzyme in the center of two active sites .i.e., in the middle of the electrostatic channel. The crystal structure of Hu DHFR (4m6k) was docked with WA. This was superimposed with Hu DHFR ternary crystal complex of MTX and NADPH (1u72) and the crystal structure of Hu DHFR complex of NADP⁺ and folate (4m6k). It was observed that all three ligands viz. WA, DHFA, and MTX are binding in the same pocket. DHFA is the substrate, and MTX is the competitive inhibitor of Hu DHFR. WA is also competing for the active site and thus

might be acting as a competitive inhibitor. No H-bonding was observed and the B.E of WA is -9.9 Kcal/mol (fig 4.17).

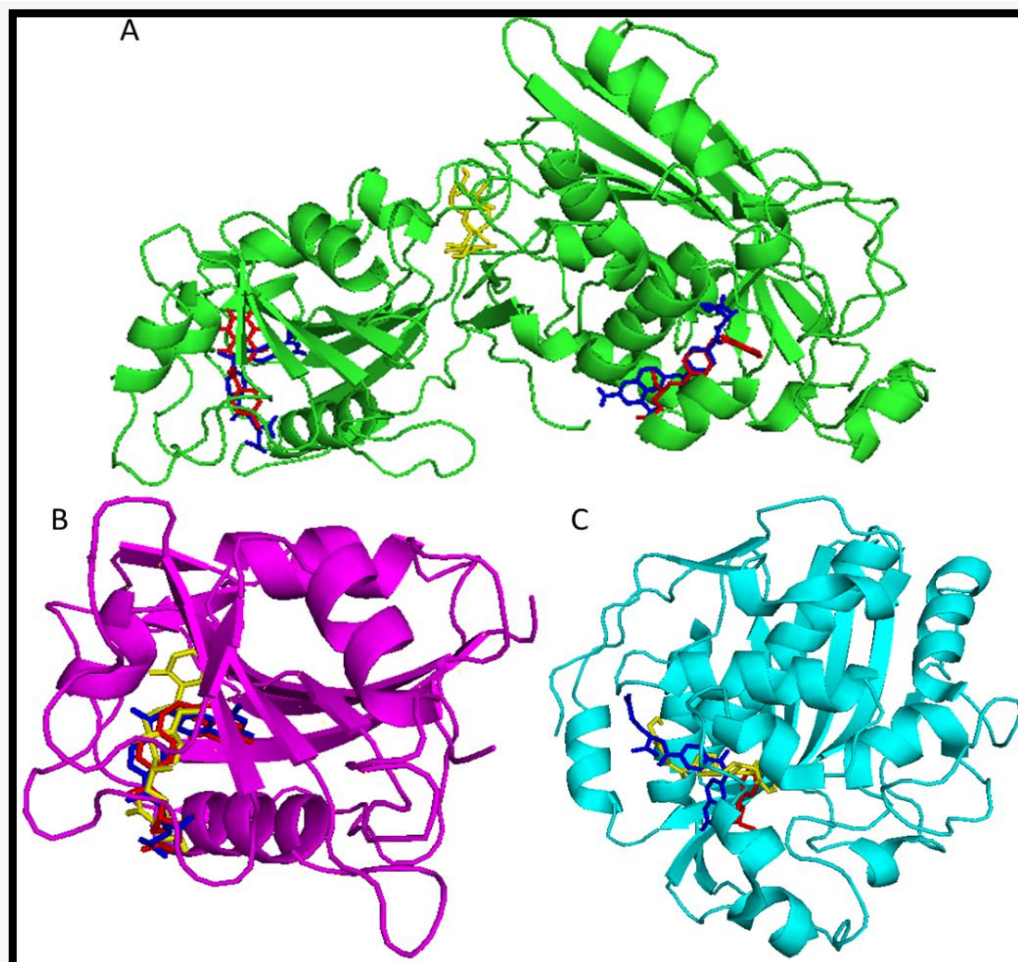


Fig 4.17: (A) Substrate DHFA (red) binds to the two active sites of *Ld* DHFR-TS where the electrostatic channel is formed and the substrate channeling between both the active sites is observed. Competitive inhibitor MTX (blue) competes with DHFA and binds to the two active sites of *Ld* DHFR-TS. Inhibitor WA (yellow) is binding to *Ld* DHFR-TS enzyme by blocking the electrostatic channel. (B) Substrate DHFA (red), Competitive inhibitor MTX (blue) and inhibitor WA (yellow) binding to Hu DHFR enzyme (C) Substrate dUMP (red), inhibitors MTX (blue) and WA (yellow) binding to Hu TS enzyme.

The Crystal structure of Hu TS (1hzw) was docked with WA and later superimposed with Hu TS complex of dUMP and MTX (5x66). dUMP is the substrate and MTX binds to dUMP binding site. It was observed that WA, dUMP, and MTX are binding at the same site. Phe 80, His 196, Leu 221 and Asn 226 form H-bonds with WA and the B.E of WA is -9.5 Kcal/mol. The ligand WA competes for the active site and thus might be a competitive inhibitor. Lys 173 forms H-bond with WA. No H-bonding with WA was observed in Hu DHFR and Phe 80, His 196, Leu 221 and Asn 226 form H- bonds with

WA in Hu TS. The reason why WA is not binding to an active site in *Ld* DHFR-TS but is binding in human enzymes is that of the difference in these interacting residues (fig 4.17).

Docking of Hu DHFR and TS with WA suggests that WA could be competing for the substrate binding sites in case of both the human enzymes. So WA could be a competitive inhibitor for the human enzymes but an uncompetitive inhibitor for the *Ld* DHFR-TS. WA could be a better drug than MTX because of its high B.E. Even though WA binds to both, parasite and host enzymes, still it could be a potent drug molecule as the B.E for *Ld* DHFR-TS is higher than the Human enzymes.

Table 4.11: Binding energies of WA with *Ld* DHFR-TS, Human DHFR, and TS

<i>Ld</i> DHFR-TS	Human DHFR	Human TS
-10.2kcal/mol	-9.9kcal/mol	-9.5kcal/mol

4.14 Molecular Dynamic Simulations:

The MDS of proteins and the protein-WA complexes were carried out to characterize the stabilizing interactions and evaluate the B.Es of WA with *Ld* DHFR-TS, Hu DHFR, and Hu TS. Initial analysis of the root mean square deviations (RMSD) showed that at the end of the simulation all the proteins attained almost stable conformations (fig. 4.18) and their overall RMSD values are comparable. Addition of WA did not show much change in the RMSD of human proteins whereas it slightly increased in *Ld* DHFR-TS. The RMSD of ligand alone was around 0.15 nm in all the proteins throughout the simulation suggests that the bound conformation was stable. Further, the root means square fluctuations (RMSF) of the individual residues were computed by considering their C α atoms as the reference (fig. 4.18). The RMSF of β 5-loop in the DHFR domain and β 1', β 4' loops in the TS domain slightly increased in the ligand-bound state of *Ld* DHFR-TS whereas the RMSF of β 4 and β 6 loops of DHFR domain reduced. In WA bound Hu DHFR, fluctuations around β 2, β 3, and β 6 loops were reduced. In case of WA bound Hu TS protein, the RMSF of β 1 loop was reduced whereas β 3 was increased. In all three proteins, changes in the fluctuations were observed largely at the sites away from the ligand binding sites. Therefore, their contribution on the ligand affinity towards respective proteins might be considered insignificant.

During the binding of WA with *Ld* DHFR-TS, it was observed that WA formed H-bonds with the backbone of F483 and the side chains of Arg275, Asn199, and Asn231. H-bonds

were identified between WA and the backbone of Gly7 and the side chain of Gln48 in Hu DHFR. WA formed H-bonds with Arg163 and Ile 78 of Hu TS.

The B.Es of the ligands were calculated by the MM-PBSA using the last 10 ns of the simulation data where the RMSD of the proteins were found to be more stable. The calculated B.Es are given in table 4.12. The analysis clearly indicates that the binding affinity of WA is more towards *Ld* DHFR-TS than the Human enzymes. Increase in the affinity is majorly contributed by an increase in the hydrophobic interactions between WA and *Ld* DHFR-TS which could be recognized from an increase in van der Waals and the non-polar solvation energies during the ligand binding.

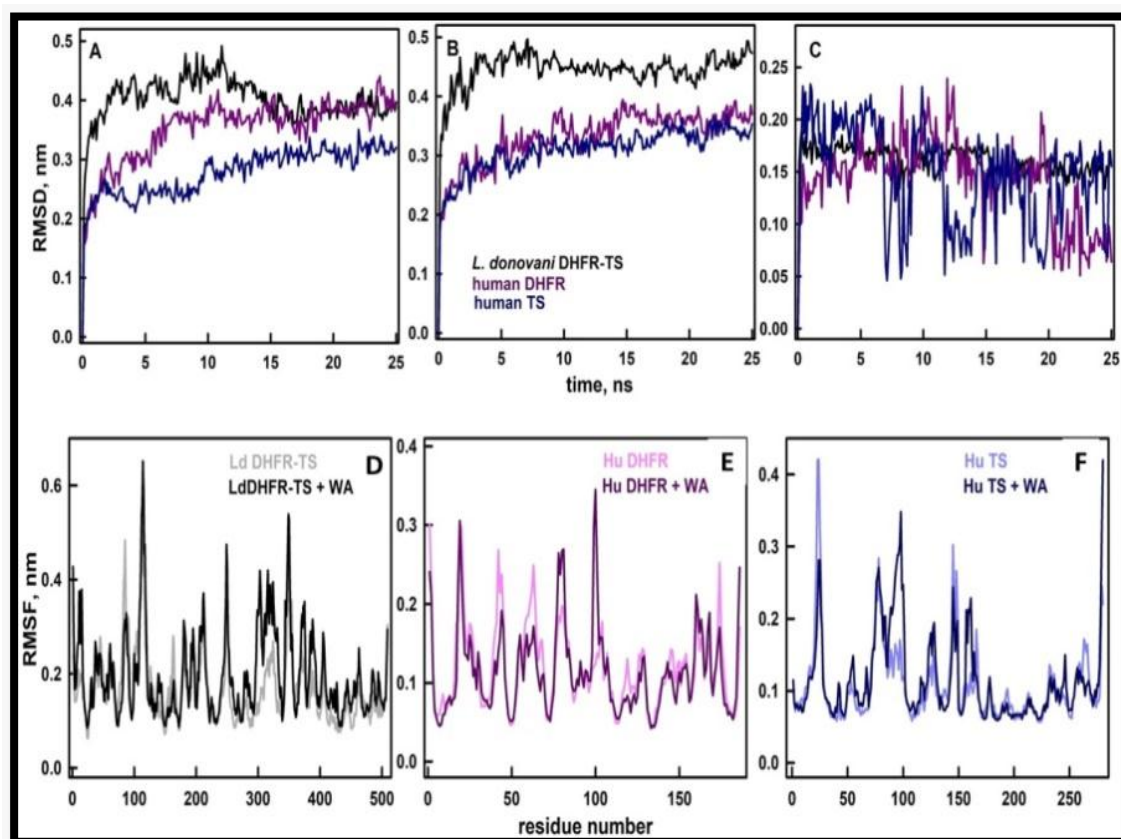


Fig 4.18: RMSD of *Ld* DHFR-TS (black), Hu DHFR (magenta) and Hu TS (purple) in the absence (a) and presence of WA (b) and WA bound in different in different proteins (c). RMSF of C α atoms of residues of proteins *Ld* DHFR-TS (d), Hu DHFR (e) and Hu TS (f) in absence and presence of WA. The color codes are presented in labels.

Table 4.12: Binding energy contributions of different interactions calculated using MM-PBSA

Types of Energy (kJ/mol)	<i>Ld</i> DHFR-TS	Hu DHFR (kJ/mol)	Hu TS
van der Waal energy	-240.828 ±14.111	-152.257 ± 20.412	-130.454 ±11.349
Electrostatic energy	-29.298 ±9.846	-24.299 ±13.315	-49.324 ±14.361
Polar solvation energy	161.597 ±20.010	95.665 ±23.352	122.969 ±30.393
Non-polar solvation energy	-23.375 ±1.019	-16.934 ±2.120	-15.405 ±2.536
Binding energy	-131.904 ±15.686	-97.826 ±24.200	-72.214 ±18.570

4.15 Cloning, Expression, and Purification of Recombinant *L. donovani* DHFR-TS Protein:

The Gradient PCR was performed with the annealing temperatures ranging from 62°C to 72°C, to find the proper conditions for amplifying a distinctive single amplicon without any non-specificity (fig 4.19). It was observed that the annealing temperature of 70°C is ideal and this condition was used further. The amplicon that codes for *Ld* DHFR-TS was cloned into the pET 28a vector and amplicon was purified and ligated using the T4 DNA ligase. The cloning was validated by a colony PCR and the double digestion of the recombinant plasmid using Nde I and Hind III restriction enzymes and also by the Sanger sequencing (fig. 4.20 and 4.21).

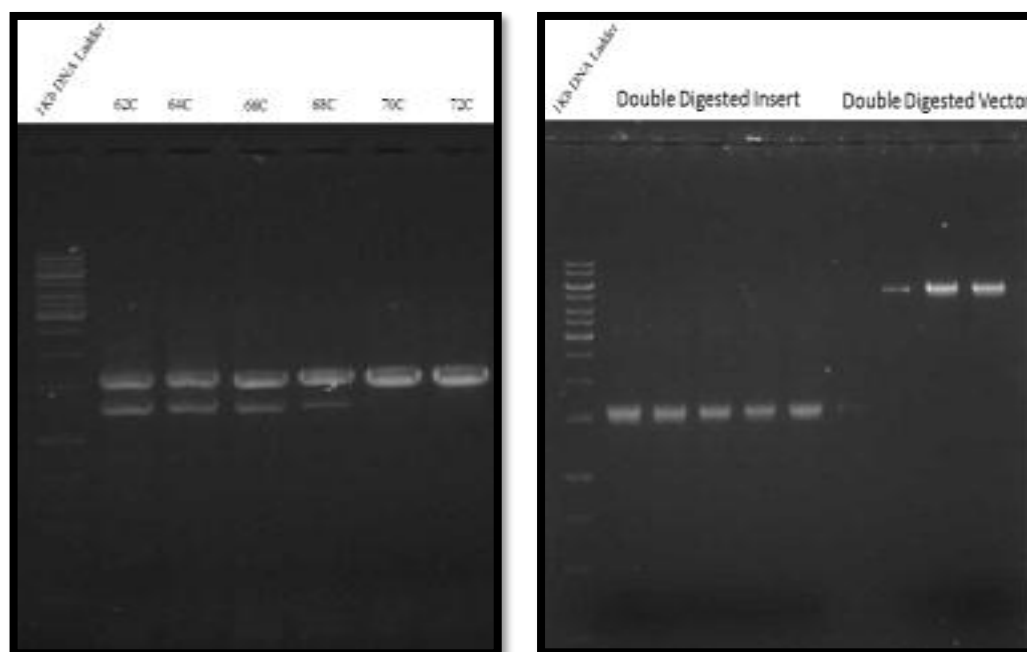


Fig 4.19: Agarose gels showing the Gradient PCR and double digested insert and vector.

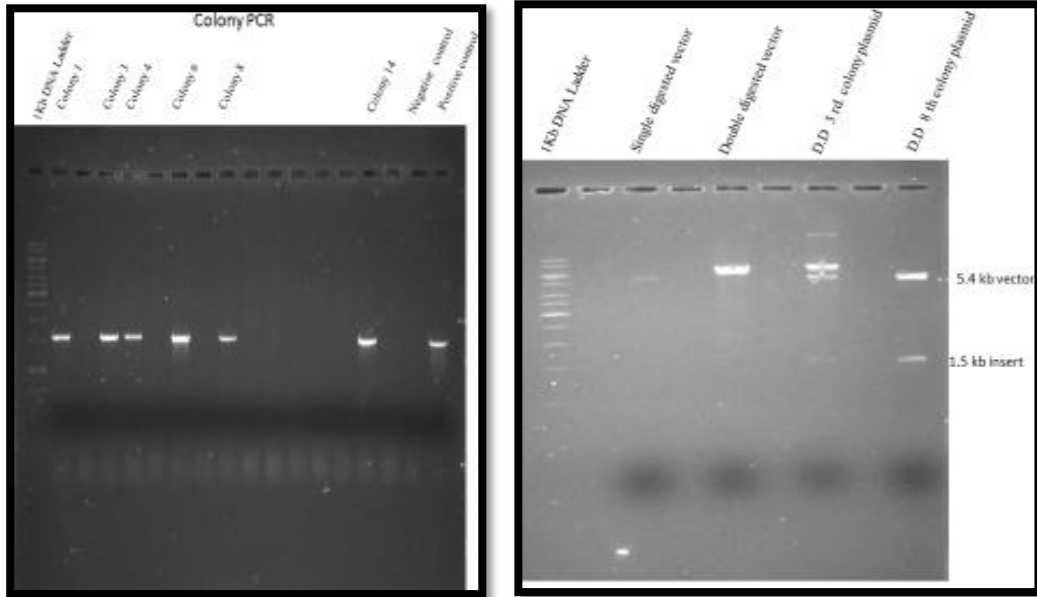


Fig 4.20: Agarose gels showing the colony PCR double digested recombinant vector releasing of the insert.



Fig 4.21: The recombinant plasmid sequenced by the Sanger sequencing with the forward and reverse primers and its alignment with the DHFR-TS gene.

Expression of Recombinant *DHFR-TS* protein:

E.coli BL21 cells were used to express the recombinant protein, using 1 mM IPTG (Sigma-Aldrich) for 4 hours at 37°C. As shown in the fig 4.23, the protein was detected in the cell lysate of the *E.coli* cells incubated with the IPTG. The identity of the protein was confirmed using the western blotting.

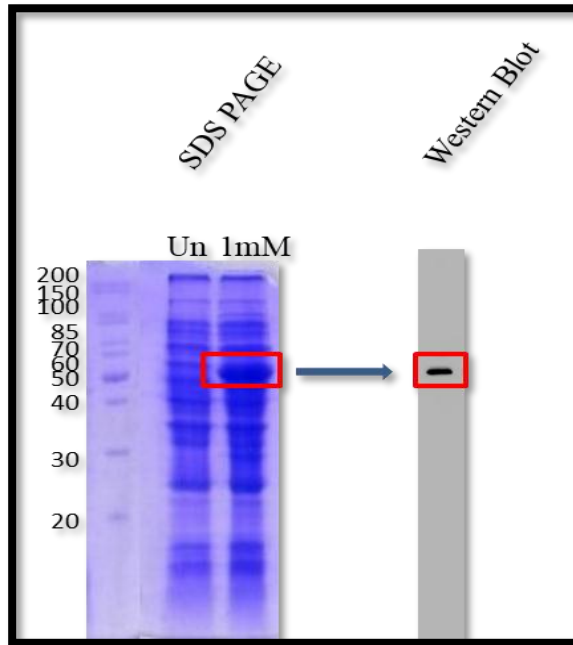


Fig 4.22: Acrylamide gel showing the expression of recombinant DHFR-TS Protein and the transferred blot

Purification of Recombinant DHFR-TS protein:

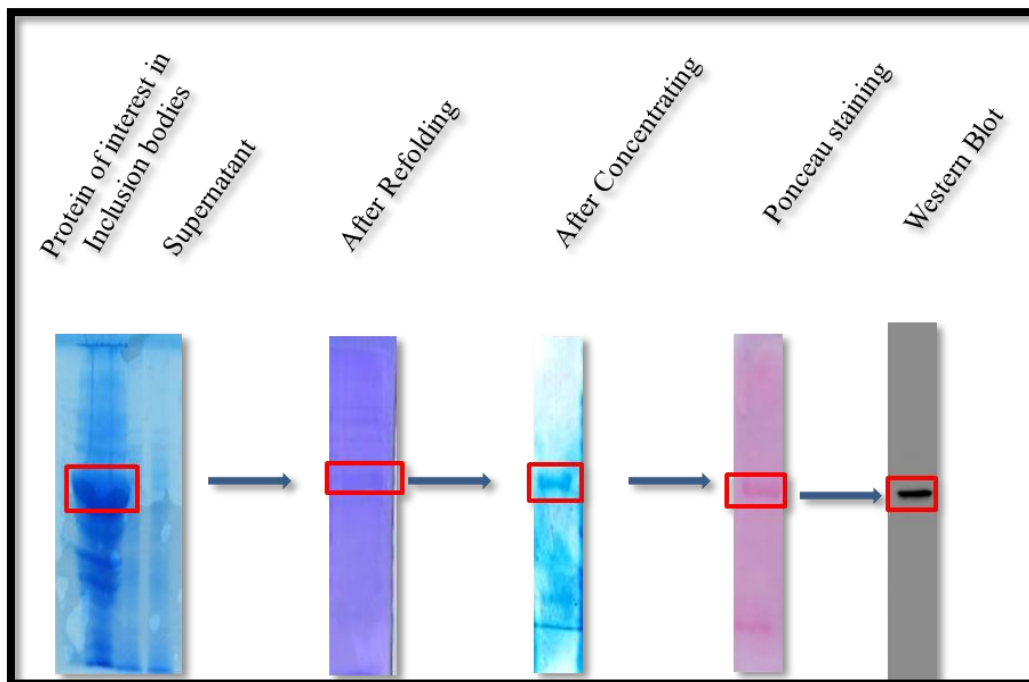


Fig 4.23: The expression of DHFR-TS Protein in inclusion bodies, its purification, concentration and transferred blot

The bacterial cells were sonicated and the lysate and the pellet were analysed for the presence of the protein. The protein was noticed in the pellet fraction instead of supernatant. The protein was thus purified from the pellet fraction and refolded (fig 4.23). Later it was concentrated using the protein concentrator.

4.16 Enzyme Assay:

Incubation of the recombinant protein with the substrate resulted in the decrease of absorbance indicating that the purified protein is properly folded and is active.

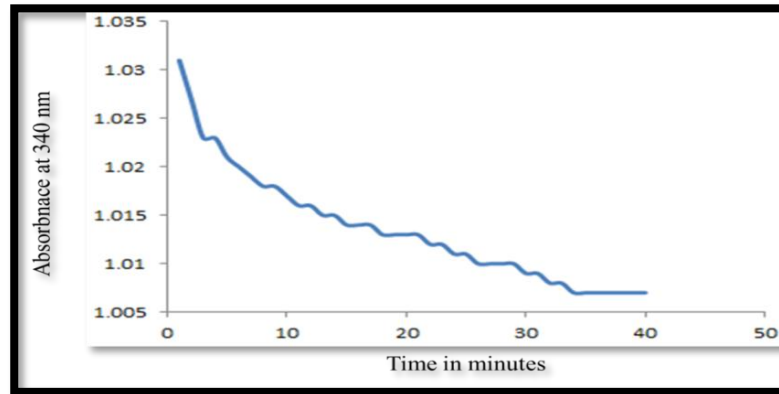


Fig 4.24: Enzyme activity of DHFR-TS Enzyme

Later, the reaction time was limited to 7 mins and the activity with the substrate DHFA and inhibition with MTX, the competitive inhibitor, and WA were performed. As MTX is a competitive inhibitor, it competed for the active site for some time and later the reaction was inhibited whereas WA showed a flat inhibition from the beginning thus acting as an uncompetitive inhibitor, as it is binding to the Enzyme-Inhibitor complex.

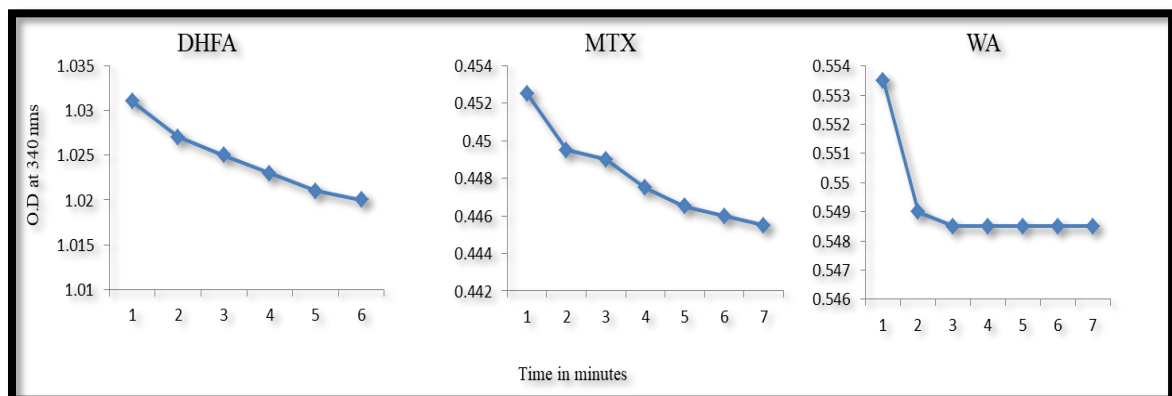


Fig 4.25: The enzyme activity of DHFR-TS and inhibition with MTX and WA

Objective III

Determination of the Additive Effect of WA on Milt in the Treatment of Experimental Visceral Leishmaniasis

4.17 Estimation of IgG2a and IgG1 Titers in Serum by Indirect ELISA:

In contrast to the infected group, a notable hike in the serum IgG2a in the combination group was observed. The treatment increased the IgG2a indicating a Th1 polarisation. An increase in the IgG1 titer indicates a Th2 polarisation but there was no significant change in all the groups. In contrast to the infected group, a significant inflation in the IgG2a /IgG1 ratio in the combination group suggests an additive effect of WA + Milt (fig 4.26).

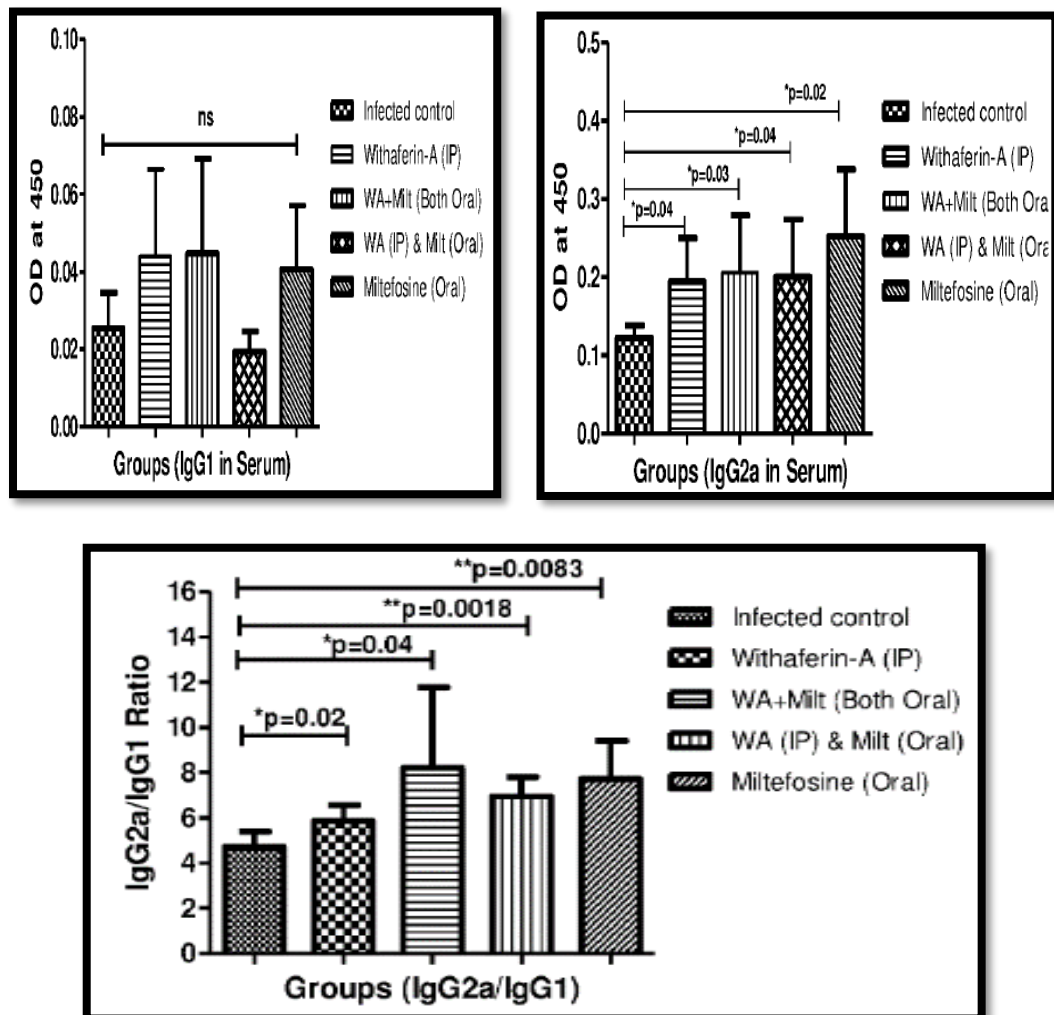


Fig 4.26: Quantitation of IgG1 and IgG2a titers in the serum

4.18 Determination of Spleen Parasite Load:

In comparison to the infected control, the combination group mice showed a significant decline in the spleen parasite population (fig 4.27).

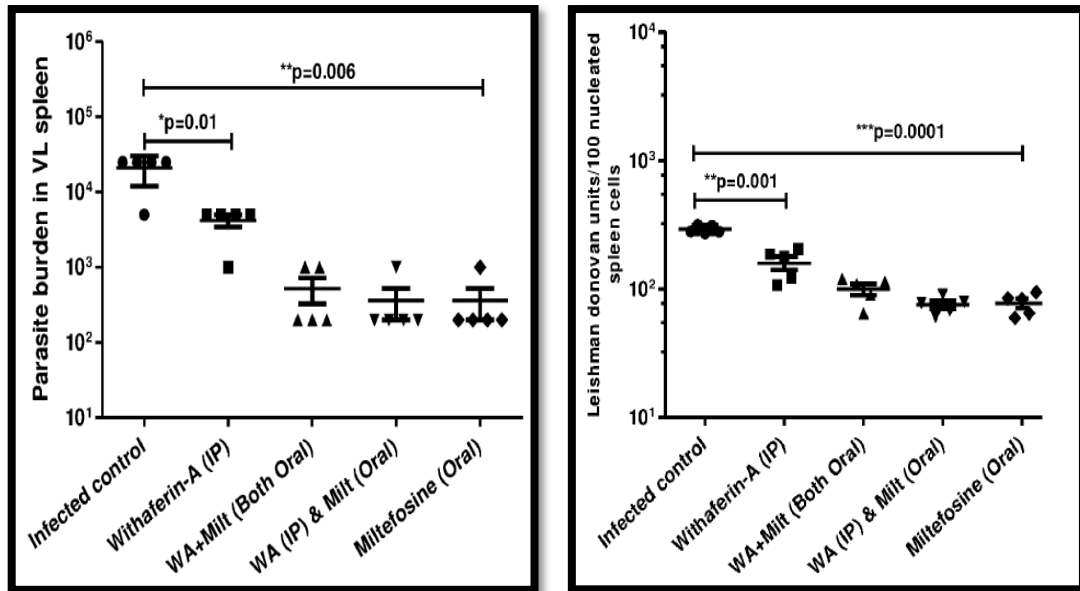


Fig 4.27: Parasite Burden in the spleen of infected and treated mice

4.19 Histopathological Examination of Liver Tissue and Estimation of Granuloma Formation:

When compared to the infected control, the combination group mice showed a significant decline in the liver granuloma formation (fig. 4.28).

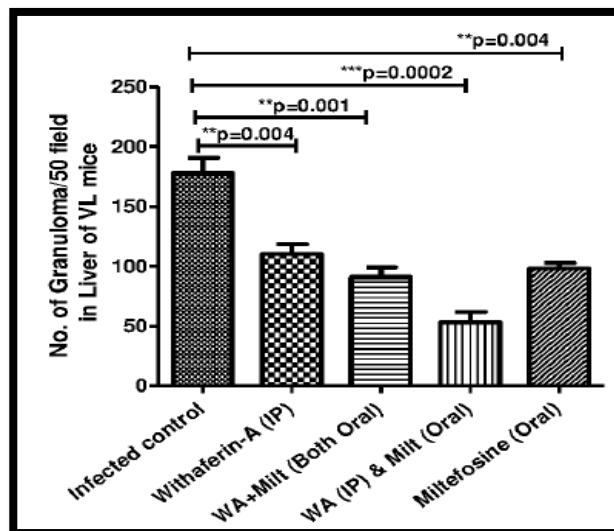


Fig 4.28 Estimation of Granuloma Formation in Liver

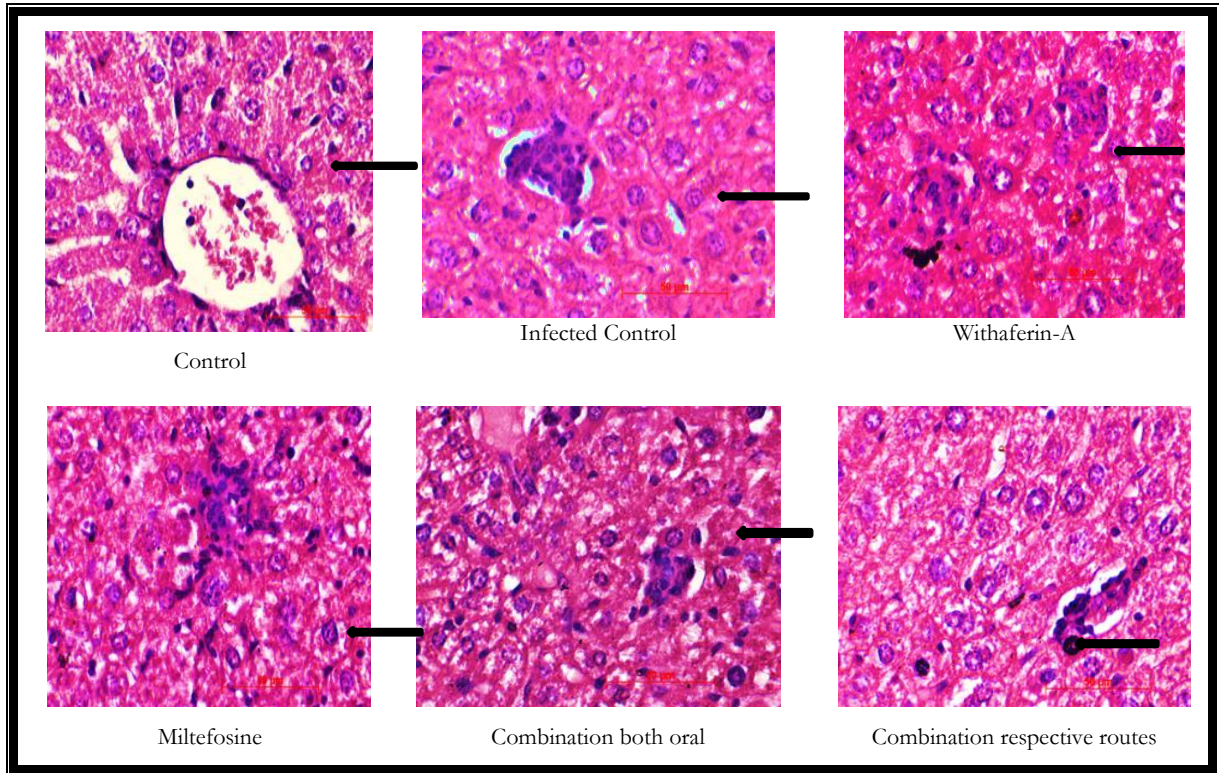


Fig 4.29: Hematoxylin and Eosin stained Liver sections of different groups (40X Magnification)

During the infection, the T lymphocytes infiltrate and develop into a granuloma in which the amastigotes are present, which is cleared with time. A number of granulomas were counted in all the treated groups and were checked with the infected group. The infected mice show a fatty degeneration and a high number of dense, tight granulomas (fig 4.29). In WA and Milt alone treatment, granuloma pattern is dense, tight and almost same in number as the infected liver. The combination of both oral group also showed the granuloma formation similar to WA and Milt treated groups. The combination respective routes group has shown a significant difference from the others with a comparatively low number of granulomas which were less dense, loose and scattered.

4.20 Estimation of Other Parameters:

No appreciable change in the total body weight, spleen weight, serum cholesterol, TAG, and glucose levels in any of the groups was observed suggesting that WA, Milt either individually or in combination were not significantly affecting these parameters (fig 4.30 and 4.31).

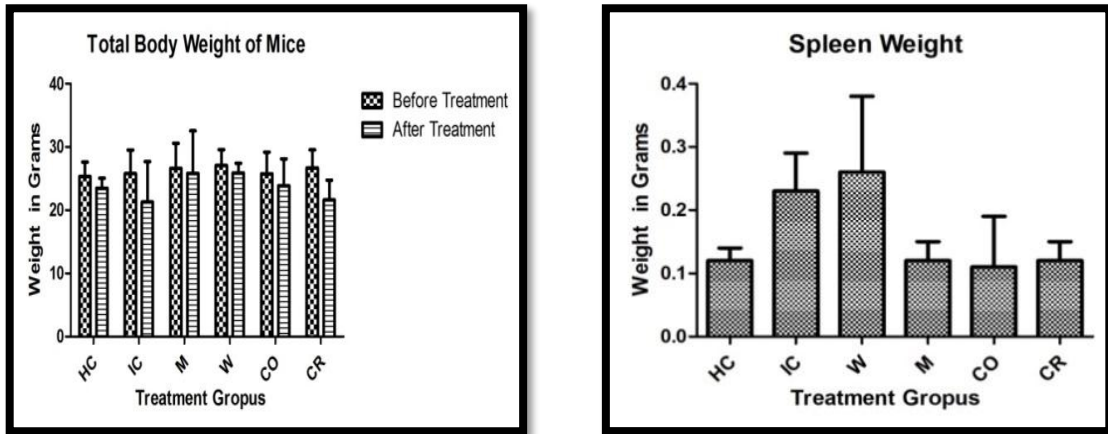


Fig 4.30: Total body weight and spleen weight of mice

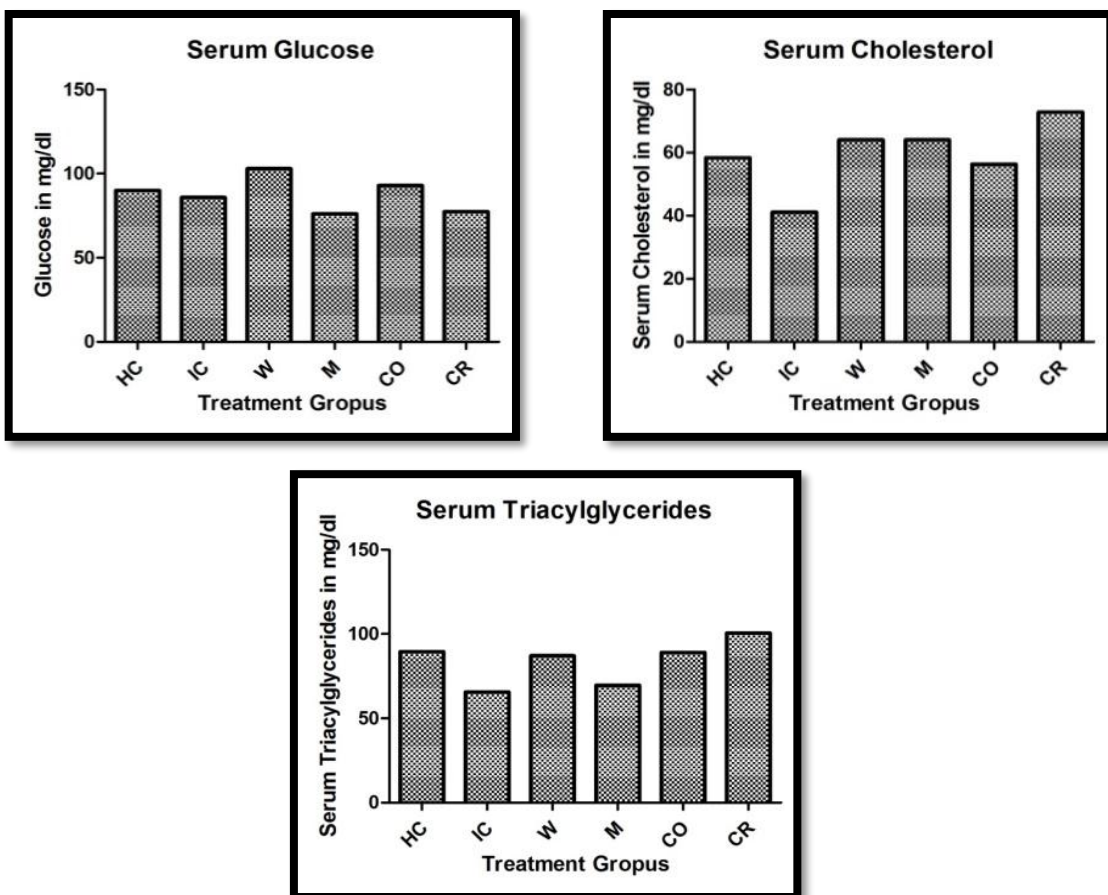


Fig 4.31: Serum glucose cholesterol and triacylglyceride concentrations

The results of the combination trial suggest that an oral administration of Milt (2.5 mg/kg BW) with an *i.p* delivery of WA (2 mg/kg BW) can be considered safe, effective and show an additive effect. WA + Milt combination may reduce the drug resistance problem in the endemic areas. However, the combination study requires further research after which it can be developed for the control of VL in the endemic regions.

4.21 Discussion:

The natural products have remarkable properties and a great potential to improve our health and wellbeing. They have been used in the traditional medicine in a holistic way, in almost every country in the world and their demand is increasing day by day. The natural products are a source of potentially powerful medicines and are making their way into the mainstream medicine once again. The natural products can be used to cure a number of diseases including the infectious ones, as they are more accessible, affordable, and acceptable to people. It is well-known fact that more than 25-30% of all the modern medicines have been derived from the natural products which have been used in the traditional medicine (Kaul and Wadhwa 2017). The natural compounds can be separated from the roots, stems, leaves, seeds, and barks of the medicinal plants and can be characterized, screened for novel bioactive lead molecules. Using the natural products in the drug discovery is innovative and needs rigorous scientific proof to demonstrate their efficacy. The time taken for the discovering a new drug and getting consent to bring it in to usage is much longer and may take up to 15-20 years, investing up to 800 million dollars. The natural compounds are crucial substitutes to the chemotherapeutics (Kaul and Wadhwa 2017; Mir et al. 2012; Singh et al. 2011). The systems biology approach is being applied in the present day drug discovery and diagnosis where a deeper knowledge of the interactions between the systems and the networks is being considered, apart from understanding the mechanisms at a molecular level. The modern 'omics' technologies are being applied in identifying and isolating the bioactive compounds and analyzing their levels and activities. To probe into the molecular targets and the mechanisms of action of pure compounds or phyto-complexes, chemo-genomics, network pharmacology, poly-pharmacokinetic principles are being applied. The knowledge of compatibility between different compounds has come from a better understanding of the synergetic interactions (Nisha Singh et al. 2014)..

Many potential target molecules in *Leishmania* is known because of the accessibility of entire genome sequence and the discovery of methods for the quantification of gene expression levels. The difference between the expression levels (of mRNA or protein) in the infected and the control parasites, drug-treated and untreated parasites and their effect on the biological pathways provide deep perception regarding the parasite biology and the disease mechanism and can accelerate the identification of potential drug targets and also help in understanding the mechanism of action of the drug. Various proteins from

pathways like DNA repair, apoptosis, cell cycle, stress response, proteasomal degradation, and receptors playing a role in the signaling pathways, kinases, proteases are being considered as the potential drug targets. The enzymes involved in the crucial biochemical and metabolic pathways which are unique to the parasites are considered as the best targets. Pinpointing the target molecule is the crucial step in the drug discovery. A biological target with the 3D structure has to be identified which gives information about the environment, surface area, structural information and chemical nature of the binding pockets. The enzyme's binding pocket can be either an active site or an allosteric site which can be a potential target site for WA which brings significant conformational changes and alters the function upon binding. The nature of binding pocket residues conveys information about the binding pose and the binding energy. Once the target molecules are identified, the interaction of the natural products with these molecules can be studied using the computational methods like docking and MDS which reveal the mechanism of action. Many of the computer-aided prediction tools for various physical-chemical properties, drug-likeness, and biological activities are free on the Internet. This is advantageous for the medicinal chemists from academia because they have limited resources for purchasing licenses for commercially available software's and they cannot send the details of their lead molecules due to the data integrity issues. However, the predictions and the wet lab evaluations may or sometimes may not correlate. So it is better to evaluate the predictions for accuracy (Chawla and Madhubala 2010; Drews 2000; Drummelsmith et al. 2003; Drummelsmith et al. 2003).

Based on the previous findings, this part of the research hypothesized that WA has multiple targets and inhibits *Ld* DHFR-TS, the other enzyme in the folate biosynthesis pathway. WA can act in combination with existing antileishmanial drugs showing an additive effect. It has been hypothesized that WA + Milt combination might improve efficiency; reduce the duration and lower the treatment failure. It has been predicted that WA has drug-like properties, obeys the Lipinski's rule of five, does not cross the BBB, absorbed in the GI tract and does not affect the CNS (as it is effluxed out by the P-glyco protein), has good oral bioavailability, no cardiac toxicity, and enzymes as the most probable targets. The exclusive pathways of *Trypanosomatids* provide exceptional drug targets among which the folic acid pathway is one. Another mode of action of WA is by blocking the electrostatic channel between the two active sites of *Ld* DHFR-TS. The MDS studies revealed that the B.E and affinity of WA are more towards *Ld* DHFR-TS than the

Human enzymes. WA inhibited *Ld* DHFR-TS in an uncompetitive mode. So WA can inhibit multiple enzymes of the same pathway simultaneously. The CMI drives a potent Th1 type of immune response, which controls VL. During the infection, increased Th2 cytokines exacerbate VL and are responsible for its progression. So treatment should ideally elevate Th1 immune response (Wadhone et al. 2009).

The *Leishmania* species have developed resistance to existing antileishmanial drugs which are very few in numbers, toxic and costly. So there is a necessity to develop novel, safe less toxic, efficacious and affordable drugs. The combination of a chemotherapeutic drug with a natural compound can be the most rational alternative approach as they have multiple benefits obtained from both the drugs. As individual treatment with the existing antileishmanial drugs have several drawbacks, the combinations of antileishmanial drugs with the plant compounds and other natural products have been explored earlier *in vitro*, and *in vivo*. It was reported that an *in vitro* combination of Nicotinamide or Vitamin B3 with the trivalent antimony showed an additive effect and decreased the burden of *L. infantum*, *L. amazonensis* and *L. braziliensis* (Gazanion et al. 2011). The green propolis water extract with free or liposomal meglumine antimoniate decreased the liver and spleen parasite population and protected from lesions (Ferreira et al. 2014). Allicin along with Amb reduced the spleen and liver parasite burden through a partial additive effect in *L. infantum* infected hamsters (Corral et al. 2014). Nano Curcumin and miltefosine together have demonstrated synergism, augmented *in vivo* antileishmanial effect escorted by hiked ROS, RNS, phagocytic activity and lymphocyte proliferation (Tiwari et al. 2017). In sync with the above research findings, our combination trial with Milt and WA showed a significant increase in Th1 specific IgG2a antibody levels but no significant decrease in Th2 specific IgG1 antibody levels. The H-E staining of liver tissues and a decrease in the parasite burden in the spleen indicate a successful clearance of the parasites. When the parasite enters the hepatic tissue, the host immune cells rush towards the infection site resulting in the granuloma formation which clears the parasite with time. Later the granuloma structures disappear. With the treatment of miltefosine and WA combination, there was a reduction in the number of granulomas and the parasite population in the granuloma, proving the potency of the combination.

In conclusion, we propose that WA has multiple modes of antileishmanial activity out of which the inhibition of DHFR-TS is important. In the combination with miltefosine, it has an additive effect on *L. donovani* prevalence of infection.

Chapter V

Summary

Leishmaniasis is a serious public health issue affecting the poor people across the continents. The conventional drugs cost high, have toxicity and resistance. As VL is not completely curable as of now, a novel approach to control the disease is the need of the hour. The plant compounds are being used for treatment as they are comparatively less toxic, cost-effective, better compatible with the human body and are efficacious. They can be used along with the available antileishmanial drugs without any detrimental drug-drug cross reactivity as they have multiple advantages and can effectively cure the disease. *Ashwagandha* (*Withania somnifera*), is a sub-tropical herb, from the *Solanaceae* family having a group of naturally occurring C₂₈-steroidal lactone triterpenoid compounds called Withanolides, out of which the most abundant is Withaferin A. The Withanolides have been extracted, identified from *Withania somnifera* leaves and the *in vitro* antileishmanial activity through apoptotic-like death was reported (Chandrasekaran et.al 2013). The leaf extract of *Withania somnifera* (alcoholic fractions F5, F6) and purified WA's antileishmanial and immunomodulatory activities were evaluated, both *in vitro* and *in vivo*. (Chandrasekaran et.al 2017). The mode of antileishmanial activity of WA was through un-competitive inhibition of PTR1, a parasite-specific enzyme from the folate biosynthesis pathway (Chandrasekaran et.al 2015).

In continuation to the previous study, the current research performed *in silico* studies and predicted that WA and Milt are similar in many aspects. It has been predicted that WA has druglike properties, obeys the Lipinski's rule of five, does not cross the BBB, absorbed in the GI tract and does not affect the CNS (as it is effluxed out by the P-glycoprotein), has good oral bioavailability, no cardiac toxicity, and enzymes as the most probable targets. The folate biosynthesis pathway enzymes of the parasite, PTR1 and DHFR-TS are 13.5% similar and were not physically interacting with each other but were showing a relation called 'Gene Neighborhood'. *L. chagasi*, *L. infantum*, and *L. major* DHFR-TS enzymes have 99.2%, 99.8%, 95.7% similarity respectively with *Ld* DHFR-TS and are highly conserved. So theoretically the same inhibitor should work in all these *Leishmania* species. Humans have DHFR and TS as two separate enzymes whereas in all the *Trypanosomatids* DHFR-TS is a single polypeptide with the DHFR on amino and the TS domain on carboxy termini. *Ld* DHFR-TS (1563 bp, 520aa) is considerably different at the gene and the protein level from the Human DHFR (564 bp, 187aa) Human TS (942 bp, 313aa). The homology between the target *Ld* DHFR-TS and the template *T. cruzi* DHFR-TS-A chain was 67.32% which was used to build a good quality 3D model for *Ld* DHFR-TS. In the molecular

docking study, it has been observed that the substrate DHFA was binding to the two active sites in *Ld* DHFR-TS, one in the DHFR and one in the TS domain where an electrostatic channel is formed and the substrate channeling was reported. The competitive inhibitor MTX was binding to *Ld* DHFR-TS active sites. The ligand WA was binding at a different site and blocking the electrostatic channel between the two active sites. MTX and DHFA have common amino acids in their binding sites and have the same binding energy of -8.8 Kcal/mol, whereas WA has -10.2 Kcal/mol. WA acts as a competitive inhibitor in case of the human enzymes. The MDS revealed that the binding energy and affinity of WA is more towards *Ld* DHFR-TS than the Human enzymes. The cloning of *Ld* DHFR-TS gene was confirmed by releasing the insert from the recombinant plasmid and by Sanger sequencing. The size of the expressed protein was checked on an SDS PAGE. During the enzyme assay a reduction in OD at 340 nm was observed indicating the conversion of NADPH to NADP⁺. WA inhibited *Ld* DHFR-TS in an uncompetitive mode. Thus, WA can inhibit multiple enzymes of the same pathway simultaneously. In *in vivo* studies, a notable increase in the serum IgG2a in the combination group was observed in comparison to the infected control. The treatment increased the IgG2a indicating a Th1 polarisation. There was no significant change in the IgG1 in all groups. The increased IgG1 titer indicates a Th2 polarisation. A notable hike in the IgG2a /IgG1 ratio in the combination group in comparison to the infected control, suggests the additive effect of WA + Milt. In contrast to the infected group, there was an appreciable decline in the spleen parasite population and the liver granuloma formation in the combination group. There was no remarkable alteration in the total body weight, spleen weight, serum cholesterol, TAG, and glucose levels in any of the group suggesting that WA, Milt either individually or in combination were not significantly affecting these parameters. The results of the combination trial suggest that, an oral administration of Milt (2.5 mg/kg BW) with an *i.p* delivery of WA (2 mg/kg BW) can be considered safe, effective and show an additive effect. WA + Milt combination may reduce the drug resistance problem in the endemic areas. However, the combination study requires further research after which it can be developed for the control of VL in the endemic regions. Further, combination studies of WA with a few more available antileishmanial drugs like AmB, paromomycin etc. can be performed to know the best efficacious, nontoxic synergistic/additive combination both *in vitro* and *in vivo*. It is evident that this study has proved that WA has more than one molecular target in the parasite. A few more parasite-specific enzymes from various pathways can be targeted and their inhibition with WA *in vivo* and in the parasite

can be performed which can be the best proof for the 'Butterfly Effect of WA' in the *Leishmania* parasite. The 'Butterfly Effect' shown by many natural products includes a single or few drug molecules binding to multiple targets in the parasite and ultimately killing it; at the same time triggering a systemic protective immune response in the patient's body and ultimately curing the patient from the disease.

Chapter VI

References

- Abongomera, Charles, Francis Gatluak, Jozefine Buyze, and Koert Ritmeijer. 2016. "A Comparison of the Effectiveness of Sodium Stibogluconate Monotherapy to Sodium Stibogluconate and Paromomycin Combination for the Treatment of Severe Post Kala Azar Dermal Leishmaniasis in South Sudan-A Retrospective Cohort Study." *PLoS ONE* 11(9).
- Abraham, Mark James et al. 2015. "Gromacs: High Performance Molecular Simulations through Multi-Level Parallelism from Laptops to Supercomputers." *SoftwareX* 1–2: 19–25.
- Al-Hindawi, Muhaned K., Saadia H. Al-Khafaji, and May H. Abdul-Nabi. 1992. "Anti-Granuloma Activity of Iraqi Withania Somnifera." *Journal of Ethnopharmacology* 37(2): 113–16.
- Ali, Jogoth et al. 2012. "In Silico Prediction of Aqueous Solubility Using Simple QSPR Models: The Importance of Phenol and Phenol-like Moieties." *Journal of Chemical Information and Modeling* 52(11): 2950–57.
- Alvar, Jorge et al. 2012. "Leishmaniasis Worldwide and Global Estimates of Its Incidence." *PLoS ONE* 7(5).
- Angélica, Ana et al. 2014. "Communication Report Effectiveness of Miltefosine-Pentoxifylline Compared to Miltefosine in the Treatment of Cutaneous Leishmaniasis in C57Bl / 6 Mice." 47: 517–20.
- April C. Joice, Sihyung Yang, Abdelbasset A. Farahat, Heidi Meeds, Mei Feng, Junan Li, David W. Boykin, Michael Zhuo Wang, Karl A. Werbovetza. 2018. "Antileishmanial Efficacy and Pharmacokinetics of DB766-Azole Combinations". *Antimicrobial Agents and Chemotherapy* Volume 62 Issue 1 e01129-17.
- Arnold, Konstantin, Lorenza Bordoli, Jürgen Kopp, and Torsten Schwede. 2006. "The SWISS-MODEL Workspace: A Web-Based Environment for Protein Structure Homology Modelling." *Bioinformatics* 22(2): 195–201.
- Baell, Jonathan B., and Georgina A. Holloway. 2010. "New Substructure Filters for Removal of Pan Assay Interference Compounds (PAINS) from Screening Libraries and for Their Exclusion in Bioassays." *Journal of Medicinal Chemistry* 53(7): 2719–40.

- Balasegaram, Manica et al. 2012. "Liposomal Amphotericin B as a Treatment for Human Leishmaniasis." *Expert opinion on emerging drugs* 17(4): 493–510.
- Banerjee, A., M. De, N. Ali. 2008. "Complete Cure of Experimental Visceral Leishmaniasis with Amphotericin B in Stearylamine-Bearing Cationic Liposomes Involves Down-Regulation of IL-10 and Favorable T Cell Responses." *The Journal of Immunology* 181(2): 1386–98.
- Banerjee, Antara, Manjarika De, Nahid Ali. 2011. "Combination Therapy with Paromomycin-Associated Stearylamine-Bearing Liposomes Cures Experimental Visceral Leishmaniasis through Th1-Biased Immunomodulation." *Antimicrobial Agents and Chemotherapy* 55(4): 1661–70.
- Beck, Joanne T., Buddy Ullman. 1990. "Nutritional Requirements of Wild-Type and Folate Transport-Deficient *Leishmania Donovanii* for Pterins and Folates." *Molecular and Biochemical Parasitology* 43(2): 221–30.
- Bekersky, Ihor et al. 2002. "Pharmacokinetics, Excretion, and Mass Balance of Liposomal Amphotericin B (AmBisome) and Amphotericin B Deoxycholate in Humans." *Antimicrobial Agents and Chemotherapy* 46(3): 828–33.
- Bello, a R et al. 1994. "PTR1: A Reductase Mediating Salvage of Oxidized Pteridines and Methotrexate Resistance in the Protozoan Parasite *Leishmania Major*." *Proceedings of the National Academy of Sciences of the United States of America* 91(24): 11442–46.
- Benkert, P, S C E Tosatto, D Schomburg. 2008. "QMEAN: A Comprehensive Scoring Function for Model Quality Assessment." *Proteins-Structure Function and Bioinformatics* 71(1): 261–77.
- Berman, Jonathan. 2005. "Miltefosine to Treat Leishmaniasis." *Expert Opinion on Pharmacotherapy* 6(8): 1381–88.
- Beverley, S.M, T.E Ellenberger, J S Cordingley. 1986. "Primary Structure of the Gene Encoding the Bifunctional Dihydrofolate Reductase-Thymidylate Synthase of *Leishmania Major*." *Proceedings of the National Academy of Sciences of the United States of America* 83(8): 2584–88.

- Biasini, Marco et al. 2014. "SWISS-MODEL: Modelling Protein Tertiary and Quaternary Structure Using Evolutionary Information." *Nucleic Acids Research* 42(W1).
- Blakley RL, Benkovic SJ. 1984. *Chemistry and Biochemistry of Folates. In: Folates and Pterins.* John Wiley.
- Bordoli, Lorenza et al. 2008. "Protein Structure Homology Modeling Using SWISS-MODEL Workspace." *Nature Protocols* 4(1): 1–13.
- Bray, R, and F Modabber. 2000. "The History of Leishmaniasis." *Protozoal Diseases. New York & London: Hodder ...*: 1–10.
- Brenk, Ruth et al. 2008. "Lessons Learnt from Assembling Screening Libraries for Drug Discovery for Neglected Diseases." *ChemMedChem* 3(3): 435–44.
- Cavasotto, Claudio N., and Sharangdhar S. Phatak. 2009. "Homology Modeling in Drug Discovery: Current Trends and Applications." *Drug Discovery Today* 14(13–14): 676–83.
- Chandra, Sunandini, Dipali Ruhela, Anindita Deb, and Ram A Vishwakarma. 2010. "Glycobiology of the *Leishmania* Parasite and Emerging Targets for Antileishmanial Drug Discovery." *Expert Opinion on Therapeutic Targets* 14(7): 739–57.
- Sambamurthy Chandrasekaran, Alti Dayakar, Jalaja Veronica, Shyam Sundar, Radheshyam Maurya. 2013. "An in vitro study of apoptotic like death in *Leishmania donovani* promastigotes by withanolides." *Parasitology International* 62 (2013) 253–261.
- Chandrasekaran, Sambamurthy et al. 2015. "Exploring the Inhibitory Activity of Withaferin-A against Pteridine Reductase-1 of *L. Donovanii*." *Journal of Enzyme Inhibition and Medicinal Chemistry* 31(6): 1029–37.
- Chandrasekaran S, Veronica J, Sundar S and Maurya R. 2017. "Alcoholic Fractions F5 and F6 from *Withania somnifera* Leaves Show a Potent Antileishmanial and Immunomodulatory Activities to Control Experimental Visceral Leishmaniasis." *Front. Med.* 4:55. doi: 10.3389/fmed.2017.00055
- Chawla, Bhavna, and Rentala Madhubala. 2010. "Drug Targets in *Leishmania*." *Journal of Parasitic Diseases* 34(1): 1–13.

- Chunge, C. N., J. Owate, H. O. Pamba, and L. Donno. 1990. "Treatment of Visceral Leishmaniasis in Kenya by Aminosidine Alone or Combined with Sodium Stibogluconate." *Transactions of the Royal Society of Tropical Medicine and Hygiene* 84(2): 221–25.
- Corral, M Jesús et al. 2014. "Efficacy of Low Doses of Amphotericin B plus Allicin against Experimental Visceral Leishmaniasis." *The Journal of antimicrobial chemotherapy*: 1–7.
- Costa, Sonya, Marisa Machado, Cláudia Cavadas, and Maria do Céu Sousa. 2016. "Antileishmanial Activity of Antiretroviral Drugs Combined with Miltefosine." *Parasitology Research* 115(10): 3881–87.
- Cruz, A, S. M Beverley. 1990. "Gene Replacement in Parasitic Protozoa." *Nature* 348: 171–73.
- Cunningham, Mark L., and Stephen M. Beverley. 2001. "Pteridine Salvage throughout the Leishmania Infectious Cycle: Implications for Antifolate Chemotherapy." *Molecular and Biochemical Parasitology* 113(2): 199–213.
- Daina, Antoine, Olivier Michielin, and Vincent Zoete. 2017. "SwissADME: A Free Web Tool to Evaluate Pharmacokinetics, Drug-Likeness and Medicinal Chemistry Friendliness of Small Molecules." *Nature Publishing Group*: 1–13.
- Daina, Antoine, and Vincent Zoete. 2016. "A BOILED-Egg To Predict Gastrointestinal Absorption and Brain Penetration of Small Molecules." : 1117–21.
- Delaney, John S. 2004. "ESOL: Estimating Aqueous Solubility Directly from Molecular Structure." *Journal of Chemical Information and Computer Sciences* 44(3): 1000–1005.
- Desjeux, Philippe. 1996. "Leishmaniasis: Public Health Aspects and Control." *Clinics in Dermatology* 14(5): 417–23.
- Desjeux. 1999. "Global Control and Leishmania HIV Co-Infection." *Clinics in Dermatology* 17(3): 317–25.
- Dorlo, Thomas P C et al. 2014. "Failure of Miltefosine in Visceral Leishmaniasis Is Associated with Low Drug Exposure." *Journal of Infectious Diseases* 210(1): 146–53.
- Drews, J. 2000. "Drug Discovery: A Historical Perspective." *Science* 287(5460): 1960–64.

- Drummel-Smith, Jolyne et al. 2003. "Proteome Mapping of the Protozoan Parasite Leishmania and Application to the Study of Drug Targets and Resistance Mechanisms." *Molecular & cellular proteomics: MCP* 2(3): 146–55.
- Duncan, Robert et al. 2011. "Identification and Characterization of Genes Involved in Leishmania Pathogenesis: The Potential for Drug Target Selection." *Molecular biology international* 2011: 428486.
- Efficacy, Antileishmanial et al. 2018. "Crossm Combinations." 62(1): 1–14.
- Egan, W. J., K. M. Merz, and J. J. Baldwin. 2000. "Prediction of Drug Absorption Using Multivariate Statistics." *Journal of Medicinal Chemistry* 43(21): 3867–77.
- El-Hajj, L. et al. 2001. "Azoles and Allopurinol: A Maintenance Therapy for Visceral Leishmaniasis in HIV Patients." *Medicine et Maladies Infectieuses* 31(6): 446–47.
- Elcock, Adrian H. et al. 1996. "Electrostatic Channeling in the Bifunctional Enzyme Dihydrofolate Reductase-Thymidylate Synthase." *Journal of Molecular Biology* 262(3): 370–74.
- Ephros, Moshe et al. 1999. "Stage-Specific Activity of Pentavalent Antimony against Leishmania Donovanii Axenic Amastigotes." *Antimicrobial Agents and Chemotherapy* 43(2): 278–82.
- Ertl, Peter, and Ansgar Schuffenhauer. 2009. "Estimation of Synthetic Accessibility Score of Drug-like Molecules Based on Molecular Complexity and Fragment Contributions." *Journal of Cheminformatics* 1(1).
- Faleiro, Rebecca J., Rajiv Kumar, Louise M. Hafner, and Christian R. Engwerda. 2014. "Immune Regulation during Chronic Visceral Leishmaniasis." *PLoS Neglected Tropical Diseases* 8(7).
- Ferone, R, and S Roland. 1980. "Dihydrofolate Reductase: Thymidylate Synthase, a Bifunctional Polypeptide from Crithidia Fasciculata." *Proceedings of the National Academy of Sciences of the United States of America* 77(10): 5802–6.
- Ferreira, Flávia M. et al. 2014. "Association of Water Extract of Green Propolis and Liposomal Meglumine Antimoniate in the Treatment of Experimental Visceral Leishmaniasis." *Parasitology Research* 113(2): 533–43.

- Freitas, Vanessa C. et al. 2012. "Development of Leishmania (Leishmania) Infantum Chagasi in Its Natural Sandfly Vector Lutzomyia Longipalpis." *American Journal of Tropical Medicine and Hygiene* 86(4): 606–12.
- Frézard, Frédéric, Cynthia Demicheli, and Raul R. Ribeiro. 2009. "Pentavalent Antimonials: New Perspectives for Old Drugs." *Molecules* 14(7): 2317–36.
- Gautam, Shalini et al. 2011. "IL-10 Neutralization Promotes Parasite Clearance in Splenic Aspirate Cells from Patients with Visceral Leishmaniasis." *Journal of Infectious Diseases* 204(7): 1134–37.
- Gazanion, Elodie et al. 2011. "In Vitro Activity of Nicotinamide/antileishmanial Drug Combinations." *Parasitology International* 60(1): 19–24.
- Genheden, Samuel, and Ulf Ryde. 2015. "The MM/PBSA and MM/GBSA Methods to Estimate Ligand-Binding Affinities." *Expert Opinion on Drug Discovery* 10(5): 449–61.
- Gfeller, David et al. 2014. "SwissTargetPrediction: A Web Server for Target Prediction of Bioactive Small Molecules." *Nucleic Acids Research* 42(W1).
- Gfeller, David, Olivier Michielin, and Vincent Zoete. 2013. "Shaping the Interaction Landscape of Bioactive Molecules." *Bioinformatics* 29(23): 3073–79.
- Ghose, Arup K., Vellarkad N. Viswanadhan, and John J. Wendoloski. 1999. "A Knowledge-Based Approach in Designing Combinatorial or Medicinal Chemistry Libraries for Drug Discovery. 1. A Qualitative and Quantitative Characterization of Known Drug Databases." *Journal of Combinatorial Chemistry* 1(1): 55–68.
- Gibson, M E. 1983. "The Identification of Kala Azar and the Discovery of Leishmania Donovanii." *Medical History* 27: 203–13.
- Gossage, Sharon M., Matthew E. Rogers, and Paul A. Bates. 2003. "Two Separate Growth Phases during the Development of Leishmania in Sand Flies: Implications for Understanding the Life Cycle." *International Journal for Parasitology* 33(10): 1027–34.
- Goto, H., and J. A L Lindoso. 2004. "Immunity and Immunosuppression in Experimental Visceral Leishmaniasis." *Brazilian Journal of Medical and Biological Research* 37(4): 615–23.

- Goto, Hiro, and José Angelo Lauletta Lindoso. 2012. "Cutaneous and Mucocutaneous Leishmaniasis." *Infectious Disease Clinics of North America* 26(2): 293–307.
- van Griensven, Johan et al. 2010. "Combination Therapy for Visceral Leishmaniasis." *The Lancet Infectious Diseases* 10(3): 184–94.
- Grover, Abhinav et al. 2012. "Blocking Protein Kinase C Signaling Pathway: Mechanistic Insights into the Anti-Leishmanial Activity of Prospective Herbal Drugs from *Withania Somnifera*." *BMC genomics* 13 Suppl 7(Suppl 7): S20.
- Grumont, Raelene, Wendy L Washtien, Daniel Caputt, and Daniel V Santi. 1986. "Bifunctional Thymidylate Synthase-Dihydrofolate Reductase from *Leishmania Tropica*: Sequence Homology with the Corresponding Monofunctional Proteins (cDNA Cloning/gene Structure and Evolution/protozoan Parasite)." *Biochemistry* 83: 5387–91.
- Guex, Nicolas, and Manuel C. Peitsch. 1997. "SWISS-MODEL and the Swiss-PdbViewer: An Environment for Comparative Protein Modeling." *Electrophoresis* 18(15): 2714–23.
- Gupta, Suman et al. 2011. "CpG Oligodeoxynucleotide 2006 and Miltefosine, a Potential Combination for Treatment of Experimental Visceral Leishmaniasis." *Antimicrobial Agents and Chemotherapy* 55(7): 3461–64.
- Handman, Emanuela, and Denise V R Bullen. 2002. "Interaction of *Leishmania* with the Host Macrophage." *Trends in Parasitology* 18(8): 332–34.
- Hasker, Epcó et al. 2012. "Visceral Leishmaniasis in Rural Bihar, India." *Emerging Infectious Diseases* 18(10): 1662–64.
- Hendrickx, Sarah et al. 2017. "Combined Treatment of Miltefosine and Paromomycin Delays the Onset of Experimental Drug Resistance in *Leishmania Infantum*." *PLoS Neglected Tropical Diseases* 11(5).
- Herwaldt, B L. 1999. "Leishmaniasis." *Lancet* 354(0140–6736): 1191–99.
- Huang, Wei, Zhixiong Lin, and Wilfred F. Van Gunsteren. 2011. "Validation of the GROMOS 54A7 Force Field with Respect to β -Peptide Folding." *Journal of Chemical Theory and Computation* 7(5): 1237–43.

- Ivanetich, Kathryn M., and Daniel V. Santi. 1990. "Thymidylate Synthase-Dihydrofolate Reductase in Protozoa." *Experimental Parasitology* 70(3): 367–71.
- Jain, Keerti, and N.K. Jain. 2015. "Vaccines for Visceral Leishmaniasis: A Review." *Journal of Immunological Methods* 422: 1–12.
- Joshua Muli Mutiso, John Chege Macharia, Mustafa Barasa, Evans Taracha, Alain J. Bourdichon Michael M. Gicheru. 2011. "In Vitro and in Vivo Antileishmanial Efficacy of a Combination Therapy of Diminazene and Artesunate against *Leishmania Donovanii* in BALB /c Mice." *Rev. Inst. Med. Trop. Sao Paulo* 53(3): 53(3):129-132.
- Kaul, Sunil C, and Renu Wadhwa. "Science of Ashwagandha: Preventive and Therapeutic Potentials." Springer International Publishing AG 2017.
- Kaur, K., T. Coons, K. Emmett, and B. Ullman. 1988. "Methotrexate-Resistant *Leishmania Donovanii* Genetically Deficient in the Folate-Methotrexate Transporter." *Journal of Biological Chemistry* 263(15): 7020–28.
- Kaye, P. M., and T. Aebischer. 2011. "Visceral Leishmaniasis: Immunology and Prospects for a Vaccine." *Clinical Microbiology and Infection* 17(10): 1462–70.
- Kimutai, Robert et al. 2017. "Safety and Effectiveness of Sodium Stibogluconate and Paromomycin Combination for the Treatment of Visceral Leishmaniasis in Eastern Africa: Results from a Pharmacovigilance Programme." *Clinical Drug Investigation* 37(3): 259–72.
- Kopp, Jurgen, and Torsten Schwede. 2004. "Automated Protein Structure Homology Modeling: A Progress Report." *Pharmacogenomics* 5(4): 405–16.
- Kurup PA.1956."The antibacterial principle of the leaves of *Withania somnifera*". *Curr Sci* 25:57–58
- Kumar, Rajiv, and Christian Engwerda. 2014. "Vaccines to Prevent Leishmaniasis." *Clinical & Translational Immunology* 3(3): e13.
- Laemmli UK.1970."Cleavage of structural proteins during the assembly of the head of bacteriophage T4". *Nature*. 227: 680-685.

- Leeson, Paul D., and Brian Springthorpe. 2007. "The Influence of Drug-like Concepts on Decision-Making in Medicinal Chemistry." *Nature Reviews Drug Discovery* 6(11): 881–90.
- Lemley, Craig et al. 1999. "The Leishmania Donovanii LD1 Locus Gene ORFG Encodes a Biopterin Transporter (BT1)." *Molecular and Biochemical Parasitology* 104(1): 93–105.
- Leo, Albert, Corwin Hansch, and David Elkins. 1971. "Partition Coefficients and Their Uses." *Chemical Reviews* 71(6): 525–616.
- Liang, Po Huang, and Karen S. Anderson. 1998. "Substrate Channeling and Domain-Domain Interactions in Bifunctional Thymidylate Synthase-Dihydrofolate Reductase." *Biochemistry* 37(35): 12195–205.
- Po-Huang Liang and Karen S. Anderson. 1998. "Kinetic Reaction Scheme for the Dihydrofolate Reductase Domain of the Bifunctional Thymidylate Synthase-Dihydrofolate Reductase from Leishmania major." *Biochemistry* 1998, 37, 12206-12212.
- Liew, F. Y, C. A. O'Donnell. 1993. "Immunology of Leishmaniasis." *Advances in Parasitology* 32(C): 161–259.
- Lipinski, Christopher A. 2004. "Lead- and Drug-like Compounds: The Rule-of-Five Revolution." *Drug Discovery Today: Technologies* 1(4): 337–41.
- Lipinski, Christopher A, Franco Lombardo, Beryl W. Dominy, Paul J. Feeney. 2012. "Experimental and Computational Approaches to Estimate Solubility and Permeability in Drug Discovery and Development Settings." *Advanced Drug Delivery Reviews* 64: 4–17.
- Loría-Cervera, Elsy Nalleli, and Fernando José Andrade-Narváez. 2014. "Animal Models for the Study of Leishmaniasis Immunology." *Revista do Instituto de Medicina Tropical de São Paulo* 56(1): 1–11.
- Luba, J et al. 1998. "Leishmania Major Pteridine Reductase 1 Belongs to the Short Chain Dehydrogenase Family: Stereochemical and Kinetic Evidence." *Biochemistry* 37(12): 4093–4104.

- Lux, Henning et al. 2000. "Ether-Lipid (Alkyl-Phospholipid) Metabolism and the Mechanism of Action of Ether-Lipid Analogues in Leishmania." *Molecular and Biochemical Parasitology* 111(1): 1–14.
- Lyne, Paul D. 2002. "Structure-Based Virtual Screening: An Overview." *Drug Discovery Today* 7(20): 1047–55.
- Mahajan, Raman et al. 2015. "Combination Treatment for Visceral Leishmaniasis Patients Coinfected with Human Immunodeficiency Virus in India." *Clinical Infectious Diseases* 61(8): 1255–62.
- Makwali, J A et al. 2012. "Combination and Monotherapy of Leishmania Major Infection in BALB/c Mice Using Plant Extracts and Herbicides." *Journal of Vector Borne Diseases* 49(3): 123–30.
- Malde, Alpeshkumar K. et al. 2011. "An Automated Force Field Topology Builder (ATB) and Repository: Version 1.0." *Journal of Chemical Theory and Computation* 7(12): 4026–37.
- Martin, Yvonne C. 2005. "A Bioavailability Score." *Journal of Medicinal Chemistry* 48(9): 3164–70.
- Mesquita, Juliana T., Andre G. Tempone, and Juliana Q. Reimo. 2014. "Combination Therapy with Nitazoxanide and Amphotericin B, Glucantime, Miltefosine and Sitamaquine against Leishmania (Leishmania) Infantum Intracellular Amastigotes." *Acta Tropica* 130(1): 112–16.
- Mir, Bilal Ahmad et al. 2012. "Botanical, Chemical and Pharmacological Review of Withania Somnifera (Indian Ginseng): An Ayurvedic Medicinal Plant." *Indian Journal of Drugs and Diseases* 1(6): 147–60.
- Modabber, Farrokh. 2010. "Leishmaniasis Vaccines: Past, Present and Future." *International Journal of Antimicrobial Agents* 36(SUPPL. 1).
- Monte-Alegre, Adriano, Ali Ouaiissi, and Denis Sereno. 2006. "Leishmania Amastigotes as Targets for Drug Screening." *Kinetoplastid Biology and Disease* 5.

- Moriguchi, Ikuo, Shuichi hirono, Izumi nakagome, and Hiroyuki hirano. 1994. "Comparison of Reliability of Log P Values for Drugs Calculated by Several Methods." *Chemical & Pharmaceutical Bulletin* 42(4): 976–78.
- Muegge, I., S. L. Heald, and D. Brittelli. 2001. "Simple Selection Criteria for Drug-like Chemical Matter." *Journal of Medicinal Chemistry* 44(12): 1841–46.
- Murray, H W, and C F Nathan. 1999. "Macrophage Microbicidal Mechanisms in Vivo: Reactive Nitrogen versus Oxygen Intermediates in the Killing of Intracellular Visceral Leishmania Donovanii." *The Journal of experimental medicine* 189(4): 741–46.
- Murray, Henry W., and June Hariprasad. 1996. "Activity of Oral Atovaquone Alone and in Combination with Antimony in Experimental Visceral Leishmaniasis." *Antimicrobial Agents and Chemotherapy* 40(3): 586–87.
- Musa, Ahmed et al. 2012. "Sodium Stibogluconate (Ssg) & Paromomycin Combination Compared to Ssg for Visceral Leishmaniasis in East Africa: A Randomised Controlled Trial." *PLoS Neglected Tropical Diseases* 6(6).
- Mwololo, Samuel W et al. 2015. "In Vitro Activity and in Vivo Efficacy of a Combination Therapy of Diminazene and Chloroquine against Murine Visceral Leishmaniasis." *Journal of biomedical research* 29(3): 214–23.
- Nare, Bakela, Larry W. Hardy, Stephen M. Beverley. 1997. "The Roles of Pteridine Reductase 1 and Dihydrofolate Reductase- Thymidylate Synthase in Pteridine Metabolism in the Protozoan Parasite Leishmania Major." *Journal of Biological Chemistry* 272(21): 13883–91.
- Naula, Christina, Marilyn Parsons, Jeremy C. Mottram. 2005. "Protein Kinases as Drug Targets in Trypanosomes and Leishmania." In *Biochimica et Biophysica Acta - Proteins and Proteomics*, , 151–59.
- Nylén, S. et al. 2003. "Live Leishmania Promastigotes Can Directly Activate Primary Human Natural Killer Cells to Produce Interferon-Gamma." *Clinical and Experimental Immunology* 131(3): 457–67.
- Nylén, Susanne, David Sacks. 2007. "Interleukin-10 and the Pathogenesis of Human Visceral Leishmaniasis." *Trends in Immunology* 28(9): 378–84.

- Oliveira, Fabiano, Augusto M. de Carvalho, Camila I. de Oliveira. 2013. "Sand-Fly Saliva-Leishmania-Man: The Trigger Trio." *Frontiers in Immunology* 4: 1–8.
- Otranto, Domenico et al. 2013. "Prevention of Canine Leishmaniosis in a Hyper-Endemic Area Using a Combination of 10% Imidacloprid/4.5% Flumethrin." *PLoS ONE* 8(2).
- Owais, M., K. S. Sharad, A. Shehbaz, and M. Saleemuddin. 2005. "Antibacterial Efficacy of *Withania Somnifera* (Ashwagandha) an Indigenous Medicinal Plant against Experimental Murine Salmonellosis." *Phytomedicine* 12(3): 229–35.
- Pak-Lam Yu, Jia Zhao, Ming Yu, Ralph Reid, and Daniel V. Santi. 1996. "Functional Expression of the Dihydrofolate Reductase Domain of *Leishmania major* Dihydrofolate Reductase Thymidylate Synthase Bifunctional Protein." *PROTEIN EXPRESSION AND PURIFICATION* 8, 23–27.
- Pal, C. et al. 2002. "Combination Therapy with Indolylquinoline Derivative and Sodium Antimony Gluconate Cures Established Visceral Leishmaniasis in Hamsters." *Antimicrobial Agents and Chemotherapy* 46(1): 259–61.
- Paris, Caroline, Philippe M. Loiseau, Christian Bories, and Jaqueline Bréard. 2004. "Miltefosine Induces Apoptosis-Like Death in *Leishmania Donovanii* Promastigotes." *Antimicrobial Agents and Chemotherapy* 48(3): 852–59.
- Pastor Jacinta, Marley García, Silvia Steinbauer, William N. Setzer, Ramón Scull, Lars Gille, Lianet Monzote. 2015. "Combinations of ascaridole, carvacrol, and caryophyllene oxide against *Leishmania*." *Acta Tropica* 145 31–38
- Pérez-Victoria, F. Javier, Santiago Castanys, and Francisco Gamarro. 2003. "Leishmania *Donovani* Resistance to Miltefosine Involves a Defective Inward Translocation of the Drug." *Antimicrobial Agents and Chemotherapy* 47(8): 2397–2403.
- Pérez-Victoria, F. Javier, María P. Sánchez-Cañete, Santiago Castanys, and Francisco Gamarro. 2006. "Phospholipid Translocation and Miltefosine Potency Require Both L. *Donovani* Miltefosine Transporter and the New Protein LdRos3 in *Leishmania* Parasites." *Journal of Biological Chemistry* 281(33): 23766–75.

- Quinnell, R. J., and O. Courtenay. 2009. "Transmission, Reservoir Hosts and Control of Zoonotic Visceral Leishmaniasis." *Parasitology* 136(14): 1915–34.
- Rahman, Ridwanur et al. 2017. "Safety and Efficacy of Short Course Combination Regimens with AmBisome, Miltefosine and Paromomycin for the Treatment of Visceral Leishmaniasis (VL) in Bangladesh." *PLoS Neglected Tropical Diseases* 11(5).
- Ramesh, V, Ruchi Singh, Poonam Salotra. 2007. "Short Communication: Post-Kala-Azar Dermal Leishmaniasis - An Appraisal." *Tropical Medicine and International Health* 12(7): 848–51.
- Ramesh, Venkat, Kumar Avishek, Vanila Sharma, and Poonam Salotra. 2014. "Combination Therapy with Amphotericin-B and Miltefosine for Post-Kala-Azar Dermal Leishmaniasis: A Preliminary Report." *Acta Dermato-Venereologica* 94(2): 242–43.
- Ready, Paul D. 2014. "Epidemiology of Visceral Leishmaniasis." *Clinical Epidemiology* 6(1): 147–54.
- Reithinger, Richard et al. 2007. "Cutaneous Leishmaniasis." *The Lancet Infectious Diseases* 7(9): 581–96.
- Rishton, Gilbert M. 2003. "Nonleadlikeness and Leadlikeness in Biochemical Screening." *Drug Discovery Today* 8(2): 86–96.
- Roberts, C. W. et al. 2003. "Fatty Acid and Sterol Metabolism: Potential Antimicrobial Targets in Apicomplexan and Trypanosomatid Parasitic Protozoa." *Molecular and Biochemical Parasitology* 126(2): 129–42.
- Rodolpho C. Braga, Vinicius M. Alves, Meryck F. B. Silva, Eugene Muratov, Denis Fourches, Luciano M. Lião, Alexander Tropsha, and Carolina H. Andrade. 2015. "Pred-hERG: A Novel web-Accessible Computational Tool for Predicting Cardiac Toxicity". *Mol Inform.* 34(10): 698–701.
- Sachdeva, Heena, Rakesh Sehgal, and Sukhbir Kaur. 2014. "Tinospora Cordifolia as a Protective and Immunomodulatory Agent in Combination with Cisplatin against Murine Visceral Leishmaniasis." *Experimental Parasitology* 137(1): 53–65.
- Savoia, Dianella. "Review Recent Updates and Perspectives on Leishmaniasis."

- Sangwan NS, Sangwan RS. 2013. "Applied plant cell biology secondary metabolites of traditional medical plants: a case study of Ashwagandha (*Withania somnifera*)". *Plant Cell Monogr* 22:325–367
- Sambrook J, Fritsch EF, Maniatis T. 1989. "Molecular cloning: A laboratory manual (2nd Edition)." Cold Spring Harbour Press.
- Schrevel, J., and P.M. Loiseau. 2016. "Sitamaquine." In *Reference Module in Biomedical Sciences*,
- Schwede, Torsten, Jürgen Kopp, Nicolas Guex, and Manuel C. Peitsch. 2003. "SWISS-MODEL: An Automated Protein Homology-Modeling Server." *Nucleic Acids Research* 31(13): 3381–85.
- Scott, David A., Graham H. Coombs, and Barbara E. Sanderson. 1987. "Folate Utilisation by *Leishmania* Species and the Identification of Intracellular Derivatives and Folate-Metabolising Enzymes." *Molecular and Biochemical Parasitology* 23(2): 139–49.
- Sen, N et al. 2007. "Apoptosis Is Induced in Leishmanial Cells by a Novel Protein Kinase Inhibitor Withaferin A and Is Facilitated by Apoptotic Topoisomerase I–DNA Complex." *Cell Death and Differentiation* 14: 358–67.
- Serrano-Martín, Xenón et al. 2009. "Amiodarone and Miltefosine Act Synergistically against *Leishmania Mexicana* and Can Induce Parasitological Cure in a Murine Model of Cutaneous Leishmaniasis." *Antimicrobial Agents and Chemotherapy* 53(12): 5108–13.
- Shakya, Nishi et al. 2011. "Improved Treatment of Visceral Leishmaniasis (Kala-Azar) by Using Combination of Ketoconazole, Miltefosine with an Immunomodulator-Picroliv." *Acta Tropica* 119(2–3).
- Shakya, Nishi, Shraddha A. Sane, Wahajul Haq, and Suman Gupta. 2012. "Augmentation of Antileishmanial Efficacy of Miltefosine in Combination with Tuftsia against Experimental Visceral Leishmaniasis." *Parasitology Research* 111(2): 563–70.

- Shakya, Nishi, Shraddha A. Sane, Preeti Vishwakarma, and Suman Gupta. 2012. "Enhancement in Therapeutic Efficacy of Miltefosine in Combination with Synthetic Bacterial Lipopeptide, Pam3Cys against Experimental Visceral Leishmaniasis." *Experimental Parasitology* 131(3): 377–82.
- Sharma, Veena, Sadhana Sharma, Pracheta, and Ritu Paliwal. 2011. "Withania Somnifera: A Rejuvenating Ayurvedic Medicinal Herb for the Treatment of Various Human Ailments." *International Journal of PharmTech Research* 3(1): 187–92.
- Da Silva, Sydney M. et al. 2012. "Efficacy of Combined Therapy with Liposome-Encapsulated Meglumine Antimoniate and Allopurinol in Treatment of Canine Visceral Leishmaniasis." *Antimicrobial Agents and Chemotherapy* 56(6): 2858–67.
- Singh, Gaganmeet, K.G. Jayanarayan, Chinmoy S. Dey. 2008. "Arsenite Resistance in Leishmania and Possible Drug Targets." *Advances in Experimental Medicine and Biology* 625: 1–8.
- Singh, G, P K Sharma, R Dudhe, and S Singh. 2010. "Biological Activities of Withania Somnifera." *Annals of Biological Research* 1(3): 56–63.
- Singh, Narendra, Mohit Bhalla, Prashanti de Jager, and Marilena Gilca. 2011. "An Overview on Ashwagandha: A Rasayana (Rejuvenator) of Ayurveda." *African Journal of Traditional, Complementary and Alternative Medicines* 8(5 SUPPL.): 208–13.
- Singh, Nisha et al. 2014. "Natural Product Based Leads to Fight against Leishmaniasis." *Bioorganic and Medicinal Chemistry* 22(1): 18–45.
- Singh, Sarman. 2006a. "New Developments in Diagnosis of Leishmaniasis." *Indian Journal of Medical Research* 123(3): 311–30.
- Singh, Sarman. 2006b. "New Developments in Diagnosis of Leishmaniasis." *Indian Journal of Medical Research* 123(3): 311–30.
- Solgi, Ghassem et al. 2006. "Effects of Combined Therapy with Thalidomide and Glucantime on Leishmaniasis Induced by Leishmania Major in BALB/c Mice." *The Korean journal of parasitology* 44(1): 55–61.
- Subramanian SS, Sethi PD.1969."Withaferin–A from Withania somnifera coagulants roots". *Current science* 38:267–268.

- Sundar, S et al. 1994. "Clinicoepidemiological Study of Drug Resistance in Indian Kala-Azar." *BMJ (Clinical research ed.)* 308(6924): 307.
- Sundar, Shyam et al. 2007. "Injectable Paromomycin for Visceral Leishmaniasis in India." *N.Engl.J.Med.* 356(1533–4406: 2571–81.
- Sundar, Shyam et al. 2002. "Oral Miltefosine for Indian Visceral Leishmaniasis." *The New England journal of medicine* 347(22): 1739–46.
- Sundar, Shyam et al.2007. "Injectable Paramomycin for Visceral Leishmaniasis in India." *The New England Journal of Medicine* 356(25): 2571–81.
- Sundar, Shyam et al.2010. "Single-Dose Liposomal Amphotericin B for Visceral Leishmaniasis in India." *The New England journal of medicine* 362(6): 504–12.
- Sundar, Shyam et al.2011. "Ambisome plus Miltefosine for Indian Patients with Kala-Azar." *Transactions of the Royal Society of Tropical Medicine and Hygiene* 105(2): 115–17.
- Sundar, Shyam et al. 2012. "Efficacy of Miltefosine in the Treatment of Visceral Leishmaniasis in India after a Decade of Use." *Clinical Infectious Diseases* 55(4): 543–50.
- Sundar, Shyam, and Mitali Chatterjee. 2006. "Visceral Leishmaniasis - Current Therapeutic Modalities." *The Indian journal of medical research* 123: 345–52.
- Szklarczyk, Damian et al. 2015. "STRING v10: Protein-Protein Interaction Networks, Integrated over the Tree of Life." *Nucleic Acids Research* 43(D1): D447–52.
- Tavares, C. A P, Ana Paula Fernandes, and Maria Norma Melo. 2003. "Molecular Diagnosis of Leishmaniasis." *Expert Review of Molecular Diagnostics* 3(5): 657–67.
- Teague, Simon J., Andrew M. Davis, Paul D. Leeson, and Tudor Oprea. 1999. "The Design of Leadlike Combinatorial Libraries." *Angewandte Chemie - International Edition* 38(24): 3743–48.
- Thöny, B, G Auerbach, and Nenad Blau. 2000. "Tetrahydrobiopterin Biosynthesis, Regeneration and Functions." *The Biochemical journal* 347 Pt 1: 1–16.
- Tiuman, Tatiana S. et al. 2011. "Recent Advances in Leishmaniasis Treatment." *International Journal of Infectious Diseases* 15(8).

- Tiwari, Brajendra et al. 2017. "Nanotized Curcumin and Miltefosine, a Potential Combination for Treatment of Experimental Visceral Leishmaniasis." *Antimicrobial Agents and Chemotherapy* 61(3).
- Trott, Oleg, and Arthur J. Olson. 2010. "AutoDock Vina: Improving the Speed and Accuracy of Docking with a New Scoring Function, Efficient Optimization, and Multithreading." *Journal of Computational Chemistry* 31(2): 455–61.
- Varma, Neelam, and Shano Naseem. 2010. "Hematologic Changes in Visceral Leishmaniasis/Kala Azar." *Indian Journal of Hematology and Blood Transfusion* 26(3): 78–82.
- Weber, Daniel F et al. 2002. "Molecular Properties That Influence the Oral Bioavailability of Drug Candidates." *Journal of medicinal chemistry* 45: 2615–23.
- Veras, P. S T et al. 1999. "A Dhfr-Ts- Leishmania Major Knockout Mutant Cross-Protects against Leishmania Amazonensis." *Memorias do Instituto Oswaldo Cruz* 94(4): 491–96.
- Verma, Navin K., and Chinmoy S. Dey. 2004. "Possible Mechanism of Miltefosine-Mediated Death of Leishmania Donovanii." *Antimicrobial Agents and Chemotherapy* 48(8): 3010–15.
- Vishwanathan, B., B. M. Gurupadaya, and K. Venkata Sairam. 2016. "In Silico and Antithrombotic Studies of 1,3,4-Oxadiazoles Derived from Benzimidazole." *Bangladesh Journal of Pharmacology* 11(1): 67–74.
- Volf, P., and V. Volfova. 2011. "Establishment and Maintenance of Sand Fly Colonies." *Journal of Vector Ecology* 36: S1–9.
- Vries, Henry J C De, Sophia H Reedijk, and Henk D F H Schallig. 2015. "Cutaneous Leishmaniasis: Recent Developments in Diagnosis and Management." : 99–109.
- Wadhone, Pallavi et al. 2009. "Miltefosine Promotes IFN-Gamma-Dominated Anti-Leishmanial Immune Response." *Journal of immunology* 182(11): 7146–54.
- Wang, J et al. 1997. "Pterin and Folate Reduction by the Leishmania Tarentolae H Locus Short-Chain Dehydrogenase/reductase PTR1." *Archives of biochemistry and biophysics* 342(2): 197–202.

- Wasunna, Monique et al. 2016. "Efficacy and Safety of AmBisome in Combination with Sodium Stibogluconate or Miltefosine and Miltefosine Monotherapy for African Visceral Leishmaniasis: Phase II Randomized Trial." *PLoS Neglected Tropical Diseases* 10(9): 1–18.
- Wheeler, Richard J., Eva Gluenz, and Keith Gull. 2011. "The Cell Cycle of Leishmania: Morphogenetic Events and Their Implications for Parasite Biology." *Molecular Microbiology* 79(3): 647–62.
- Whiteley JM, Xuong NH, Varughese KI. 1993. "Is Dihydropteridine Reductase an Anomalous Dihydrofolate Reductase, a Flavin-like Enzyme, or a Short-Chain Dehydrogenase?" *Adv Exp Med Biol* 338: 115–21.
- WHO technical report series. 2010. "Control of the Leishmaniasis: Report of a Meeting of the WHO Expert Committee on the Control of Leishmaniasis, Geneva, 22-26 March 2010." *World Health Organization technical report series* 949(March): 202.
- Widodo, Nashi et al. 2007. "Selective Killing of Cancer Cells by Leaf Extract of Ashwagandha: Identification of a Tumor-Inhibitory Factor and the First Molecular Insights to Its Effect." *Clinical Cancer Research* 13(7): 2298–2306.
- Wildman, Scott A., and Gordon M. Crippen. 1999. "Prediction of Physicochemical Parameters by Atomic Contributions." *Journal of Chemical Information and Computer Sciences* 39(5): 868–73.
- Winters, Marie. 2006. "Ancient Medicine, Modern Use: Withania Somnifera and Its Potential Role in Integrative Oncology." *Alternative Medicine Review* 11(4): 269–77.
- Zhao, Yuan H et al. 2002. "Rate-Limited Steps of Human Oral Absorption and QSAR Studies." 19(10): 1446–57.
- Zijlstra, E. E. et al. 2003. "Post-Kala-Azar Dermal Leishmaniasis." *Lancet Infectious Diseases* 3(2): 87–98.

Publications

RESEARCH NOTE

Open Access



Homology modelling, molecular docking, and molecular dynamics simulations reveal the inhibition of *Leishmania donovani* dihydrofolate reductase-thymidylate synthase enzyme by Withaferin-A

Bharadwaja Vadloori¹, A. K. Sharath², N. Prakash Prabhu² and Radheshyam Maurya^{1*} 

Abstract

Objective: Present in silico study was carried out to explore the mode of inhibition of *Leishmania donovani* dihydrofolate reductase-thymidylate synthase (*Ld* DHFR-TS) enzyme by Withaferin-A, a withanolide isolated from *Withania somnifera*. Withaferin-A (WA) is known for its profound multifaceted properties, but its antileishmanial activity is not well understood. The parasite's DHFR-TS enzyme is diverse from its mammalian host and could be a potential drug target in parasites.

Results: A 3D model of *Ld* DHFR-TS enzyme was built and verified using Ramachandran plot and SAVES tools. The protein was docked with WA-the ligand, methotrexate (MTX)-competitive inhibitor of DHFR, and dihydrofolic acid (DHFA)-substrate for DHFR-TS. Molecular docking studies reveal that WA competes for active sites of both *Hu* DHFR and TS enzymes whereas it binds to a site other than active site in *Ld* DHFR-TS. Moreover, Lys 173 residue of DHFR-TS forms a H-bond with WA and has higher binding affinity to *Ld* DHFR-TS than *Hu* DHFR and *Hu* TS. The MD simulations confirmed the H-bonding interactions were stable. The binding energies of WA with *Ld* DHFR-TS were calculated using MM-PBSA. Homology modelling, molecular docking and MD simulations of *Ld* DHFR-TS revealed that WA could be a potential anti-leishmanial drug.

Keywords: *Leishmania donovani*, DHFR-TS, *Withania somnifera*, Ashwagandha, Molecular docking, Withaferin-A, Methotrexate, Dihydrofolicacid, Antileishmanial drug

Introduction

Withaferin-A (WA) is among the most effective withanolide isolated from *W. somnifera* and has various effects like anti-bacterial, anti-inflammatory, anti-proliferative and potent anti-cancer properties [1–4]. Recently we demonstrated in vitro, that withanolides show potent anti-leishmanial activity [5] and a drastic reduction in parasite load in vivo [6].

Availability of complete genome sequence of *Leishmania* opens new windows to identify a potential drug target [7]. Many enzymes of *Leishmania* are extensively explored as drug targets as they are diverse from mammalian hosts [8, 9]. Trypanosomatids including *Leishmania* are pteridine auxotrophs and require an exogenous source of folate/biopterin [10, 11]. Folate and biopterin are served as cofactors only in their fully reduced forms, H4-folate and H4-biopterin, respectively (Fig. 1a). In *Leishmania* DHFR along with TS forms DHFR-TS complex and occurs as a bifunctional enzyme [12–17]. However, as de novo biopterin synthetic pathway is absent, DHFR-TS shows no activity with biopterin [18–21].

*Correspondence: rmusl@uohyd.ernet.in; radhemaurya@rediffmail.com

¹ Department of Animal Biology, School of Life Sciences, University of Hyderabad, Prof. C.R. Rao Road, Gachibowli, Hyderabad 500046, India
Full list of author information is available at the end of the article



SCIENTIFIC REPORTS

OPEN

Leptin regulates Granzyme-A, PD-1 and CTLA-4 expression in T cell to control visceral leishmaniasis in BALB/c Mice

Alti Dayakar, Sambamurthy Chandrasekaran , Jalaja Veronica, Vadloori Bharadwaja & Radheshyam Maurya 

Visceral leishmaniasis (VL) is responsible for several deaths in malnourished children accompanied by diminished circulating leptin and impaired cell-mediated immunity. Typically, leptin deficiency is associated with the Th2 polarization that markedly coincides with the pathogenesis of VL. The aim of the present study was to unravel the prophylactic role of leptin in malnutrition-coupled VL mice. Interestingly, we observed that *L. donovani* infection itself reduces the serum leptin levels in malnutrition. Exogenous leptin restored severe body weight loss and parasite load in the spleen and liver of malnourished infected mice compared to controls. Leptin increases functional CD8⁺ T-cell population, Granzyme-A expression down-regulates anergic T-cell markers such as PD-1 and CTLA-4. It was also noticed that, leptin suppresses GM-CSF mRNA expression in parasite favored monocytes and reduced arginase activity in bone marrow derived macrophage indicate macrophages dependent T-cell activation and proliferation. Leptin-induced IFN- γ , IL-2, and TNF- α cytokines in the culture supernatant of splenocytes upon soluble leishmanial antigen (SLA) stimulation and significantly up-regulates serum IgG2a titers, which help to generate Th1 immune response in VL. Furthermore, leptin induced a granulomatous response and restored *L. donovani* induced tissue degeneration in the liver. Altogether, our findings suggest the exogenous leptin can restore T cell mediated immunity in malnourished VL mice.

Visceral Leishmaniasis (VL) is a vector borne infectious disease caused by the protozoan parasite *Leishmania donovani* in the Indian subcontinent. VL majorly affects the undernourished population especially children (5–14 years) in endemic regions of tropical and subtropical countries, and it is the most severe clinical form of the disease characterized by systemic infection to vital lymphoid organs such as lymph nodes, liver, spleen, and bone marrow¹. The global burden of VL is about 400,000 new cases and >40,000 deaths per year². The most affected countries are Sudan, Ethiopia, Brazil, and the Indian subcontinent, which is accounted for 90% of cases³.

Successful treatment of VL depends on the induction of cellular immunity together with the production of the proinflammatory cytokines owing to Th1 response primed mostly by interleukin IL-12 produced from dendritic cells and macrophages^{4,5}. Production of IL-12 by antigen-presenting cells (APCs) and interferon IFN- γ by T-cells is crucial for controlling parasite growth by inducing nitric oxide (NO) signalling^{6,7}. The host immune response was skewed towards IL-10, transforming growth factor (TGF)- β , or IL-4 producing Th2 cytokines and IL-10 producing T-regulatory cells, suppressing host immunity and help parasite survival^{8,9}. However, IL-10 also protects the host from tissue damage caused by excessive inflammatory cytokines¹⁰. Exhaustion of CD8⁺ T-cells has been defined as antigen-specific effector T-cells dysfunction with sustained expression of inhibitory receptors including programmed death-1 (PD-1) and decreased effector cytokine production in chronic parasitic diseases as in toxoplasmosis and cutaneous leishmaniasis^{11,12}. A chronic murine infection with arginase-deficient *L. major* demonstrated that impaired priming of T-cells can result in PD-1 overexpression, impairment of acquired immunity, and CD8⁺ T-cell exhaustion¹³. Although VL is asymptomatic, protein-energy deficiency increases the risk of rapid development of the symptomatic clinical disease.

Department of Animal Biology, University of Hyderabad, Hyderabad, 500 046, India. Correspondence and requests for materials should be addressed to R.M. (email: rmusi@uohyd.ernet.in)

Studies on the Inhibitory and Additive Effects of Withaferin A in Experimental Visceral Leishmaniasis

by Bharadwaja Vadloori

Submission date: 20-Jun-2018 03:34PM (UTC+0530)

Submission ID: 977221123

File name: Bharadwaja_Vadloori_13laph01_thesis_for_anti-plagiarism_1.pdf (3.58M)

Word count: 31752

Character count: 166827

Studies on the Inhibitory and Additive Effects of Withaferin A in Experimental Visceral Leishmaniasis

ORIGINALITY REPORT

9%

SIMILARITY INDEX

5%

INTERNET SOURCES

7%

PUBLICATIONS

3%

STUDENT PAPERS

PRIMARY SOURCES

- 1** Bharadwaja Vadloori, A. K. Sharath, N. Prakash Prabhu, Radheshyam Maurya. "Homology modelling, molecular docking, and molecular dynamics simulations reveal the inhibition of *Leishmania donovani* dihydrofolate reductase-thymidylate synthase enzyme by Withaferin-A", *BMC Research Notes*, 2018
Publication 1%
- 2** "Science of Ashwagandha: Preventive and Therapeutic Potentials", Springer Nature, 2017
Publication 1%
- 3** www.nature.com
Internet Source <1%
- 4** rhizobium.net
Internet Source <1%
- 5** Submitted to University of Hyderabad, Hyderabad
Student Paper <1%

Mark L. Cunningham, Stephen M. Beverley.